




8-2012

Pretreatment and Pyrolysis of Rayon-based Precursor for Carbon Fibers

Kokouvi Akato
kakato@utk.edu

Follow this and additional works at: https://trace.tennessee.edu/utk_gradthes

 Part of the [Other Materials Science and Engineering Commons](#), and the [Polymer and Organic Materials Commons](#)

Recommended Citation

Akato, Kokouvi, "Pretreatment and Pyrolysis of Rayon-based Precursor for Carbon Fibers. " Master's Thesis, University of Tennessee, 2012.
https://trace.tennessee.edu/utk_gradthes/1311

This Thesis is brought to you for free and open access by the Graduate School at TRACE: Tennessee Research and Creative Exchange. It has been accepted for inclusion in Masters Theses by an authorized administrator of TRACE: Tennessee Research and Creative Exchange. For more information, please contact trace@utk.edu.

To the Graduate Council:

I am submitting herewith a thesis written by Kokouvi Akato entitled "Pretreatment and Pyrolysis of Rayon-based Precursor for Carbon Fibers." I have examined the final electronic copy of this thesis for form and content and recommend that it be accepted in partial fulfillment of the requirements for the degree of Master of Science, with a major in Polymer Engineering.

Gajanan Bhat, Major Professor

We have read this thesis and recommend its acceptance:

Roberto Benson, Kevin Kit

Accepted for the Council:

Carolyn R. Hodges

Vice Provost and Dean of the Graduate School

(Original signatures are on file with official student records.)

Pretreatment and Pyrolysis of Rayon-based Precursor for Carbon Fibers

A Thesis

Presented for the
Masters of Science

Degree

The University of Tennessee, Knoxville

Kokouvi Mawuko Akato

August 2012

DEDICATION

I dedicate my master's thesis to my fiancée, parents, and family especially my sister Ablavi Akato. I have been truly blessed that the people closest to me always supported all my endeavors and continue to support me in all that I do.

ACKNOWLEDGEMENTS

I am very grateful to everyone who helped me complete this thesis. I would like to express deep gratitude to my major advisor Dr. G. Bhat. He has given me the opportunity to grow professionally and has provided a great example to follow. I would also like to express my sincere thanks to Dr. R. Benson for his valuable questioning and suggestions, which have given me better insight into my work. I would also like to express my gratitude to all members of my thesis committee: Dr. K. Kit. Finally I would like to thank all my friends and colleagues at UTNRL. Their never-ending support and friendship provided me with the mental fortitude to complete this research.

Special thanks are due to Dr. West Hoffman, Edwards AFB, CA and Dr. Farhad Mohammadi, Advanced Cerametrics, Lumbertville, NJ for their support to this project. I am also thankful to Lenzing, Austria for providing the commercial rayon fiber. Partial support from Center for Materials Processing, UTK was also helpful in completing my thesis.

ABSTRACT

In this work, two rayon fibers were investigated as carbon fiber precursors. A detailed consideration has been applied to a domestically produced cellulose fiber to carbon fiber (CF) transition. This transition of precursor to carbon fiber can be subdivided into two stages: pyrolysis (thermal decomposition) of cellulose in air and high temperature treatment in an inert atmosphere. The specific objectives were to investigate the stabilization stage of the produced rayon with respect to changes taking place during thermal decomposition, and to evaluate the effects on the properties of the carbonized fiber. Changes taking place during the conversion process of the domestic precursor are compared with respect to the commercial rayon fiber.

Phosphoric acid was used as a catalyst and a flame retardant during stabilization. It was observed that the acid plays a multirole of heat absorption, catalytic dehydration by lowering the required temperatures, and acts as a protection during carbonization. The effects of time and temperature during stabilization were studied systematically. The temperature affects the structural changes taking place, and the time required for completion of stabilization reactions. The thermal behaviors of rayon fibers were analysed by Thermogravimetry Analysis (TGA) and Differential Scanning Calorimetry (DSC). The results showed that the phosphoric acid treated fibers underwent pyrolysis under lower temperatures and over a wider temperature range. Wide Angle X-ray Diffraction (WAXD) was used to analyse the degree of cristallinity of the precursor and the subsequent carbon fibers. The highly ordered and oriented precursor becomes totally amorphous after pyrolysis. The crystallite order was reinduced during carbonization under tension. Fourier Transform Infrared Spectroscopy (FTIR) was utilized to investigate the chemical transition during the heat treatment. The intensity of peaks corresponding to chemical groups present in the precursor decreased by the end of low temperature pyrolysis and disappeared during carbonization indicating the fibers were mostly carbon. The mechanical properties, morphology and structure of the precursor and the obtained carbon fibers were studied by Scanning Electron Microscopy (SEM). An increase in applied tension during carbonization increased the carbon content slightly leading to better quality fibers.

TABLE OF CONTENTS

CHAPTER 1: INTRODUCTION.....	1
CHAPTER 2: LITERATURE REVIEW.....	5
2.1 Carbon fibers through the years.....	5
2.2 Solution Process for Rayon Fibers.....	7
2.3 Thermal Processes of Carbon Fibers.....	8
2.3.1 PAN-based carbon fibers.....	9
2.3.2 Pitch-based carbon fibers.....	10
2.3.3 Rayon-based carbon fibers.....	11
2.4 Pretreatment effects on pyrolysis of cellulose.....	14
2.5 Chemistry and kinetics of cellulose thermal degradation.....	16
2.6 High temperature treatment of cellulose.....	25
2.7 Properties and Structure of Carbon Fibers.....	28
2.8 Application of carbon fibers.....	33
CHAPTER 3: EXPERIMENTAL	35
3.1 Materials.....	35
3.1.1 Precursor fibers.....	35
3.1.2 Phosphoric Acid.....	35
3.2 Preparation of Carbon fibers.....	35
3.2.1 Apparatus.....	35
3.2.2 Impregnation with phosphoric acid.....	38
3.2.3 Stabilization.....	38
3.2.4 Carbonization.....	39
3.3 Characterization methods.....	41
3.3.1 Color Change.....	41

3.3.2 Fiber diameter.....	41
3.3.3 Burning test.....	41
3.3.4 Thermal Analyses.....	42
3.3.5 Single fiber tensile test.....	42
3.3.6 Scanning Electron Microscopy (SEM).....	43
3.3.7 X-ray diffraction.....	44
3.3.8 Elemental Analysis.....	44
3.3.9 Fourier Transform Infrared Spectroscopy (FTIR).....	44
CHAPTER 4: RESULTS And DISCUSSION.....	45
4.1 Properties of the precursors.....	45
4.2 Precursor I: Commercial rayon fibers.....	54
4.2.1 Stabilization at low temperature.....	54
4.2.1.1 Effect of phosphoric acid.....	54
4.2.1.2 Effect of residence time and temperature.....	59
4.2.1.3 Transition and change of structure during stabilization.....	65
4.2.2 High temperature heat treatment (Carbonization).....	73
4.2.2.1 Effect of tension during carbonization.....	73
4.2.2.2 Changes during carbonization.....	75
4.2.3 Mechanical properties.....	84
4.3 Precursor II: Experimental rayon fibers.....	85
4.3.1 Low temperature heat treatment.....	85
4.3.2 High temperature heat treatment.....	90
4.3.3 Mechanical Properties.....	97
4.4 Comparison of commercial and experimental fibers.....	97
CHAPTER 5: CONCLUSIONS AND RECOMMENDATIONS FOR FUTURE WORK.....	101
5.1 Conclusions.....	101

5.2 Recommendations for future work.....	103
REFERENCES.....	104
APPENDIX.....	110
VITA.....	111

LIST OF TABLES

Table 1 Stabilization conditions (time and temperature) of commercial rayon precursor.....	39
Table 2 Stabilization conditions of the experimental rayon precursor.....	40
Table 3 Physicals and mechanical properties of the rayon fibers.....	44
Table 4 Burning test results of the untreated and soaked fibers after stabilization in air up to 380°C.....	59
Table 5 Fiber diameter of stabilized samples.....	60
Table 6 Stabilization conditions of untreated samples with color change during heat treatment.....	66
Table 7 Stabilization conditions of the treated samples with color change during heat treatment.....	66
Table 8 The carbonization conditions.....	73
Table 9 Mechanical properties, fiber diameter, and carbon content of sample 6003 and sample 6005.....	74
Table 10 Carbonization conditions (time and temperatures).....	75
Table 11 Mechanical properties and fiber diameter of the precursor, the stabilized (6001) and carbonized samples (6002, 6003).....	84
Table 12 Fiber diameter, shrinkage and burning test of the precursor and stabilized samples.....	86
Table 13 Carbonization conditions.....	90
Table 14 Mechanical properties and fiber diameter of precursor and carbonized sample.....	97
Table 15 Comparison of the commercial and experimental fibers as received precursor.....	99
Table 16 Comparison of the commercial and experimental fibers at the end of carbonization at 1200°C with commercial available carbon fibers.....	100

LIST OF FIGURES

Figure 1 Repeat unit of cellulose in rayon.....	1
Figure 2 Conversion of cellulose into carbon in the presence of hydrogen chloride.....	13
Figure 3 TGA curves of original and sulfuric acid-impregnated cellulose.....	15
Figure 4 Mass yield as weight fraction of starting cellulose at selected temperatures.....	15
Figure 5 Stylized representation of portions of neighboring cellulose chains, indicating (dashes lines) some of the hydrogen bonds that may stabilize the crystalline form of cellulose.....	16
Figure 6 Weight loss vs. temperature curve for cellulose heated in nitrogen.....	18
Figure 7 Generalized Broido-Shafizadeh mechanism.....	21
Figure 8 Banyasz model implying that the pyrolysis is the cellulose depolymerization by two pathways.....	21
Figure 9 Scheme of initiation of the cellulose auto-oxidation. It begins from the abstraction of hydrogen by oxygen at a very low degree of conversion. Either hydrogen peroxy or hydroxyl radicals affect subsequent abstraction of hydrogen.....	23
Figure 10 Reactions involved in the conversion of Rayon into carbon fibers.....	24
Figure 11 Scheme of transition of cellulose into graphite structure.....	27
Figure 12 Influence of degree of stretching in graphitization (2780-2870°C) on Young's modulus of the fiber.....	27
Figure 13 Model of longitudinal structure of carbon fiber.....	29
Figure 14 Model of transverse structure of PAN-based carbon fiber.....	30
Figure 15 Schematic of carbonization furnace.....	36
Figure 16 Temperature profile of the furnace at different temperature settings.....	37
Figure 17 Assembly for single fiber tensile test.....	43
Figure 18 X-ray patterns of the commercial rayon and experimental rayon.....	46
Figure 19 TGA curve of the commercial rayon from room temperature to 600°C in nitrogen.....	50
Figure 20 TGA curve of the experimental rayon from room temperature to 600°C in nitrogen.....	50

Figure 21 DSC curve of commercial rayon fibers from room temperature to 450°C in nitrogen.....	51
Figure 22 DSC curve of experimental rayon fibers from room temperature to 450°C in nitrogen.....	51
Figure 23 TGA curve of the commercial rayon fibers from room temperature to 600°C in air....	52
Figure 24 TGA curve of experimental rayon fibers from room temperature to 600°C in air.....	52
Figure 25 DSC curve of the commercial rayon from room temperature to 450°C in air.....	53
Figure 26 DSC curve of the experimental rayon from room temperature to 450°C in air.....	53
Figure 27 DSC curve of the as received commercial rayon precursor and the soaked precursor with phosphoric acid after drying at 110°C for 15 min.....	56
Figure 28 TGA curves of the precursor, the soaked precursor, and stabilized sample.....	57
Figure 29 SEM micrographs of the untreated and treated rayon fibers after pyrolysis at 2KX....	58
Figure 30 DSC curves of the samples after stabilization stage.....	62
Figure 31 DSC curves of selected sample after stabilization in air up to 380°C.....	63
Figure 32 TGA curves of selected samples after stabilization from room temperature to 1000°C.....	64
Figure 33 DSC curves of the untreated samples during heat treatment from 150°C to 380°C.....	67
Figure 34 DSC curves of the soaked rayon with phosphoric acid during heat treatment from 150°C to 380°C.....	68
Figure 35 The WAXD of soaked rayon during heat treatment from 150°C to 380°C.....	71
Figure 36 SEM micrographs of surface and cross-section of the treated commercial rayon at the end of pyrolysis.....	72
Figure 37 WAXD patterns of samples 6003 and 6005 with different applied tension (10g and 50g) during carbonization.....	74
Figure 38 TGA curves of the precursor, the soaked precursor, the stabilized sample, sample 6002 and sample 6003.....	77
Figure 39 The FTIR spectra of precursor, stabilized and carbonized samples.....	78
Figure 40 The WAXD of soaked sample during carbonization from 400C to 1200C in nitrogen.....	80

Figure 41 Elemental analysis results showing carbon and hydrogen content.....82

Figure 42 SEM micrographs of the surface and cross-section of the carbonized sample.....83

Figure 43 EDXA results of the commercial rayon precursor, the stabilized fibers to 380C and the carbonized fibers to 1200C respectively.....84

Figure 44 TGA curves of the precursor, the soaked precursor and the stabilized samples (502, 503 and 504) from room temperature to 1000°C in nitrogen.....88

Figure 45 DSC curves of the precursor, soaked precursor, and the stabilized samples (502, 503, 504) from room temperature to 450°C in nitrogen.....89

Figure 46 SEM micrographs of the surface and cross-section of the stabilized sample at 2KX....90

Figure 47 TGA curves of the precursor, soaked precursor, stabilized (502) and carbonized sample (506).....93

Figure 48 FTIR spectra of the experimental rayon (precursor, stabilized and carbonized samples).....94

Figure 49 The WAXD patterns of the experimental rayon (precursor, stabilized and carbonized).....95

Figure 50 Elemental analysis result showing carbon and hydrogen content.....95

Figure 51 SEM micrographs of surface (5KX) and cross-section (10KX) of the experimental rayon fiber at the end of carbonization.....96

Figure 52 EDXA results of the precursor, stabilized and carbonized samples respectively.....97

LIST OF ABBREVIATIONS

CF Carbon fiber

PAN Polyacrylonitrile

C-C Carbon-Carbon

C=O Carbon- Oxygen

FTIR Fourier Transform Infrared Spectroscopy

SEM Scanning Electron Microscopy

CHAPTER 1: INTRODUCTION

Considerable efforts have been made to develop rayon-based carbon fibers for years on a commercial scale. Aside rayon (or regenerated cellulose), PAN (Polyacrylonitrile) and pitch (petroleum and coal tar based) have been used as precursors in the commercial production of carbon fibers. Various other precursors ranging from natural materials such as lignin, wool, cotton, ramie, and jute to high performance highly crystalline aramid fibers such as Kevlar were also investigated. The primary requirement is a material that does not melt on pyrolysis in an inert atmosphere and gives sufficient carbon yield.

Rayon is produced from naturally occurring cellulose polymers (figure 1) and has excellent characteristics. It is manufactured in three types: viscose, cuprammonium, and saponified acetate [1, 2]. The viscose grade is usually used for carbon fiber production because of relatively few defects. Viscose rayon is a promising raw material because of its availability, low cost, non-melting character, low density, low metal ion content and the ease of production. These characteristics explain the high mechanical and physicochemical properties of the produced carbon fibers. The cellulose based carbon fibers present a network structure with high disorder, which gives the fiber a very low thermal conduction coefficient and the ability to be used in many applications [2].

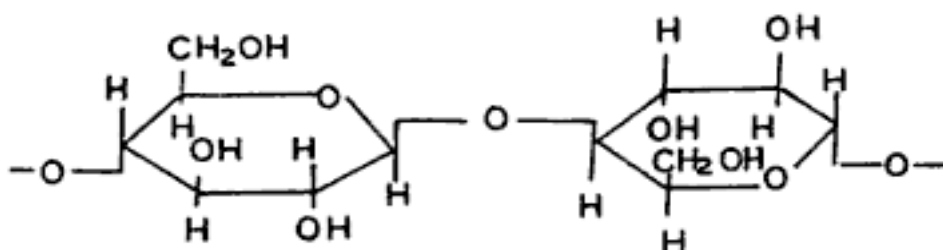


Figure 1 Repeat unit of cellulose in rayon [1].

The transition of rayon fibers to carbon fiber consist of oxidation in air at lower temperature (<300°C) also known as pyrolysis (thermal degradation); carbonization in an inert atmosphere, and graphitization in an inert environment at higher temperature up to 3000°C [3]. The typical sequence of production is as follows:

A. Stabilization. During pyrolysis of the cellulose fiber; dehydration, rearrangement, formation of carbonyl groups, evolution of carbon monoxide and carbon dioxide, and formation of carbonaceous residue occurs alongside the thermal scission of glycosidic bonds between the glycopyranose units of the cellulose. The scission produces oxygenated compounds that lead to maximum loss of the mass. Tars and coke residue are the main volatiles gaseous products formed during the thermal degradation [4]. By adding proper chemical such as impregnants or flame-retardants, one can moderate the pyrolysis mechanism by lowering the temperature range and subsequently improving the carbon yield by reducing the burning loss.

B. Carbonization. This step consists of heating the fibers between 600°C to 1300°C for a short period. This removes any non-carbon atoms from the atomic structure. At this stage, all chemical processes are completed, structural transformations take place, the coke becomes enriched with carbon, and set of fiber properties changes. The resulting fiber has tightly bonded crystalline structures with better alignment and orientation [5]. As the temperature rises, the structure of the residue becomes more complicated, in spite of simplification of the elemental composition. The effect is explained by the diversity of the transient forms of carbon and by various combinations of the bonds between the atoms of carbon.

C. Graphitization. It is the final stage of the production process. The carbonized fiber is subjected to high temperature treatment. Most of the process is energy consuming and adds to the cost of the material. Depending on their purpose and fields of application, either carbonized or graphitized carbon fiber can be the end product. The main phenomena are structural transformations and concurrent changes in the properties of the fibers. The most important processes occurring at this stage are: further aromatization of carbon, growth of the size of crystallites and of graphite like ribbons, and perfection of the orientation of the ribbons along the fiber axis [4].

It is essential to understand the effect of catalysts or impregnants as well as the effect of time, temperature, tension, protective medias, during both pyrolysis and carbonization stages. Studies have shown that the final product in the preparation of rayon-based carbon fibers is influenced to an extent by each of these variables [6, 7]. It includes the physicochemical process and changes in the properties of the product. It also leads to an improvement of the overall quality of the fibers. Lewin et al. [8] showed that most Lewis acids could be used as impregnants in rayon to carbon fiber conversion. The impregnants also serve as flame-retardants for cellulosic materials. In general, inorganic phosphates and sulfates with nitrogen have better flame retardant effects; however, which ones work best during conversion of rayon-based carbon fibers has not been reported in literature. One can improve the produced fiber by stretching and maintaining tension during carbonization and graphitization by promoting axial orientation of the carbon layers [9].

Rayon precursor can be stabilized to avoid extensive volatilization and or partial melting of the polymer. The stabilized fiber is expected to have high carbon yield and also have the same filament-like morphology as the precursor. A preferential orientation of the layer parallel to the fiber axis and a development of the graphitic basal planes by removal of their microstructural defects are required for the preparation of high modulus carbon fibers [10]. In the literature, carbon fibers are classified based on tensile modulus. The low modulus has a tensile modulus below 240 GPa. The ultrahigh modulus carbon fibers have a tensile modulus of 500 to 1000 GPa. As a comparison, steel has a tensile modulus of about 200 GPa and the strongest carbon fiber is about five times stronger than steel [11].

The aim of the present research was to investigate the feasibility of producing rayon-based carbon fibers, especially looking at a domestically produced rayon fiber, and try to optimize the production process to a certain extent. The fibers were impregnated with phosphoric acid and its effect on dehydration and decomposition of rayon was studied. The specific objectives were to evaluate the stabilization stage with respect to changes in the structure and properties of the fiber. Also the processing conditions were optimized for efficient production. Various test methods were used throughout the investigation to characterize the fibers. This investigation

was conducted as a comparison with respect to a commercial rayon fiber. The study clearly showed that by using appropriate processing conditions, it is possible to produce good quality carbon fibers from an experimental rayon precursor produced in the US.

CHAPTER 2: LITERATURE REVIEW

2.1 Carbon fibers through the years

Carbon fibers are high strength materials that have attracted worldwide attention and hold great promise. The term “Carbon fiber” is defined as a material that has been heat treated at high temperature (1000- 3000°C) and has markedly different properties and structure. The carbon fibers contain 92-99.99 % carbon [12].

Nearly a century ago, carbon fibers were produced by thermal decomposition of natural fibers like bamboo or cotton. Thomas Edison was the first to develop and use the early CF as filaments for incandescent lamps in 1880 [12]. These early carbon fibers were very weak and fragile because of the presence of pores, and were abandoned quickly. In 1950, carbon fiber development took a new direction when mechanically weak fibers were prepared by rayon pyrolysis. These rayon-based carbon fibers were used for thermal insulation but they could not compete with the glass fibers during that period.

Bacon [13] patented a continuous process using viscose rayon fibers to produce high strength, high modulus carbon fibers. The experiments resulted in commercial production of continuous lengths of CF having tensile strength between 690 and 1030 MPa and tensile modulus of elasticity values in the order of 40 MPa. Union Carbide later used stress graphitization to produce strong rayon-based CF in 1959 [14, 15]. The fibers produced possessed tensile strength between 330 and 900 MPa. The stress graphitization process is a solid state transformation of non-graphitic carbon into graphite by heat treatment combined with application of mechanical stress, resulting in a defined degree of graphitization being obtained at a lower temperature and /or after shorter time of heat treatment than in the absence of applied stress.

Concurrently, the conversion of polyacrylonitrile (PAN) fibers into high modulus carbon fibers was investigated. Shindo [16] showed the variation in the tensile strength and modulus of PAN based CF with heat treatment temperature and also investigated their electrical properties. Watt and his colleagues at the Royal Aircraft Establishment in England developed a commercial

process for PAN based fibers [17]. In 1966, Courttelle introduced a specially prepared PAN fiber that could be oxidized at temperatures around 200°C under tension, while exothermic oxidation reactions were avoided. Subsequent carbonization at 1000°C resulted in CF with tensile modulus in the range 155 to 190 GPa, and the value could be increased to 350 - 420 GPa after heat treatment at 2500°C [18]. Since 1966, numerous patents on PAN-based carbon fibers were granted [19-21] .

The quest for lower processing cost led to the possibility of pitch as precursors of carbon fibers. Otani [22] used polyvinyl chloride (PVC) pitch as a raw material in 1965. Kureka Chemical Company built a commercial plant with production capacity of 200 tons per year of carbon fiber from petroleum pitch [23]. The company was one of the leading producer of Pitch based CF in the world. Improvements to early pitch based CF were reported by Hawthorne in 1970 and 1971 [24, 25]. By stretching the fibers during the initial stage of carbonization at temperatures above 2500°C, a high degree of basal plane preferred orientation could be induced, and also tensile strength as high as 2585 MPa and tensile moduli of elasticity in excess of 480 GPa could be attained. In 1973, mesophase state liquid was developed from pitch and spun into precursor fibers [26]. These fibers were transformed to CF by oxidizing and subsequent carbonization at 1000 - 3000°C leading to fibers with high degree of preferred orientation because the liquid crystalline state was formed prior to spinning.

Studies and innovations in CF have increased over the years. Researchers are developing new methods to improve overall quality of the fiber and make it available for suitable applications while relying on early findings [27-31]. Despite the early developments in rayon based CF, it is carbon fibers from PAN and mesophase pitch (MP) precursors that now dominate the market. Today more than half of the commercially marketed carbon fibers are made from PAN. PAN based carbon fibers possess higher strength, modulus and failure strain with high yield compared to fibers made from pitch or rayon [32]. Many consider pitch based CF for special applications because they present properties not readily obtained with PAN based CF such as good thermal and electrical properties [33]. In the last half-century, U.S, Asian and European companies have successfully manufactured and commercialized PAN-based and pitch-based

carbon fibers. Rayon-based carbon fibers became almost forgotten. CF industry has recently experienced a significant resurgence due to increasing demand for the technology in wide range of applications after years of prosperity followed by rapid decrease in interest.

2.2 Solution Process for of Rayon Fibers

Rayon is a manufactured fiber composed of cellulose obtained mainly from plants (cotton linters and pulps). Rayon is called a semi-synthetic fiber because it has a long polymer chain structure that is supplied by nature and is only modified and degraded in part by chemical process[1]. The manufacture of rayon fibers involves basic principles. During production, pure cellulose is dissolved chemically and then regenerated in acid solution. The dissolved cellulose is passed through a spinneret into a bath of solution that regenerates pure cellulose fibers. Literature suggests different methods to convert cellulose to soluble form and then regenerate it[1, 34]. Rayon fibers are named according to the production methods: viscose, cuprammonium, and saponification.

The viscose method is the most used, and is also referred to as the Xanthate process. The process consists of treating the raw material with relatively high α -cellulose content, with sodium hydroxide and carbon bisulfate to form a metastable liquid that can be shaped into long-fiber product by extrusion through spinnerets. A wide range of properties can be obtained in viscose rayon. It is due to the versatility of the process. The properties are affected by the numerous changes that can be made during the formation of the viscose solution or spinning. The production of viscose rayon presents technical difficulties; therefore new novel approaches were developed. Stepanik [35] demonstrated that the electron treatment of pulps could replace the ageing step in conventional viscose process. In the Electron treatment process, radical-mediated reactions are initiated and lead to cleavage of cellulose chains, reducing the DP.

Cuprammonium rayon is made by adding drops of aqueous ammonia to a saturated copper (II) sulfate solution to form the copper (II) hydroxides precipitates. Summerlin and Ealy [36]

suggested the method. Kauffman [1], later developed a new method by using 1M sodium hydroxide instead of concentrated aqueous ammonia to make copper (II) hydroxide and 1M copper (II) sulfate as a source of copper (II) ion. The ammonia solution of copper (II) hydroxide is usually referred to as Schweizer's reagent.

Saponified cellulose acetate is another type of rayon based on the acetylation of cellulose by acetic anhydride. Paul Schutzenberger [37] was the first to develop this method. In the process of making cellulose acetate, only three hydroxyl groups per cellulose unit can be esterified, and the existence of higher acetate is attributed to degradation of the cellulose. Unlike other types of rayon, acetate fiber is not insoluble regenerated cellulose but is soluble in acetone, methylene chloride or chloroform.

Rayon fibers are attractive candidates for carbon fiber production because they originated from a renewable resource, cellulose, which is nature's most abundant polymer. Rayon fibers are more environmentally friendly than completely synthetic fibers with regards to the total energy required for their production.

2.3 Thermal Processes of Carbon Fibers

According to the literature, carbon fibers are produced by thermal treatment of a large variety of precursors (PAN, pitch, rayon) [3, 38]. Polymeric materials such as phenolic resins have also been investigated as precursors [38]. The conversion of a precursor into a high modulus CF generally can be subdivided in three main stages: stabilization of the precursor, longitudinal orientation, and development of the crystalline ordering. Depending on the nature of the precursor, the orientation process can take place simultaneously with the stabilization or with the graphitization step

2.3.1 PAN - based Carbon Fibers

PAN- based carbon fibers represent by far the most important carbon fibers used today [32]. The PAN-based carbon fibers offer a broad range of excellent structural properties; ready compatibility with matrix system, and well established manufacturing capabilities and positions in expanding application. Production of PAN based carbon fiber consists of three main stages:

- 1- Oxidative stabilization under tension
- 2- Carbonization under tension
- 3- Graphitization under tension

The oxidation stabilization is carried out in the range of 200 - 300°C. The key factor in producing good carbon fibers from PAN is the cyclization of the pendant nitrile groups and the incorporation of oxygen to yield oxidized ladder polymer parallel to the fiber axis [39]. The stabilization step converts the precursor to a thermally stable structure capable of withstanding high temperature processing at high rates with good yield.

The stabilization chemistry of PAN is complex. It is clear that in the presence of oxygen, chain scission, crosslinking, dehydrogenation and cyclization take place. To preserve and improve the molecular orientation, fiber stress must be maintained during the stabilization process by limiting shrinkage to less than 15%. Stabilization is the most time consuming step in the production of CF. Attempts have been to modify the conventional stabilization procedures to reduce the time [39-41]. It has been found that the stabilization rate is enhanced by modifying the chemical composition of the precursor fiber either by addition of comonomer [42] or additive or by impregnation with certain chemicals [43-45].

After stabilizing the stretched structure of the molecular chains, the tows of PAN fibers are subjected to thermal pyrolysis in an inert atmosphere. Most of the time nitrogen or argon is used as inert gas. Mainly two types of reactions occur: removal of the heteroatoms in the ladder polymer and development of the graphitic structure. The principal scission products released in the temperature range of 400-1000°C are HCN, NH₃, and N₂. Depending on the extent of preoxidation, variable amount of H₂O, CO, and CO₂ resulting from the attack of the

carbon backbone are also formed. In addition, small quantities of H₂ and CH₄ are released during the carbonization process. In the early stage of carbonization, the hydroxyl groups present in the oxidized PAN fibers start crosslinking with condensation reactions, which help in organization and coalescence of the cyclized sections. The cyclized structures undergo dehydrogenation and begin to link up in the lateral direction, producing graphite like structure consisting of 3 hexagons in the lateral direction and bounded by nitrogen [46, 47].

The mechanical properties of the final CF depend on the rate of heating and the final heat treatment temperature during carbonization, although the final heat treatment temperature during stabilization remains the properties determining step. The carbonized fibers have graphite-like structure. The overall properties of the carbonized fiber can be improved with heat treatment at higher temperature. Further heat treatment at even higher than 2500°C improves the ordering and orientation of crystallites in the direction of the fiber axis. This results in better mechanical properties of the final carbon fiber. It has been demonstrated that Young's modulus of the PAN based CF is related directly to the final heat treatment temperature during graphitization [32].

2.3.2 Pitch - based Carbon Fibers

Pitch is readily available in large quantities and is attractive as a precursor for large-scale carbon fiber manufacture because of its significantly lower cost compared to other precursor fibers. There are other advantages that make pitch based precursors an attractive alternative like less energy required to convert an essentially aromatic graphitizing material, and smaller percentage of hydrogen, nitrogen and other non-carbon elements [48, 49]. The carbon fiber fabrication from pitch generally consists of the following:

- 1- Pitch preparation
- 2- Spinning and drawing
- 3- Oxidative treatment
- 4- Carbonization, followed by an optimal step graphitization.

Step 1 involves an adjustment in the molecular weight, viscosity, and crystal orientation for spinning and further heating. Spinning and drawing convert the pitch into filaments, with some alignment in the crystallites to achieve the directional characteristics.

Coal or petroleum based pitches are isotropic, and were used to produce the early pitch based CF [50]. The physical properties of these early fibers were poor and could be substantially enhanced by hot stretching at high temperatures, but the procedure was difficult and costly. Pitch, while still in a liquid state could form an intermediate, highly oriented, optically anisotropic liquid crystal phase known as mesophase when heated for a certain period of time above 350°C.

The oxidation process is slow for the isotropic pitch to ensure stabilization of the fiber by crosslinking and rendering it infusible. However upon carbonization, relaxation of the aromatic molecules takes place, which gives CF with no significant preferred orientation [48]. Hence, as with rayon-based carbon fiber, stress is found to be advantageous during the heat treatment (150 - 200°C) to obtain an increase of the elastic modulus. The length of oxidation step and the resulting low quality CF with no strain graphitization make the isotropic pitch less attractive. Mesophase pitch precursors are usually oxidized at temperatures around 300°C for periods up to two hours. Crosslinking reactions take place between the aromatic units, forming layers, which are considerably greater in extent than those produced at a similar stage with PAN. The mesophase pitch based precursor fibers are essentially graphitizable materials. The spinning process has to be perfectly controlled to obtain fiber of high quality. The mesophase pitch does not require tension during stabilization or graphitization, in contrast to rayon and PAN precursors.

2.3.3 Rayon - based Carbon Fibers

Thermally produced rayon-based carbon fibers acquired commercial meaning in late 1950 and were dominant during the 1960s and early 1970s. The production requires carbonization of rayon fiber into high modulus carbon filaments. The early low strength fibers were followed by

a substantially improved high strength, high modulus yarn [51, 52], but at much higher processing cost. The steps required to convert rayon fibers into high modulus carbon fiber are:

- 1- Stabilization in air (200-350°C)
- 2- Carbonization in an inert environment at (1000 - 2000°C)
- 3- Graphitization in an inert atmosphere (with or without strain) up to 3000°C

In the first stage, extensive decomposition occurs and 50 – 60% of the initial precursor weight is lost. The low temperature oxidation is carried out in the presence of air, chlorine, HCl, and ZnCl₂ to improve yield and inhibit tar formation [47]. Pyrolysis studies in HCl vapor using weight loss measurements, X-ray diffraction, and IR analysis of the residual species showed that pyrolysis started as early as 110°C and the weight of the fiber decreased in a step manner mainly through the elimination of water [50]. Figure 2 shows the conversion of cellulose into carbon in the presence of hydrogen chloride. The ultimate yield of the fiber corresponds to a yield of five carbon atoms from each cellulose ring unit. Chain fragmentation eliminates any orientation present in the precursor, necessitating application of stress in later steps to improve the properties; the resulting product is an amorphous char. In the carbonization step, there is further weight loss with the early development of a carbon layer structure. It was found that high temperature increases the size and perfection of the layers. Stretch graphitization process can also be used to obtain fibers with modulus as high as 620 GPa and tensile strength of 3.1 GPa [13]. This Hot stretching process however was inefficient and very expensive.

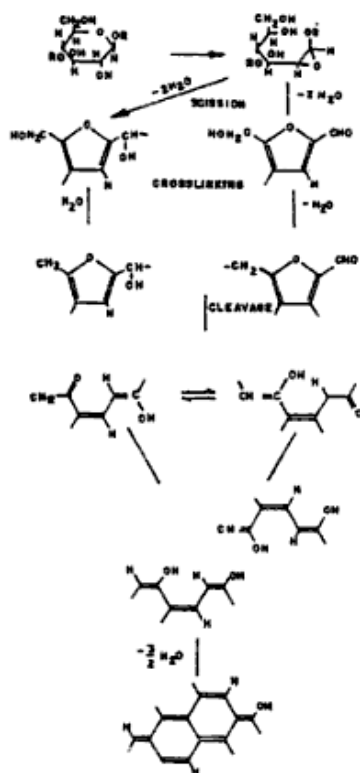


Figure 2 Conversion of cellulose into carbon in the presence of hydrogen chloride [50].

2.4 Pretreatment effects on pyrolysis of cellulose

Thermal decomposition of cellulose has been studied for a longtime. The final product is determined by various factors including substrate type, environment, heating conditions, and catalysis. The role of catalysis is important for the production of carbon fibers from rayon. Various inorganic compounds have been studied in regard of their effect on cellulose pyrolysis. Bryne [53] evaluated the thermal decomposition of cotton fabric containing different flame-retardants (bromoform, phosphorous compounds, urea, mixture of borax and boric acid). The results showed that not only the nature, but also the quantity of the flame retardant affects the composition of the pyrolysis products. Shafizadeh [54] observed that 5% Phosphoric acid increases the yield of levoglucose up to 11% at high heating rate.

It appears that flame-retardants favor the decomposition pathway of cellulose by shifting the maximum rate and onset of dehydration into the region of lower temperature and consequently increase the amount of H₂O, CO₂ and char formed. The increase in the amount of char residues formed acts as a thermal barrier reducing heat transfer to the interior, and also obstructing the outward flow of combustive gases and hence, reducing the extent of cellulose decomposition. Flame-retardants also stabilize the reaction intermediates and reduce the formation of secondary char or coke. These observations are consistent with the results of Qingfeng [55] in his study of the effects of three flame-retardants on a wood-derived rayon fiber thermal decomposition in an inert atmosphere using thermogravimetry-mass spectrometry. Pappa [56] used the chemometric methods to study the effects of (NH₄)₂SO₄ and (NH₄)₂HPO₄ on cellulose pyrolysis. Two observations were made: a decrease in the evolution of flammable products and an increase in the evolution of lower flammability products like phenolic compounds and acetic acid. The findings were similar to the observations using quantitative thermogravimetry-mass spectrometric techniques by Statheropoulos [57].

Addition of dehydrating agents, such as zinc chloride, sulfuric acid and phosphoric acid, were also reported to influence pyrolysis of cellulose. Kim [58] studied carbonization of cellulose with sulfuric acid impregnation up to 800°C. He observed that the mass yield of carbon after 800°C

treatment in nitrogen increased to 2-3 times by addition of small amounts of sulfuric acid (figure 3 and 4).

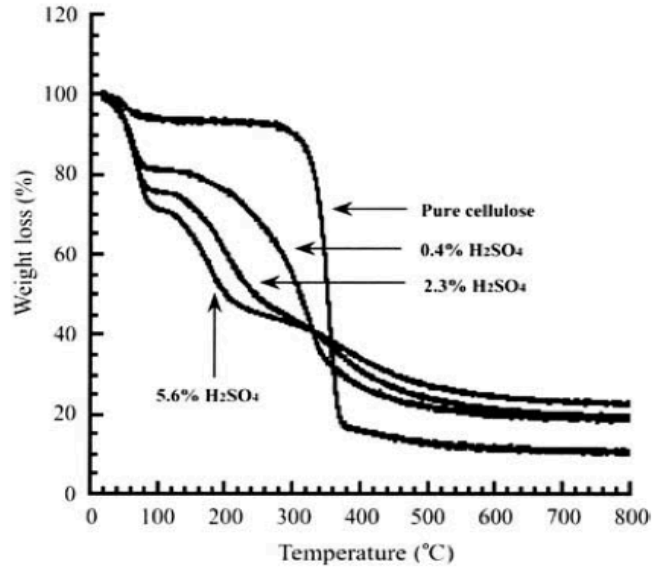


Figure 3 TGA curves of original and sulfuric acid-impregnated cellulose [58].

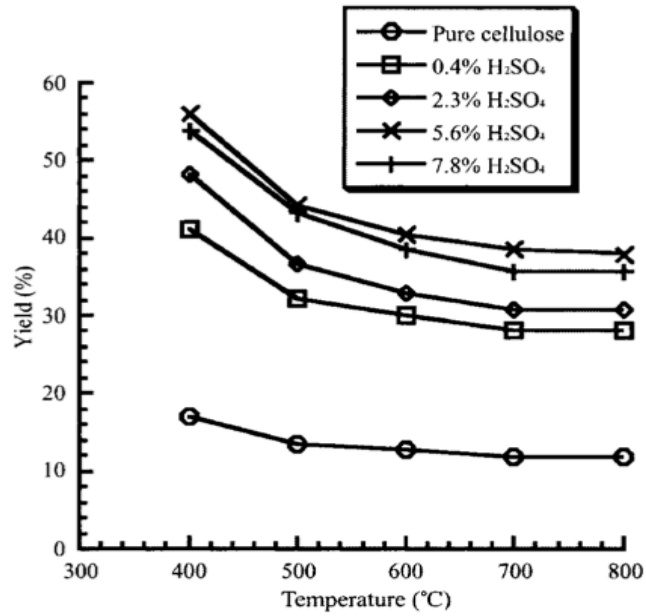


Figure 4 Mass yield as weight fraction of starting cellulose at selected temperatures [58].

2.5 Chemistry and kinetics of cellulose thermal degradation

Cellulose is a complex heterocyclic polymer containing thermolabile hydroxyl groups and acetal bonds between the units (Figure 5). Cellulose has crystalline and amorphous zones. The amorphous zone is more active than the crystalline zone, adding complexities in thermal decomposition of cellulose. The elaboration of a process for producing carbon fiber from cellulosic materials gave rise to the study of the mechanism of pyrolysis of cellulose [54, 59]. The mechanism is a complicated process involving multiphase reactions, complex chemical pathway, highly unstable intermediates, and heat and mass transfer effects. There are some major unresolved issues regarding the mechanism and chemistry of cellulose decomposition. Fortunately, knowledge of both low and high temperature degradation chemistry has not changed greatly over the years.

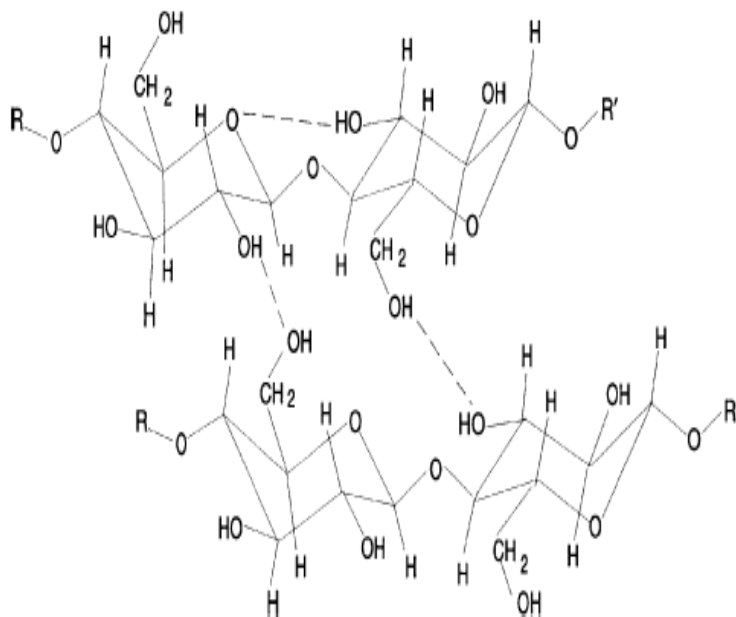


Figure 5 Stylized representation of portions of neighboring cellulose chains, indicating (dashes lines) some of the hydrogen bonds that may stabilize the crystalline form of cellulose [60].

For cellulose, high degree of degradation is characteristic, which proceeds within a narrow range of temperatures. Figure 6 shows graphical display of the rate of weight loss of cellulose vs. temperature, as measured by TGA. Three regions are clearly defined on the curves: the initial region (< 120°C) features a small loss of the mass; second region (temperature of 300 to 350°C) is characterized by an intensive loss of the mass; the third region (> 350°C) features a deceleration of the mass again. The maximum rate of loss of the mass corresponds approximately to 250°C. Within 200 to 300°C the loss of the mass reaches 50% and the carbon content in the residue increases from 44.5% to 65-70%, the DP drops from 350 down to 200. It is believed that cellulose undergoes a high degree of degradation at this stage. At temperatures above 300 - 350°C considerable contribution is made by reactions leading to aromatization of carbon and to the commencement of formation of graphite-like structure.

Tang and Bacon used IR spectroscopy to investigate the process of pyrolysis and concluded that four stages are required [47]:

- 1- Desorption of chemically bonded water (up to 150°C)
- 2- Dehydration of cellulose (150 - 240°C)
- 3- Destruction of the 1,4-glycosidic bond, of the ring bonds $-C-O-C-$, of some part of the $C-C$ bonds by the radical mechanism)
- 4- Aromatization of carbon (above 400°C)

Early findings summarized that low temperature delays the initial process of pyrolysis, corresponding to a reduction in the degree of polymerization and the formation of anhydrocellulose or active cellulose; and high temperature hydrolysis of cellulose is expressed by two competitive degradation reactions, first essentially to char and gas, the second to tars mainly levoglucosan.

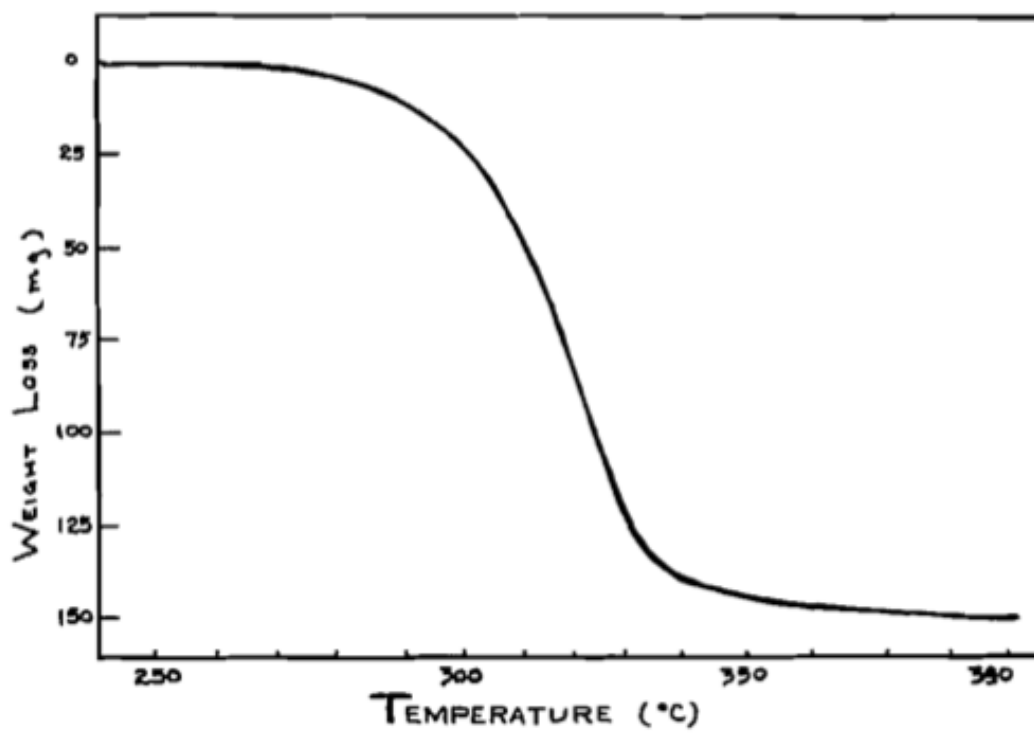


Figure 6 Weight loss vs. temperature curve for cellulose heated in nitrogen [61]

As a result of the findings summarized above, two major processes are recognized to be concurrently occurring during the thermal decomposition of cellulose: an initial reaction and a propagation reaction with activation energies of 165 and 112 KJ mol⁻¹, respectively. The competitive mechanism has been disclosed in the famous publication of Kilzer and Broido [62, 63]. The mechanism was based on the notion of anhydrocellulose that is formed due to crosslinking caused, in term, by the dehydration of cellulose. According to their assumption, the anhydrocellulose is an intermediate for the subsequent charring and the formation of light gases. Both processes have high activation energies, K_{tar} and K_{gas} (Figure 7). Mamleev provided important insights into the competitive mechanism by evaluating the kinetic constants under conditions usual for thermogravimetry and concluded that tar formation is the dominant pathway during thermal decomposition of cellulose and the process is controlled by the reaction of transglycosylation with $K_{tar} \sim 190 - 200$ KJ/mol [64].

In 1970 Shafizadeh and co-workers [65] developed a three step kinetics model in which an initiation step forms "active cellulose", which subsequently decomposes by two competitive first order reactions, one yielding volatiles and the other forming char gas. It was later found that this empirical model failed to describe the decomposition mechanism in detail despite the fact that it was widely accepted. The kinetics of slow pyrolysis is very complicated because of charring of cellulose. The pathway of charring cannot coincide with the pathway of gas formation at least by reason of one experimental fact; namely, a yield of light gases grows with increasing heating rate, while the Broido-Shafizadeh model predicts a decrease of this yield together with a yield of char. The gas formation and charring are certainly competitive processes. On the basis of the general rule, the char formation should have lower activation energy in comparison to that of the fragmentation. Indeed, charring is caused by dehydration, while fragmentation occurs with a scission of C-C bonds.

In the recent works, the notion of anhydrocellulose is excluded and solely two competitive reaction channels explain the decomposition. The first ascribed to the formation of tars (mainly levoglucosan) and chars, the other to the light gases. Following this approach, Piskorz [66] confirmed the formation of anhydrocellulose but the formation of light gases is considered not

directly to be related to the low temperature step or anhydrocellulose. Similarly, Banyasz [67] fully excluded the notion of anhydrocellulose and explained the experimental facts solely by cellulose depolymerization passing through two reaction channels (Figure 8). This hinders an explanation of the effects of preheating at low temperatures. However one can assume that the preheating at low temperatures below the boiling point of levoglucosan results in solidification of isolated tar.

Other kinetic schemes have been proposed, mainly first-order reactions [68, 69], to give better representation of the experimental cellulose pyrolysis. Alves and Figueiredo observed a decrease in the rate of conversion of cellulose during pyrolysis. The decrease could be explained by the strong endothermic heat demand during reaction, which could cool the sample and slow the reaction rate. They attributed their observation to three consecutive, first order reactions with almost identical activation energies [70]. Agarwal [69] suggested that cleaving of the pyranose ring by 1-5 scissions of the hemiacetal linkage leads to char formation and gas formation competitively, and the breaking of the 1-4 glucosidic bonds leads to tar and volatile formation. However, the C1-O-C5 linkage is known to be quite stable while it is part of the full acetal group that includes the glucosidic linkage, but very labile in reduction sugars. This fact would indicate that 1-5 scissions take place more easily at reducing termini. Since reducing termini are produced by random glycosidic hydrolysis, it is easy to conclude that char formation may be promoted by the presence of water. However those kinetic models have largely simplified the complexity of primary and secondary reactions during cellulose pyrolysis.

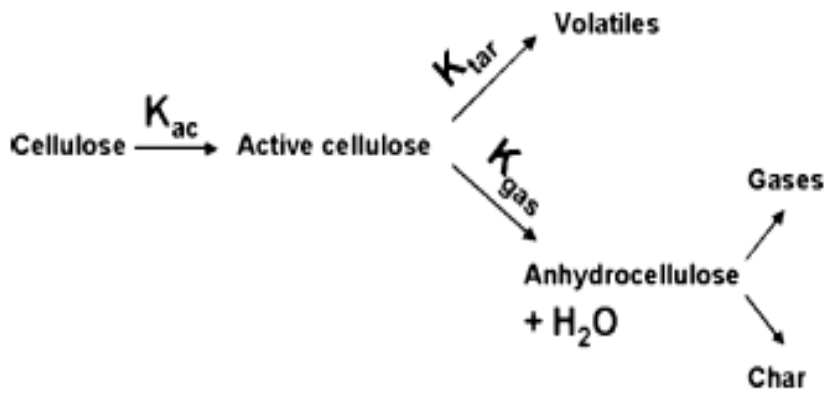


Figure 7 Generalized Broido-Shafizadeh mechanism [62, 65].

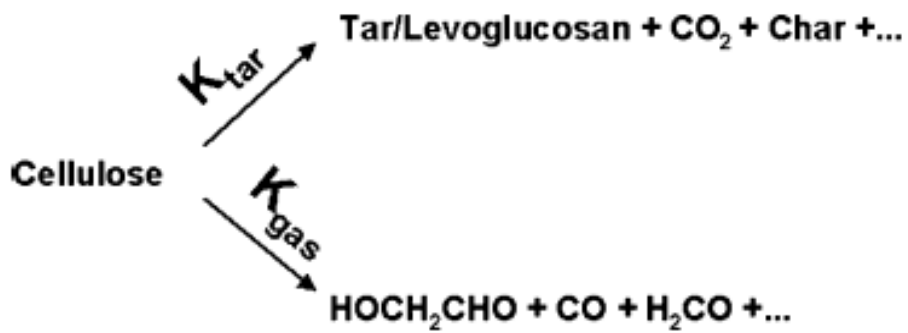


Figure 8 Banyasz model implying that the pyrolysis is the cellulose depolymerization by two pathways [67].

According to Zhbakov [71], the formation of levoglucosan is associated with closure of the ring between C1 and C6, therefore the course of reactions is conditioned by different conformation of the hydroxyl groups of the elementary units and by its change under the action of heat. Thermal depolymerization to levoglucosan is thought to occur by direct intra-chain heterolysis scission of glucosidic linkage with formation of 1,6 epoxide through the resonance stabilized glucosyl cation. In a moist environment, the –OH group of water would be a competing nucleophile that can intercept the electron deficient site on C, and in fact the carbonium ion is known to be involved in glycosidic hydrolysis equilibrium [72].

Heating rate in cellulose pyrolysis has been shown to have an effect on the product distribution, but the aspect has been poorly understood. It is generally accepted that pyrolysis chemistry and thermal transfer resistance are strongly influenced by heating rates. According to a review by Suuberg [73], diverse kinetic parameters are described by various groups based on different heating rates. In general, the higher the heating rate, the lower the activation energy for cellulose pyrolysis. This effect has been mostly attributed to heat transfer limitations. Alongside the heating rate, structure influences the thermal decomposition of cellulose. To elucidate the role of the structure of cellulose in the process of its pyrolysis, the degree of crystallinity, the size and structures of crystallites, and DP were discussed intensively by researchers [64, 74-78].

As discussed earlier, rayon is a cellulosic material and is expected to follow the similar pathway of cellulose degradation presented above. Carbon fiber yield and the processing rate can be markedly enhanced by performing the low temperature pyrolysis of rayon in the presence of reactive atmospheres, such as air or oxygen, chlorine, and HCl vapor. The oxidative decomposition of cellulose in air includes the mechanism of auto-oxidation [79]. For general considerations, the initial step of oxidation is the abstraction of hydrogen from organic molecules by oxygen. According to Shafizadeh and Bradbury, the positions 1 and 4 are most vulnerable for the oxidation (figure 9) [65], although other positions are believed to be able to react with oxygen as well. The primary formation of the radicals subsequently leads either to the formation of peroxides or the β -scission. The latter, in turn, can cause either the dehydration or depolymerization of cellulose. Both reactions should be fast in comparison to

the reaction of the generation of radicals. During thermal decomposition of cellulose, It is believed that the weight loss of up to 200°C is due exclusively to the volatilization of water. The possible reaction scheme for the various stages of the conversion of rayon into carbon fibers is reproduced in figure 10.

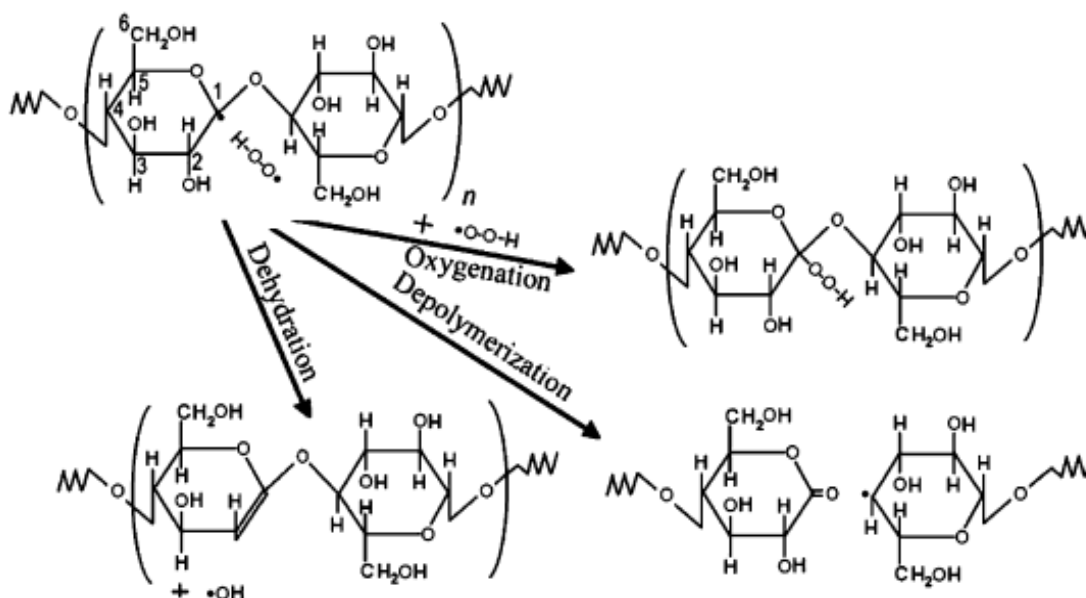


Figure 9 Scheme of initiation of the cellulose auto-oxidation. It begins from the abstraction of hydrogen by oxygen at a very low degree of conversion. Subsequent abstraction of hydrogen is effected by either hydrogen peroxy or hydroxyl radicals [64].

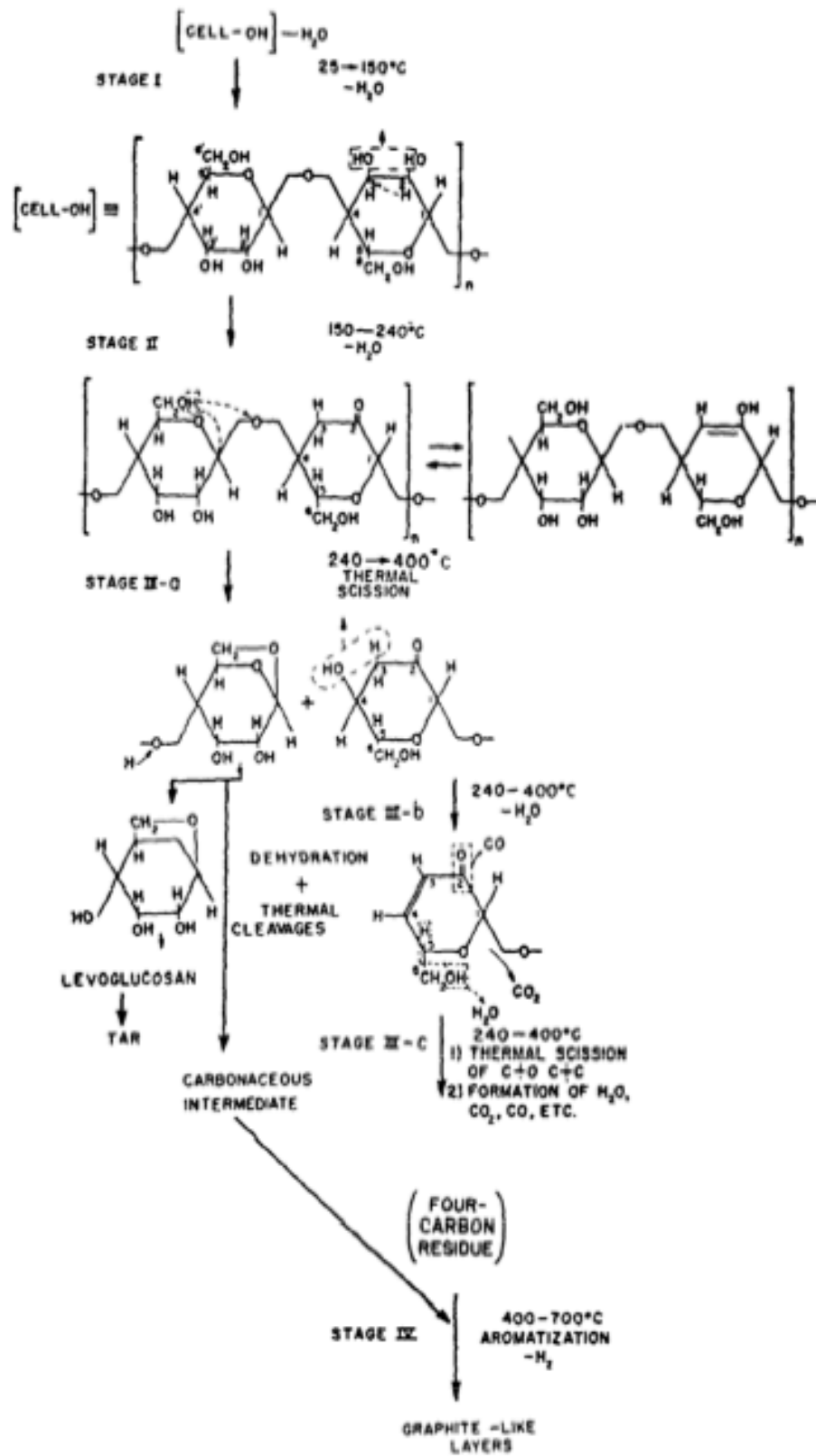


Figure 10 Reactions involved in the conversion of Rayon into carbon fibers [80].

2.6 High temperature treatment of cellulose

Complicated chemical and physical transformations occur during high temperature treatment of cellulosic materials. The high temperature treatment consists of carbonization (400°C to 1500°C), and later graphitization up to 2500°C. The main observation is an increase of carbon content and a decrease of the content of hydrogen. It is clearly established that basic microstructures of carbon are formed at lower temperature but as the temperature rises, more microcrystalline structures are gradually formed leading to an increase of the degree of orientation. High temperature treatment is usually conducted in vacuum or inert atmosphere (N₂, Ar).

Detailed descriptions of the chemical reactions occurring during high temperature treatment are not available in existing literatures but some researchers concluded that these three complex reactions occurred:

- 1- The rearrangement and aromatization of carbon atoms
- 2- Polyrecombination reactions that lead to the origination of networks
- 3- Formation of polymeric form of carbon.

Alongside the chemical reactions, physical changes also occur and include shrinkage and recrystallization. The aromatic atoms networks grow in the longitudinal and transversal direction with the decrease of crosslinking between aliphatic carbons. Physicochemical transformations of the structure lead to an increase in the strength of the fiber. Many works correlated the formation of the aromatic structure and properties of the carbon fibers. Strehlow [53] studied the axial and diameter shrinkage of rayon fibers as a function of carbonization temperatures. The results are correlated with earlier theories relating to the mechanism of cellulose pyrolysis. The appearance of the fibers observed with a polarized light microscope was found to permit useful distinction between various stages of decomposition.

In order to understand the transition of cellulose structure into graphite structure, many attempts were made. Davidson [4] used a geometric approach to develop a scheme of

transition by assuming that as the temperature increases, the chains become closer and their interaction takes place, with the formation of polycyclic rings (figure 11).

Stretching of fibers at carbonization and graphitization stages results in attaining considerable improvements in the structure and mechanical properties of carbon fibers. Figure 12 shows the correlation between the degree of stretching and Young's modulus. As the degree of stretching is increased, Young's modulus increases. The effect of stretching is explained by the resulting high degree of orientation, as the ribbons tend to orient along the axis of the fibers. Union Carbide Co. was the first to develop stretch graphitization with success.

The addition of catalysis, such as flame retardant not only influences the pyrolysis of cellulose but also plays a major role during the carbonization stage. The results are reported to be similar during the stabilization and carbonization stages. The addition leads to increase of carbon content.

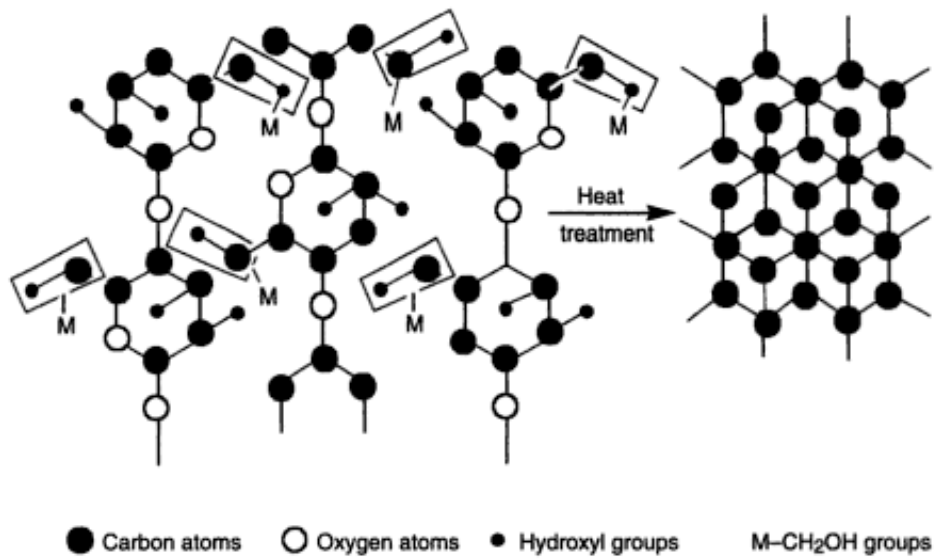


Figure 11 Scheme of transition of cellulose into graphite structure [4].

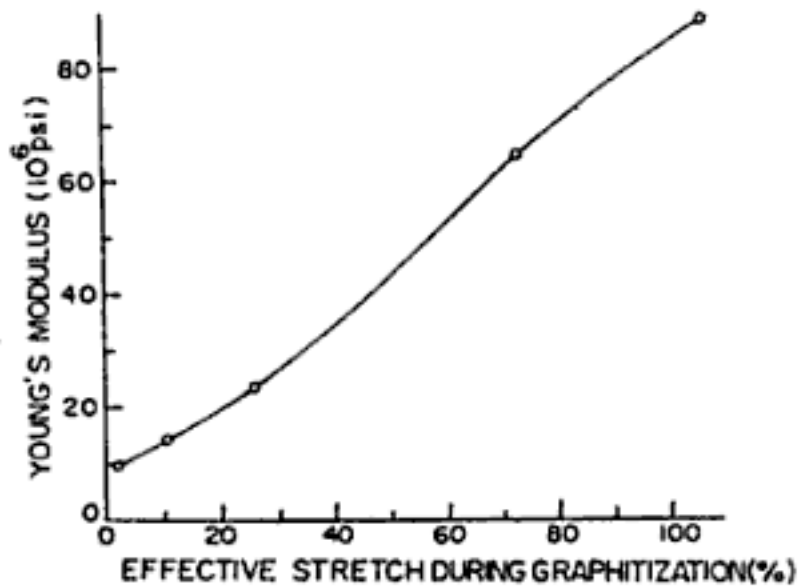


Figure 12 Influence of degree of stretching in graphitization (2780-2870° C) on Young's modulus of the fiber[53].

2.7 Properties and structure of Carbon Fibers

The word carbon came from Latin “carbo”, which means charcoal and was proposed by Lavoisier in 1798 [81]. Graphite and diamond are different form of carbon. Elemental carbon in its chemical allotropes of graphite and diamond occurs in great variety of species, such as carbon fibers, and it has been developed as a structural and functional material for a large number of highly specialized applications [3, 82, 83]. Properties of carbon fibers strongly depend on the structure. The processing of the fibers, particularly the heat treatment temperature and the ease of graphitization of the CF precursor affect the structure.

Study and understanding of CF structure have been achieved by means of indirect technique mainly X-ray scattering and electron microscopy [84-86]. Depending upon the precursor used to make the fiber, CF may be turbostratic or graphite, or have a hybrid structure with both graphite and turbostratic parts present [87, 88]. Transmission Electron Microscopy (TEM) studies by researchers revealed a fibrillar structure in CF. The model is more established in rayon based carbon fibers, but it was shown that whatever the precursor, all carbon filaments basically exhibit the same type of microstructure. Later it was found that the PAN-based fibers are essentially non- fibrillar. Different models were developed to exemplify carbon fiber structure because it is difficult to get an idea of the exact structure of individual carbon fibers. The lattice-fringe image of transverse sections reveals a very complex structure. The layer planes are essentially parallel to the superficial and region close to it. Meantime, many layer planes are folded through angles of up to 180° in a “hairpin” fashion, so that regions with layer planes at right angles to the surface are accessible if the outermost layers are removed [89]. Analysis of both the transversal and the longitudinal (Figure 13) sections led to the most appropriate schematic of features of microstructure in high modulus PAN-based CF (figure 14). The model shows skin-core heterogeneity. The formation of a skin is probably the result of layer plane ordering, which occurs as the heat treatment temperature is increased; the fiber surface presents a constraint on the number of possible orientations of surface crystallites.

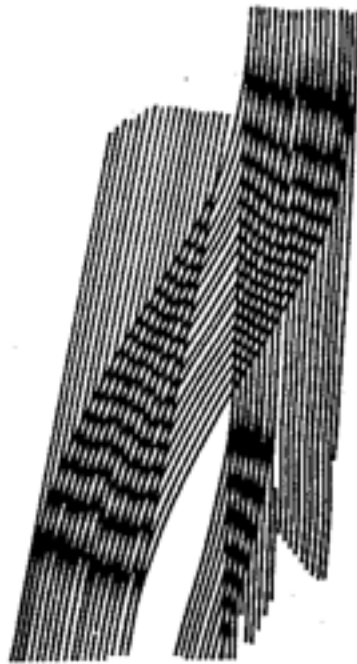


Figure 13 Model of longitudinal structure of carbon fiber [90].

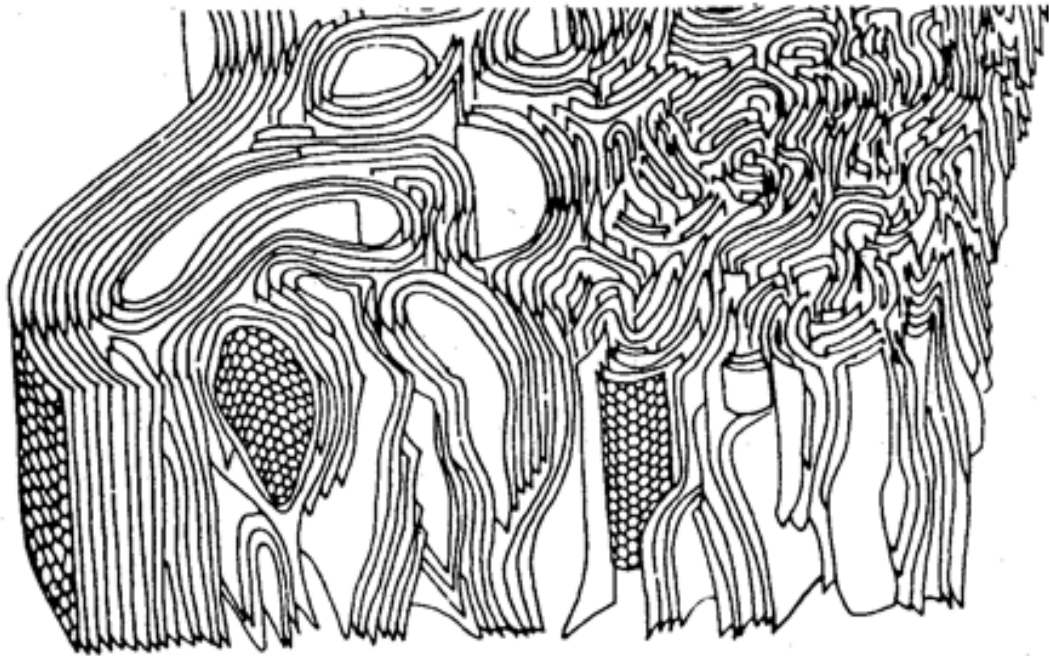


Figure 14 Model of transverse structure of PAN-based carbon fiber [90].

PAN-based CF has a high structural anisotropy. In a medium modulus fiber, sheets are smaller, less orientated, and more crosslinked than in high modulus materials, where, they are wider, thicker, and more axially oriented. The pitch based carbon fibers present a variety of microstructures and are rather more complex than PAN-based CF. Most seen structures are random, radial, flat-layer, onion-skin, radial-folded and line-origin. The pitch-based precursor is characterized by onion-skin, radial or random textures. The textures can be varied based on the spinning conditions such as melt temperature and viscosity, and that the microstructure are maintained throughout carbonization and graphitization [91]. Wu used X-ray diffraction to compare the lyocell based CF and the rayon based CF [92]. The patterns revealed that the crystalline structure of rayon fibers has two diffractions peaks at 2θ (12° and 22°). The peaks correspond to reflections of the 101 and 002 planes of the monoclinic unit cell. His findings indicated high values of crystallinity (X_c) and crystal size (L_{002}). Very little is known in the literature about detailed structure of rayon based CF but it was proven over the years that they possess attractive properties just like the pitch and PAN-based CF.

In general, properties of CF include the following: high tensile modulus and strength, low thermal expansion coefficient, thermal stability in the absence of oxygen to over 3000°C , excellent creep resistance, chemical stability, particularly in strong acids, biocompatibility, high thermal conductivity, low electrical resistivity, availability in a continuous form, decreasing cost (versus time). Most properties are interrelated for CF. An increase in the tensile modulus leads to decrease in the strain to failure and decrease in compressive strength. Also an increase in thermal conductivity leads to decrease in the coefficient of thermal expansion and vice versa.

Mechanical properties of different carbon fibers have been studied extensively [53, 88, 93-95]. The high modulus of carbon fibers stem from the fact that carbon layers, though not necessarily flat, tend to be parallel to the fibers axis. As a result, a carbon fiber has a higher modulus parallel to the fiber axis than perpendicular to the fiber axis. Similarly, the electrical and thermal conductivities are higher along the fiber axis, and the coefficient of thermal expansion is lower along the fiber axis. Prandy explained that the difference in compressive behavior between pitch-based and PAN- based CF is attributed to the strong preferred orientation of the

carbon layers in the pitch-based fibers and the more random microstructure causes the fibers to be susceptible to shearing [96]. The torsion modulus of CF has been analyzed and it was found that it is governed mostly by the cross-sectional microstructure. Mesophase pitch-based carbon fibers have low torsional modulus compared to PAN-based CF because they have an appreciable radial cross-sectional microstructure, which facilitates interlayer shear. Many works analyzed the correlation between production, structure and properties of CF. Watt and Johnson [93] have shown that there is a clear correlation between the change in length of the filament after oxidation at 220°C and the Young's modulus of the resultant CF. Since Young's modulus primarily depends on the alignment of the carbon ribbons with the fiber axis, it is clear that oxidation under strain induces a preferential orientation of the ladder polymer chains.

Most properties of carbon fibers can be improved through high temperature treatment, possibly under load. Concepts for interpretation of the relationship between the temperature and the mechanical properties of all carbon fibers have been studied in detail. Bacon and Smith [95] determined mechanical properties in the temperature range of 20 - 1900°C for rayon-based carbon fiber. They concluded that the strength had a maximum value at a temperature around 1700 - 1800°C and then a steep drop at higher temperatures. Young's modulus decreased slightly as temperature increased to 1500°C and then dropped substantially.

Mostovoi measured the mechanical properties of a PAN-Based CF in the temperature range 20-2000°C [97]. The tensile strength increased first by about 40% from room temperature to 1800°C and then it dropped at 2000°C. Young's modulus temperature dependence was similar to the one reported by Bacon and Smith. Tensile deformations were noticed at 2000°C but this feature was not discussed. Tanable analyzed a pitch-based carbon fiber in the temperature range 20-1300°C [98]. He concluded that neither tensile strength nor Young's modulus showed significant temperature dependence. In a recent work by Sauder et al., the tensile behaviors of CF were investigated at high temperatures [99]. It was found that the basal planes spacing expands with increasing temperatures, which decreases the transverse elastic moduli. Additionally, the planes perpendicular to the c-axis are subject to shear stress with increasing temperature.

2.8 Application of Carbon Fibers

Extensive application development has produced high confidence in carbon fiber composites with demonstrated materials performances, reliability, and predictability, accompanied by weight and fuel savings and manufacturing and operational cost reductions [100]. All these assets have led to performance critical military aircraft and aerospace applications as well as to other applications.

The first single component was produced in 1969 and used on the F14, military applications [101]. The applications have progressed over the years and were extended to commercial and general aviation applications. The space shuttle orbiter payload bay doors were some of the larger CF epoxy structure ever made [102]. The new Boeing 787 Dreamliner has nearly 35 tons of carbon fiber reinforced plastic (CFRP), made with 23 tons of CF [103]. It presents a great example of how far carbon fibers have come along in civil aviation. The Boeing 787 is one of the lighter aircraft and has a higher strength-to-weight ratio than traditional aircraft.

Carbon fibers are also used in the automobile industry and are still being investigated for size reduction, improved engine efficiency and better dynamics. They have proved to be an advantage in racing cars. The first automotive application of CF sheet molded composite was made in nine components of the 2003 Dodge Viper convertible to provide structural performance and to achieve significant weight saving [104]. An important consideration in the vehicle development is the judicious application of new technologies that potentially can be extended to higher volume car and truck line.

Carbon fibers are also used for sporting goods applications that include: golf club, shafts, tennis rackets, and lightweight fishing rods. In the medical field, carbon fibers are used as prosthetic devices, artificial limbs and surgical implants. Nowadays, carbon fibers are used in industrial machining to enable higher operating speeds at reduced noise levels and longer lifetimes. They are also used in business machine and computer applications.

Carbon fiber cost is principally determined, independent of the usual volume price relationships, by precursor cost and related mass yield in conversion and capital and intensity.

The carbon fiber business has developed into a complex and unusual multinational network of interlocking corporate arrangements dominated in manufacturing capacity by Japan and in consumption by the United States. Cheaper and newer versions of carbon fibers are being produced from new raw materials. Novel applications are also being developed. Nonwoven carbon fibers are being tested as possible high temperature fire-retardant insulation [105].

As carbon fibers for different applications require different properties and performance, which in turn is dependent on the structure of the fibers, carbon fibers continue to be produced from different precursors and there is continuing investigation on the possibility of using different precursors. Because of this continuing interest, rayon fibers, especially the ones produced in the US, as no commercial rayon is being produced in the US today, are investigated as a precursor for possible military applications.

CHAPTER 3: EXPERIMENTAL

3.1 Materials

3.1.1 Precursor fibers

Two different rayon fibers were used in the present work. A commercial grade rayon fiber was obtained from Lenzing, Austria and an experimental rayon fiber from Advanced Cerametrics, Lambertville, NJ. The precursors were multifilament bundles. The physical and mechanical properties of both precursors are listed in section 4.1. The characteristics were measured as described in the later sections.

3.1.2 Phosphoric Acid

Phosphoric acid (H_3PO_4), reagent ACS plus from Fisher Scientific of 85% assay was used. One normal (1N) solution was prepared by adding distilled water to the desired quantity for sample treatment.

3.2 Preparation of Carbon fibers

3.2.1 Apparatus.

The method of heating and the design of appropriate apparatus is a complex problem. The apparatus designed for the present investigation is a tubular oven mounted on rails. The furnace has two inlets at both ends through which the desired gas is fed into the furnace to control the environment. The inlet flow into the furnace was kept constant. A programmable temperature controller maintained the temperature of the heater at set points. A thermocouple attached to a temperature indicator was used to determine the temperature profile inside the furnace at different temperature settings. The wheels on the mounting table allow moving the furnace freely without removing the fibers to heat the furnace to the working temperature when needed. Figure 15 shows a schematic of the furnace and the fiber set up.

The temperature profile inside the furnace along the thread line for various temperature settings are shown in Figures 16. The working temperatures are maintained in the middle 15 centimeters of the furnace. The temperature distribution is broad and decreases towards the entrance of the furnace as expected. The temperature profile was checked regularly before the experiments.

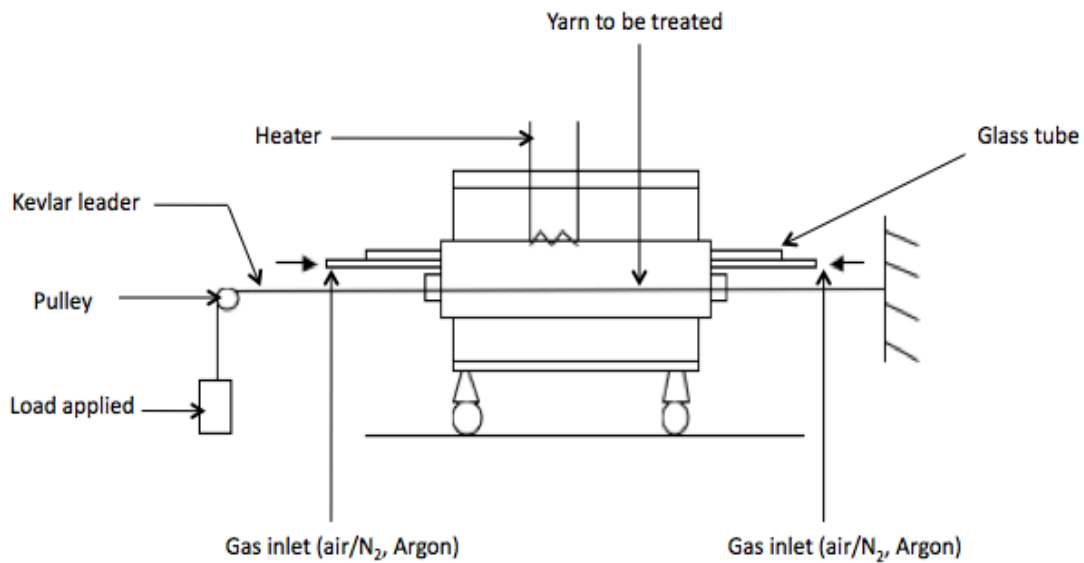


Figure 15 Schematic of the furnace used for stabilization and carbonization.

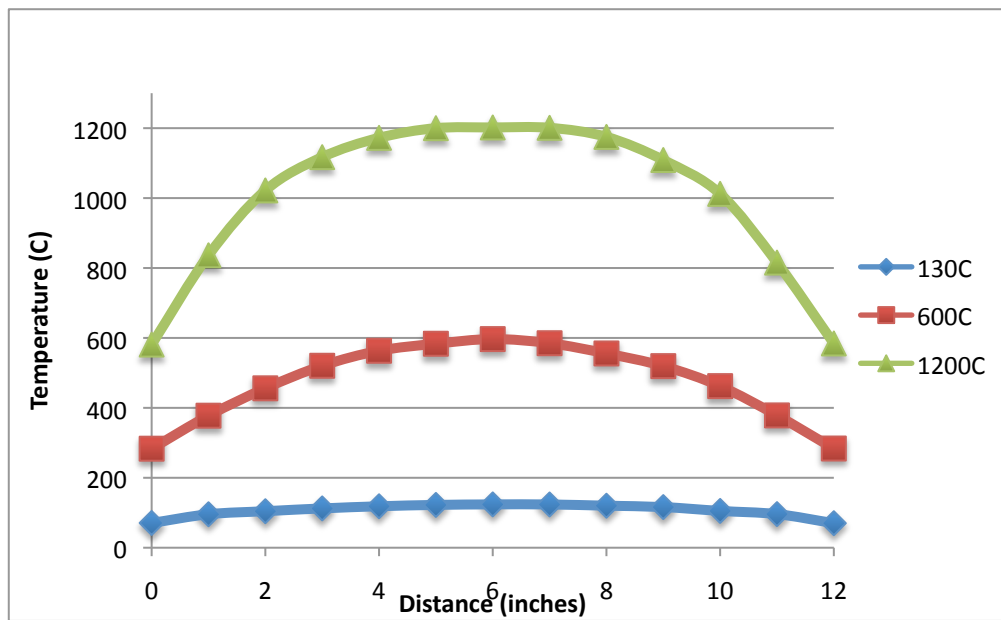


Figure 16 Temperature profile of the furnace at different temperature settings.

3.2.2 Impregnation with phosphoric acid

The rayon fibers were impregnated in a one normal solution of phosphorous acid. Sufficient amount of the catalytic solution was prepared and the rayon fibers were kept immersed in it for 5 hours. The fibers were dried at room temperature at least two hour after removal from the acidic bath.

3.2.3 Stabilization

The rayon fibers were kept in the central zone of the tubular furnace where the temperature is maintained at desired range. Air was pumped into the furnace chamber at a rate of 60cc/min. The oven was preheated to the required starting temperature before the samples were inserted horizontally. The stabilization temperature was from 110°C to 380°C. A light tension was applied during the process. Continuous and periodic heating action was used for optimization. The stabilization temperature and time were varied during the investigation. Samples treated for various conditions were collected for further testing and analysis (Table 1 and Table 2).

Table 1 Stabilization conditions (time and temperature) of commercial rayon precursor.

Sample ID	Treated with Phosphoric acid	Temperatures (°C) and stabilization time (min)						Total time (min)
		150 °C	200°C	250°C	300°C	350°C	380°C	
5012		30	30	30	30	30	30	180
5053P	Yes	30	30	30	30	30	30	180
5009		30	60	30	30	30	30	210
5052P	Yes	30	60	30	30	30	30	210
5011		120	60	30	30	30	30	300
5050P	Yes	120	60	30	30	30	30	300
5010		240	60	30	30	30	30	420
5051P	Yes	240	60	30	30	30	30	420

Note: The oven is preheated to 110°C then the time showing in the table is the time it took to reach the next temperature. Example: For sample 5012, it took 30 minutes to go from 110°C to 150°C and another 30 minutes to go from 150 to 200°C and so on.

Table 2 Stabilization conditions of the experimental rayon precursor.

Sample ID	Temperature (°C)	110	150	200	250	300	350	380	Total time (min)
502	Continuous heating	10	30	30	30	30	30	30	190
503	Hold at temp.	10	20	20	20	20	20	20	130
504	Continuous heating	10	20	20	20	20	20	20	130

Note:

- 1- Sample 503 was heated in two steps. First, it was programmed to reach each set point in 10 min and held at the set point for 20 min. The total time for stabilization is 190 min.

3.2.4 Carbonization

The samples stabilized for optimum conditions, based on the results from initial investigation were used for carbonization. At the end of stabilization stage, the gas in the furnace was switched from air to ultra high purity nitrogen. The nitrogen flow was kept constant at 80cc/min. Oxygen was purged out of the furnace chamber by letting nitrogen flow for at least 15 minutes and temperature kept at 380°C. This ensured an inert atmosphere before the carbonization process started. The stabilized samples were carbonized to a temperature of 1200°C under tension. The carbonization stage was carried out at different heating rates.

3.3 Characterization methods

3.3.1 Color Change

Changes in the color of the samples as stabilization proceeded were monitored visually. The colors were recorded as white, yellow, deep yellow, brown, dark brown and black.

3.3.2 Fiber Diameter

From the SEM macrographs, fiber diameter was quantitatively measured using automated image analysis based software (Image Pro). For precursor fibers, fiber diameters were measured using the optical microscope. The reported diameters are the average of ten measurements.

3.3.3 Burning Test

The flammability of the stabilized samples was determined before proceeding to carbonization stage. The samples were thrust into a match flame and combustibility was evaluated. The samples that do not burn are generally suitable for carbonization without disintegration

3.3.4 Thermal Analyses

Thermal analysis of the samples was carried out in air and nitrogen by differential scanning calorimetry (DSC) using the Mettler DSC 821e. The scans were run from room temperature (25°C) to 450°C at a heating rate of 10°C/min. Selected samples were dried inside the DSC for 15 minutes at 110°C to remove moisture before the scan.

The weight loss of the samples was measured in air and nitrogen atmosphere by thermogravimetric analysis (TGA) with Mettler TGA 867. The scans were run from 25°C to 1000°C at a heating rate of 10°C/min. The sample weights were kept around 6mg.

3.3.5 Single Fiber Tensile Test

Tensile properties of the precursors, the stabilized and the carbonized fibers were measured using the EJA Tensile Tester. Single fiber was isolated from the bundles and glued to two metallic plates with holders on the sides to allow the assembly to be stable (Figure 17). The gauge length was set to 25mm. The assembly was held between the pneumatic grips of the tensile tester. After careful alignment of the grips, the side holders were cut to transfer the load to the fiber. The crosshead speed was set to 0.1mm/s. The tensile strength was calculated from the peak load value and the estimated cross-sectional area of the single fiber. The elongation at break was also recorded. Ten readings per sample were obtained and the average values are reported.

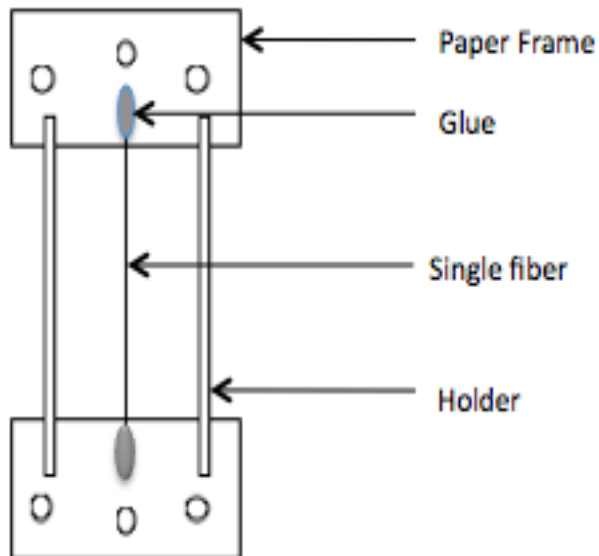


Figure 17 Assembly for single fiber tensile test.

3.3.6 Scanning Electron Microscopy (SEM)

The samples were coated with gold by an ion sputter coater, and studied using a Leo 1525 scanning electron microscope. Both the fibers cross-sections and surface morphology were observed and micrographs were generated.

Energy dispersive X-ray analysis (EDXA) was carried out on selected samples to confirm the carbon content and to verify if carbonized samples showed the presence of phosphor.

3.3.7 X-ray Diffraction

The crystal structures were measured by scanning the fibers in the 2θ ranges of 5 to 70° (2θ) using the Rigaku wide angle X-ray diffractometer (WAXD). The X-ray beam was generated from synchrotron radiation using $\text{CuK}\alpha$ radiation ($\lambda = 1.541 \text{ \AA}$). The sample to detector distance was 36 mm.

3.3.8 Elemental Analysis

Selected samples were sent to Atlantic Microlab, Inc, Norcross GA for elemental analysis for C and H. The samples were dried at 110°C for 15 min before the test. Elemental analysis is accomplished by combustion analysis. In this technique, a sample is burned in an excess of oxygen, and various traps collect the combustion products—carbon dioxide, water, and nitric oxide. The masses of these combustion products are used to calculate the composition of the unknown sample. The detection limit is 0.25% and the error is less than 0.3%.

3.3.9 Fourier Transform Infrared Spectroscopy (FTIR)

The precursor, the stabilized and carbonized fibers were analyzed for chemical structure. The test was completed at ambient temperature by BIO RAD FTS 6000 Fourier transform infrared spectrometer (FTIR). Co-add 1024 scans were collected for peak analysis.

CHAPTER 4: RESULTS and DISCUSSION

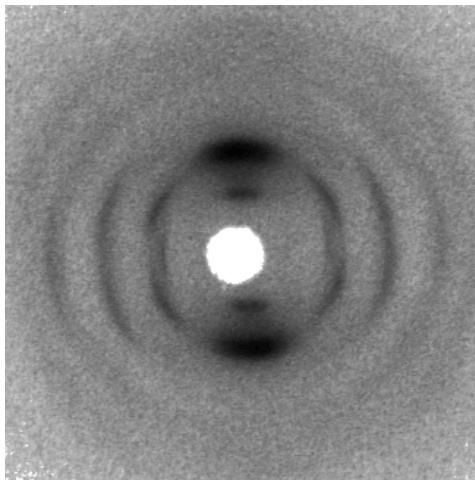
4.1 Properties of the precursors

Two different types of viscose rayon used in the present investigation were, a commercial grade rayon fiber from Lenzing, Austria, and an experimental rayon fiber from Advanced Cerametrics, Lumbertville, NJ USA. The physical and mechanical properties of the fibers are presented in table 3. The obvious differences are that the experimental rayon fiber diameter was higher and tensile properties were poorer compared to that of the commercial fiber. Both precursors have good amount of order and orientation as evident from WAXD patterns shown in figure 18. The patterns revealed that the crystalline structure of the rayon fibers has two diffractions peaks at 2θ of 12° and 22° . The peaks correspond to reflections of the 101 and 002 planes of the monoclinic unit cell. The orientation and crystallinity were induced during fiber production. It was reported that the physical and chemical properties of the fibers strongly depend on the crystallinity and orientation. The tensile strength and the elongation of rayon fibers change several percent when the chain orientation is changed from random to parallel. The common method used to increase orientation in fibers is stretching.

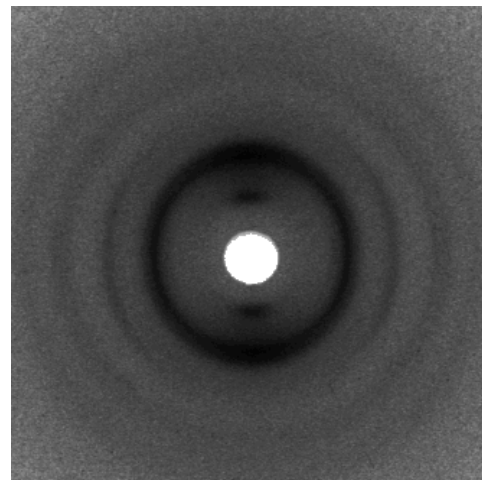
The thermal behaviors of the precursors are important during the production of carbon fibers. The thermal behaviors influence the stabilization and carbonization stages and hence the yield of carbon. During stabilization, thermal transformation of the precursor occurs by mean of different reactions. Many researchers studied the thermal degradation of cellulose and its products [47, 59, 62, 64, 65, 69, 106, 107]. TGA and DSC are effective methods to study thermal stability of organic materials. Both scans were completed with small samples (4-10mg) at a low heating rate ($10^\circ\text{C}/\text{min}$).

Table 3 Physicals and mechanical properties of the rayon fibers.

Properties	Commercial rayon	Experimental rayon
Color	White	White
Fiber diameter (Microns)	14.98	18.99
Tensile strength (MPa)	275.57	174.67
Elongation at break (%)	8.20	5.21
Young's modulus (GPa)	32.35	26.71



A



B

Figure 18 X-ray patterns of the commercial rayon (A) and experimental rayon (B).

The TGA curves obtained in nitrogen from 25°C to 600°C are shown in figure 19 and 20 respectively for the commercial rayon and the experimental rayon. The curves show different stages of degradation. There is a small weight loss in the temperatures range of 25-125°C. The mass loss was found to be 7.5% at 200°C. There is a rapid mass loss of 72.5% in the temperatures range of 240-380°C with an onset temperature of 318.°C. The mass continues to drop but slowly from 400°C. The thermal degradation curve of the experimental rayon is similar to that of the commercial rayon. It has different stages as well. There is a mass loss of 4.7% in the temperatures range up to 125°C. The mass loss is around 7.1% at 200°C. There is a rapid mass loss of 74.2% in the temperatures range of 235-370°C with an onset temperature of 304°C.

The DSC curves in nitrogen are shown in figures 21 and 22, respectively. Both curves show large endothermic peaks in the temperature range of 25-130°C for the commercial rayon and 25-135°C for the experimental rayon. There is a high temperature endothermic peak at 348°C for the commercial rayon and at 341°C for the experimental rayon.

Figure 23 and 24 represent the TGA curves in air of the commercial and experimental rayon, respectively. The shapes of the curves are similar to the TGA curves in nitrogen in the 100°C. The weight loss is about 7.3% and 8.0% at 200°C respectively for both precursors. The sharp drop for the commercial rayon is around 260°C to 350°C with an onset temperature of 305°C. The experimental rayon has the same sharp weight loss starting at 240°C and ending at 340°C with onset at 284°C. Over 95% of mass is lost at 500°C.

The DSC scans of both precursors in air are similar (figures 25 and 26). There is a large endotherm in the 100°C region, which is due to the moisture evaporation. The commercial rayon has a small exotherm peak at 324°C followed by a large exotherm from 340°C to 450°C. The experimental rayon has a small exotherm at 322°C followed by a large exothermic from 340°C to 450°C.

The quick drop in mass in the temperatures range of 25-130°C is explained by the removal of moisture and evaporation of the adsorbed water by the rayon fibers. Both DSC and TGA curves

confirm this phenomenon. This stage marks the beginning of the dehydration and decomposition processes of cellulose. Splitting up of structural water from the main cellulose chain is followed (130°C - 260°C). Dehydration of cellulose is an endothermic process and produces dehydrocellulose. It was reported that formation of C=O and C=C bonds occurs. The bonds indicate that dehydration process is intramolecular rather than intermolecular [108]. The dehydration continues through the pyrolysis stage up to 260°C. Around the same temperature, a depolymerization reaction competes for the residual cellulose by an endothermic process, and the product turns into tar. Earlier researches have shown that levoglucosan is the essential intermediate of the tarry material [61, 71]. The rapid weight loss, found in the range of 260°C - 380°C is associated with the large endothermic peak on the DSC curve. During this stage, most of the cellulose is decomposed by series of chemical reactions. The major reactions are the cleavage of C-O and C-C linkages, crosslinking, ring scission followed by evolution of H₂O, CO and CO₂. The massive weight loss results from the formation of four carbons residue from each cellulose ring unit.

The large exotherm portion after 280°C in figures 24 and 25 indicates multiple reactions are competing. The rising exotherm at 320°C, followed by large rapid exotherm on the DSC curve in air corresponds to the observed TGA results. Oxygen or oxidative environment plays a dominant role during low-temperature degradation of cellulose. Shafizadeh and Bradbury [54] reported that oxidative reactions are responsible for acceleration in the rates of weight loss and depolymerization of cellulose in air at temperature below 300°C but at temperatures above 300°C the rate of pyrolysis is essentially the same in both air and nitrogen. Their findings contradict our results. The TGA and DSC curves show that the degradation is similar below 300°C but different above 300°C. The DSC curves show endothermic peak above 300°C in nitrogen. In air, the peak is exothermic and appears at a lower temperature. During the oxidative decomposition of cellulose at low temperatures, dehydration is followed by crosslinking reactions [95]. Concurrently there is rearrangement of the cellulose structures. The rate of mass change is high in air at low temperatures. On the basis of relative decomposition temperature, shape of thermal curves, and weight loss analysis, pyrolysis in air proceeds much more intensively than pyrolysis in nitrogen. Oxidation suppresses the formation of

levoglucosan. On the other hand, it favors the formation of aldehyde and ketone. The aldehyde and ketone groups participate in the crosslinking reactions, which in turn increase the yield of carbon.

As a result of the findings described here, the thermal decomposition of cellulose cannot be explained by one step model first order reaction. There are more reactions competing. Tang [108] reported that there are second order interactions and some intramolecular rearrangements occurring. Broido [62] reported that crosslinking competes with depolymerization. Advanced investigation of the composition of gases during cellulose pyrolysis helped to conclude that at least two or more pathways compete in the decomposition. The competitive mechanism has been disclosed by Kilzer and Broido [62, 63]. The two competitive pathways are the formation of volatile tar and the formation of light gases together with char.

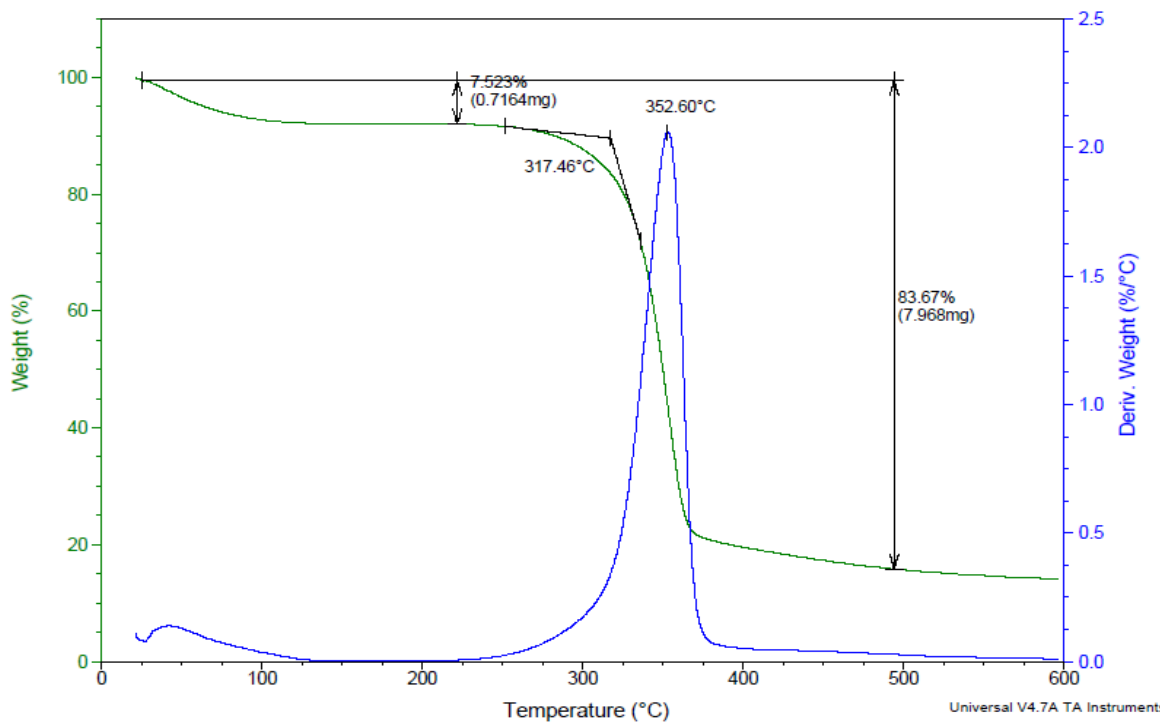


Figure 19 TGA curve of the commercial rayon from room temperature to 600°C in nitrogen

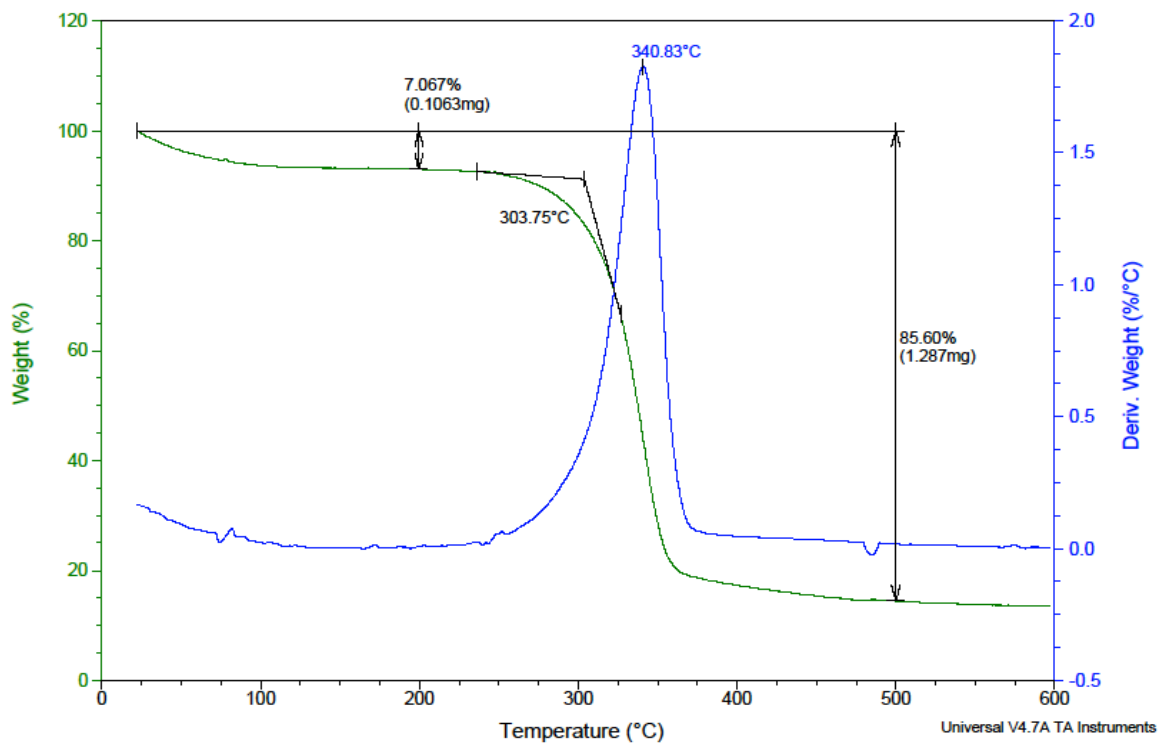


Figure 20 TGA curve of the experimental rayon from room temperature to 600°C in nitrogen

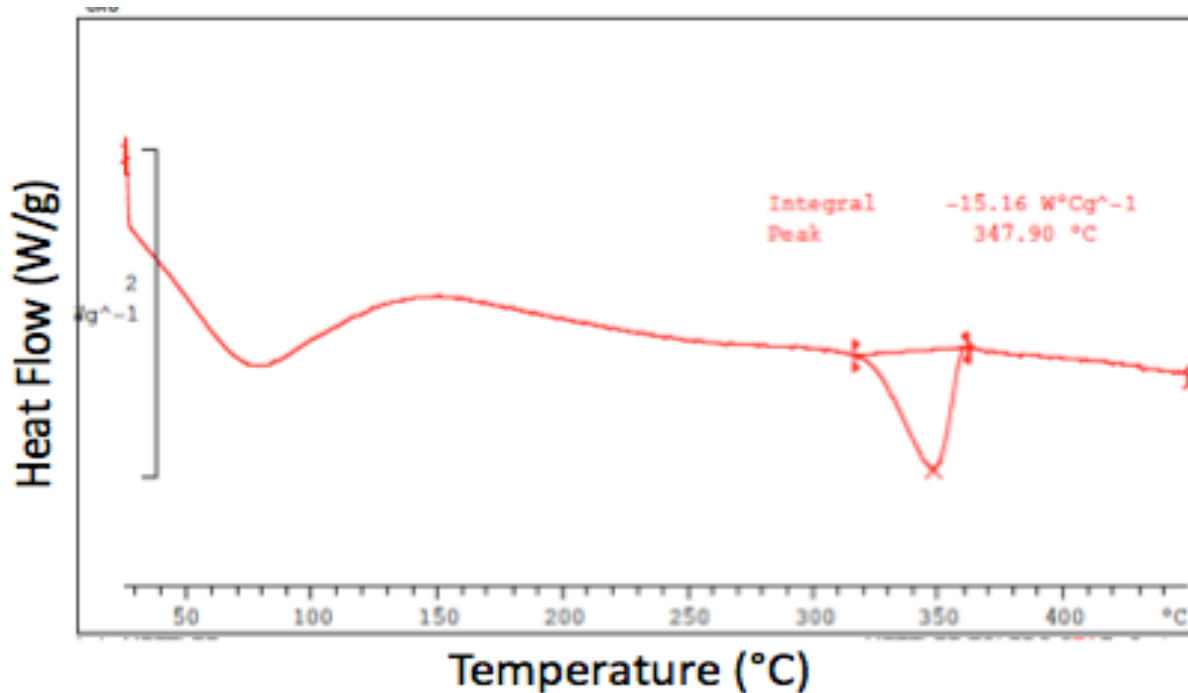


Figure 21 DSC curve of commercial rayon fibers from room temperature to 450°C in nitrogen.

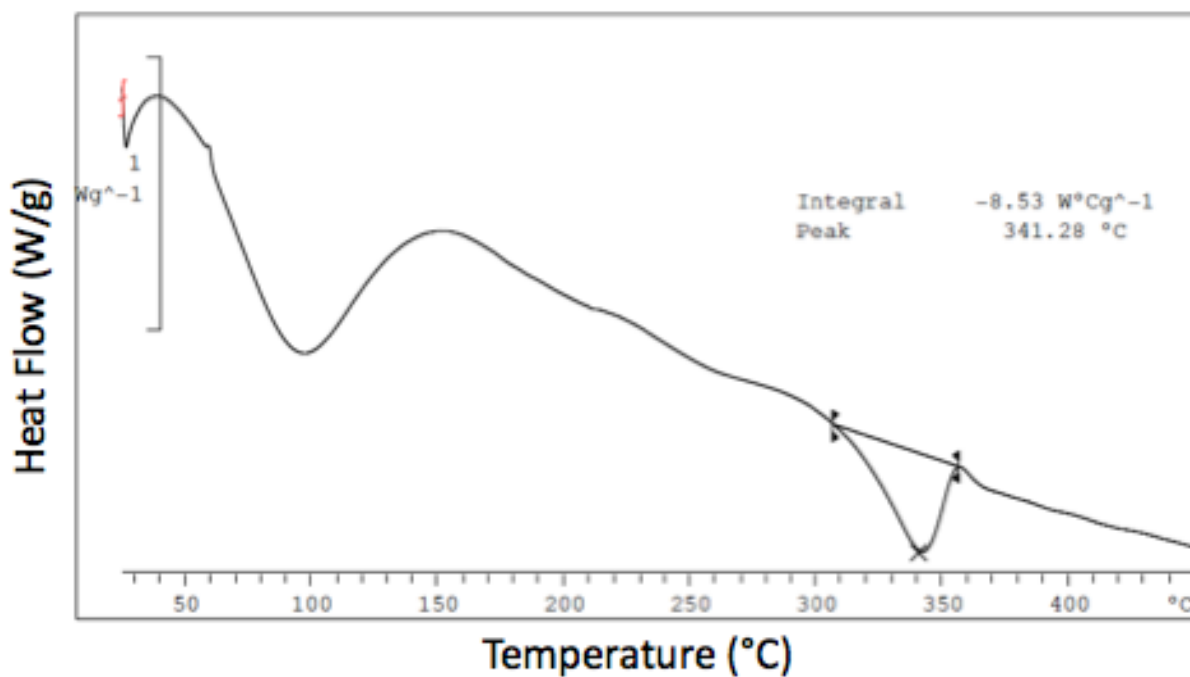


Figure 22 DSC curve of experimental rayon fibers from room temperature to 450°C in nitrogen

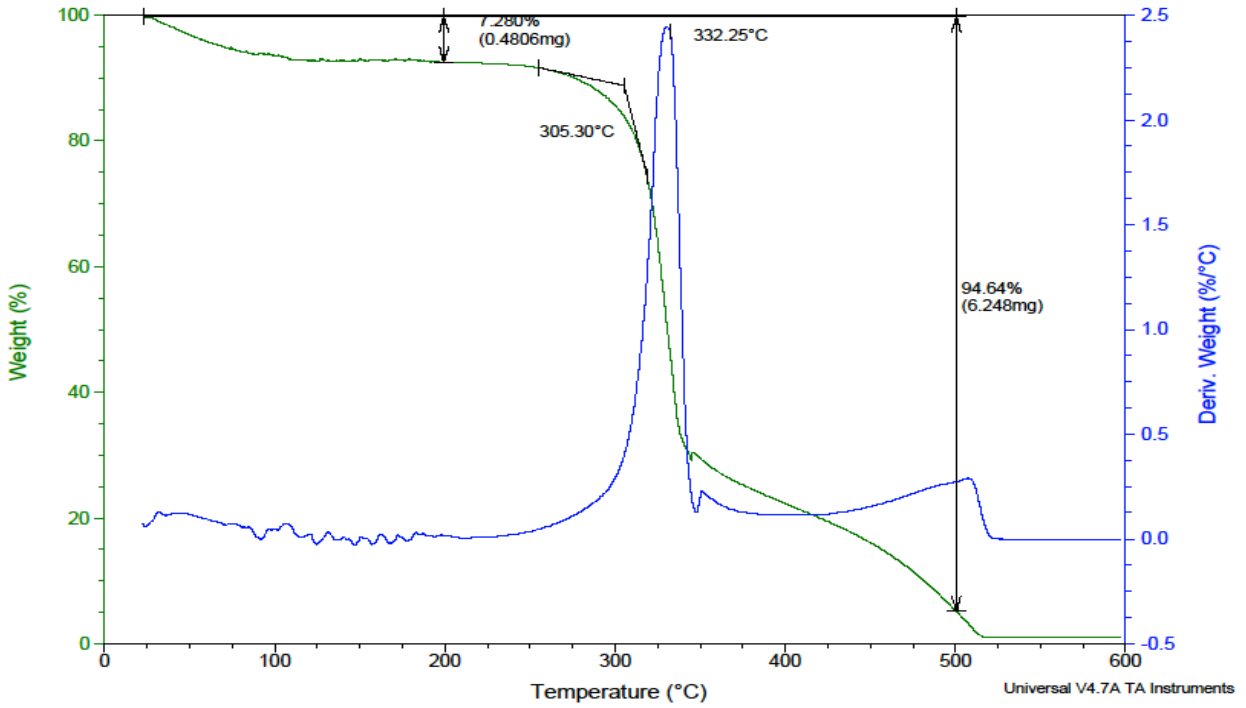


Figure 23 TGA curve of the commercial rayon fibers from room temperature to 600°C in air

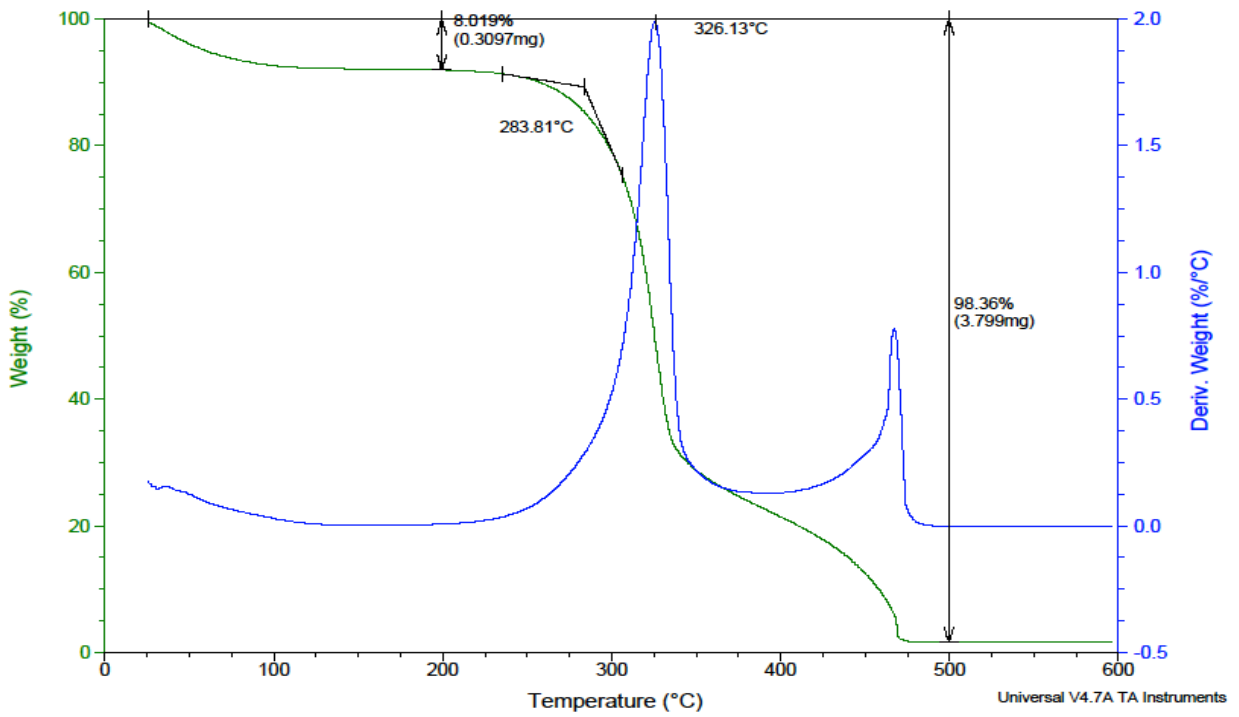


Figure 24 TGA curve of experimental rayon fibers from room temperature to 600°C in air

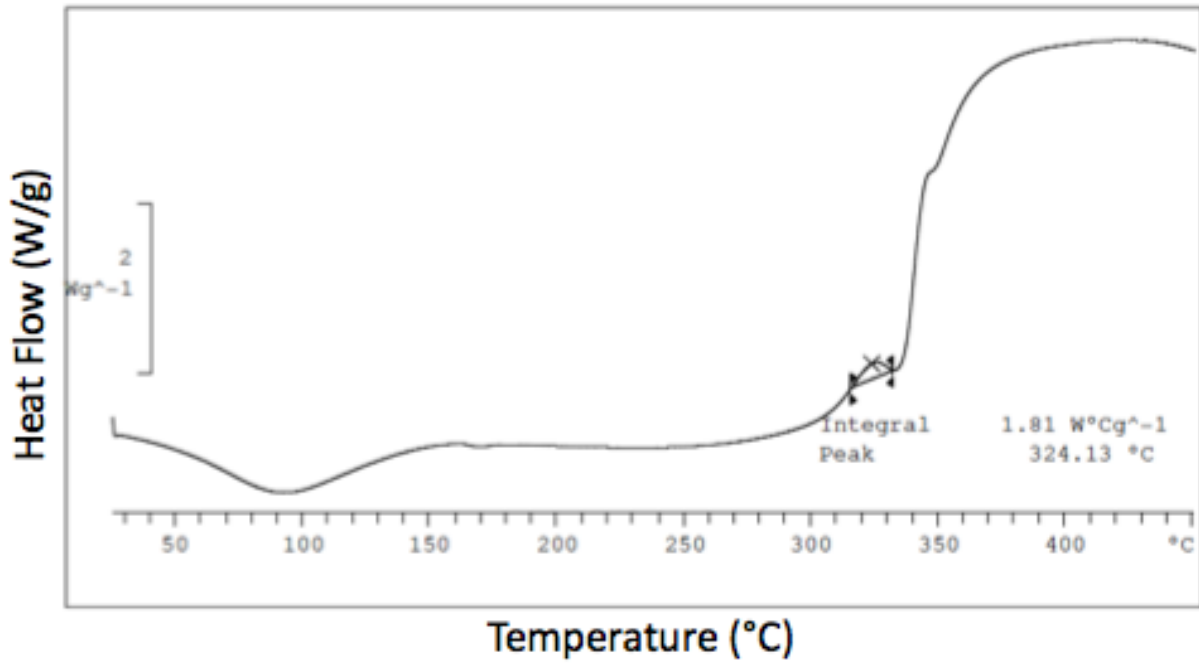


Figure 25 DSC curve of the commercial rayon from room temperature to 450°C in air.

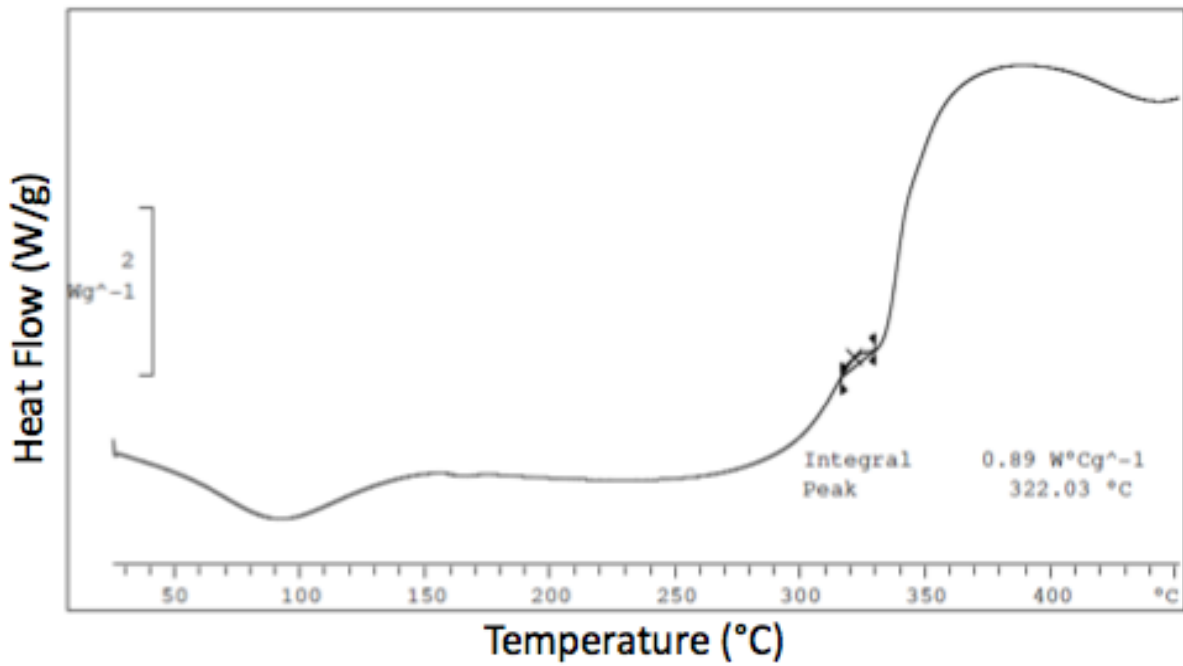


Figure 26 DSC curve of the experimental rayon from room temperature to 450°C in air.

4.2 Precursor I: Commercial rayon fibers

4.2.1 Stabilization at low temperature

4.2.1.1 Effect of pretreatment with phosphoric acid

The effects of inorganic catalysts on the pyrolysis of rayon fibers have been studied in the past [8, 58, 109-111]. Our experiment was carried out to investigate the effects of phosphoric acid pretreatment on the pyrolysis of rayon fibers.

Figure 27 shows the DSC curves of the rayon precursor and the treated precursor with phosphoric acid in nitrogen atmosphere. The samples were dried for 15 minutes at 110°C before the scan. The precursor curve presents an endothermic peak at 341°C. The endothermic peak is shifted to a lower temperature of 215°C, with another small one at 420°C with exothermic peaks at 260 and 315°C on the DSC curve of the treated precursor. For the untreated samples, the endothermic peak at 341°C indicates decomposition of cellulose macromolecule into levoglucosan at that temperature. For the treated sample, the same peak is observed but shifted to lower temperatures (about 125°C lower). The results suggested that pyrolysis reactions for the treated samples started at a much lower temperature over a wider range. There is a growth of exothermic peak at 260°C. This peak confirmed the increase of the dehydration rate.

Figure 28 shows the TGA of untreated rayon, the treated rayon and the stabilized rayon in nitrogen from 25°C to 1000°C at 10°C/min. Two main weight loss stages are observed. The precursor has around 8% mass loss at 120°C and around 78% mass loss at 380°C. The treated sample on the other hand shows a different pyrolysis behavior. It has lost about 8% of mass around 120°C and 42% at 300°C. The treated sample had the smaller weight loss at 1000°C than the untreated precursor. The stabilized sample also showed a minimal weight loss at the beginning of the curve and a sharp loss from 400°C to 780°C. The stabilized sample had the smallest weight loss at 1000°C compared to the untreated and treated samples. The presence of phosphoric acid promotes the diffusion of reactive gaseous species into the interior of the fiber, which leads to small weight loss, hence improving carbon yield. The formation of the

carbonaceous residue was promoted by the presence of phosphor ion. It is in agreement with the literature data describing the effect of phosphoric substances on cellulose decomposition [6, 86, 110]

The corresponding weight loss in the 100°C is the evaporation of moisture in the fibers. The thermal decomposition of the untreated sample starts at the highest temperature (first peak at 340°C on the DSC curve and sharp weight loss at 305°C on the TGA curve). Compared to the untreated rayon, the phosphoric acid treated one shows a much lower starting temperature and faster rate of dehydration reactions. The first peak on the DSC curve is at 220°C and rapid weight loss at 190°C. The phosphoric acid accelerated the pyrolysis reactions. Phosphoric acid, like other inorganic flame-retardants, catalyzed the dehydration reactions. During pyrolysis, the phosphoric acid reacts with the water molecule from the rayon fibers by breaking the hydrogen bond leading to water evaporation. In the temperature range of 150 to 250°C (figure 28), the weight loss is attributed exclusively to the volatilization of water. The results suggested that the phosphoric acid treated rayon fiber started to form char at a relatively lower temperature, and the beginning decomposition temperature was lower by about 60°C than that for the untreated rayon fibers. The treated rayon produced more carbon and less flammable material than the untreated sample because the acid suppressed the release of volatile organic substances by reacting with hydroxyl groups.

Figure 29 shows the SEM images of the treated and untreated carbon fiber surface at 2kX magnification and 2kV beam energy. It can be found that SEM delineated much smoother surface of fibers treated with phosphoric acid; while rougher surface with pores for untreated fibers. The main reason for the difference is that during pyrolysis, the reactions occurring are accelerated by the acid. The acid also catalyzes the dehydration reactions. When the fibers are treated with H_3PO_4 , the surface is protected and the pyrolysis reaction can happen from fiber surface to fiber core with a tempered speed. The surface protection by phosphoric acid will likely prevent the formation of the skin-core structure in the carbon fibers.

Many structural changes occur during low temperature treatment of rayon. These changes involve dehydration, rearrangement, formation of carbonyl groups, evolution of carbon

monoxide and carbon dioxide, formation of carbonaceous residue, and thermal scission of glycosidic bonds producing oxygenated compounds. The stabilized sample did not have a large mass loss till around 400°C because the pretreatment in air changed the morphology and structure of the rayon fibers. Phosphoric acid is found to be an effective catalyst of rayon decomposition based on the following functions. The acid decreases the pyrolysis temperature to a lower range. It increases the amount of char formed.

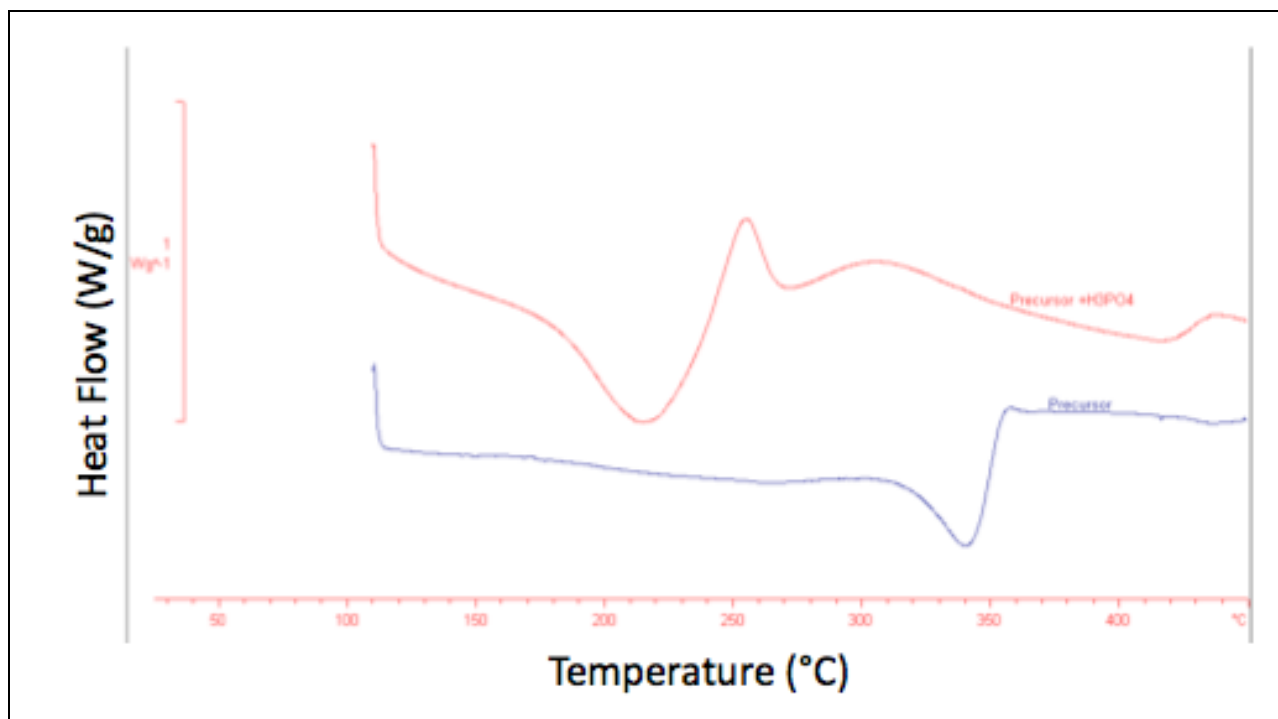


Figure 27 DSC curve of the as received commercial rayon precursor and the soaked precursor with phosphoric acid after drying at 110°C for 15 min.

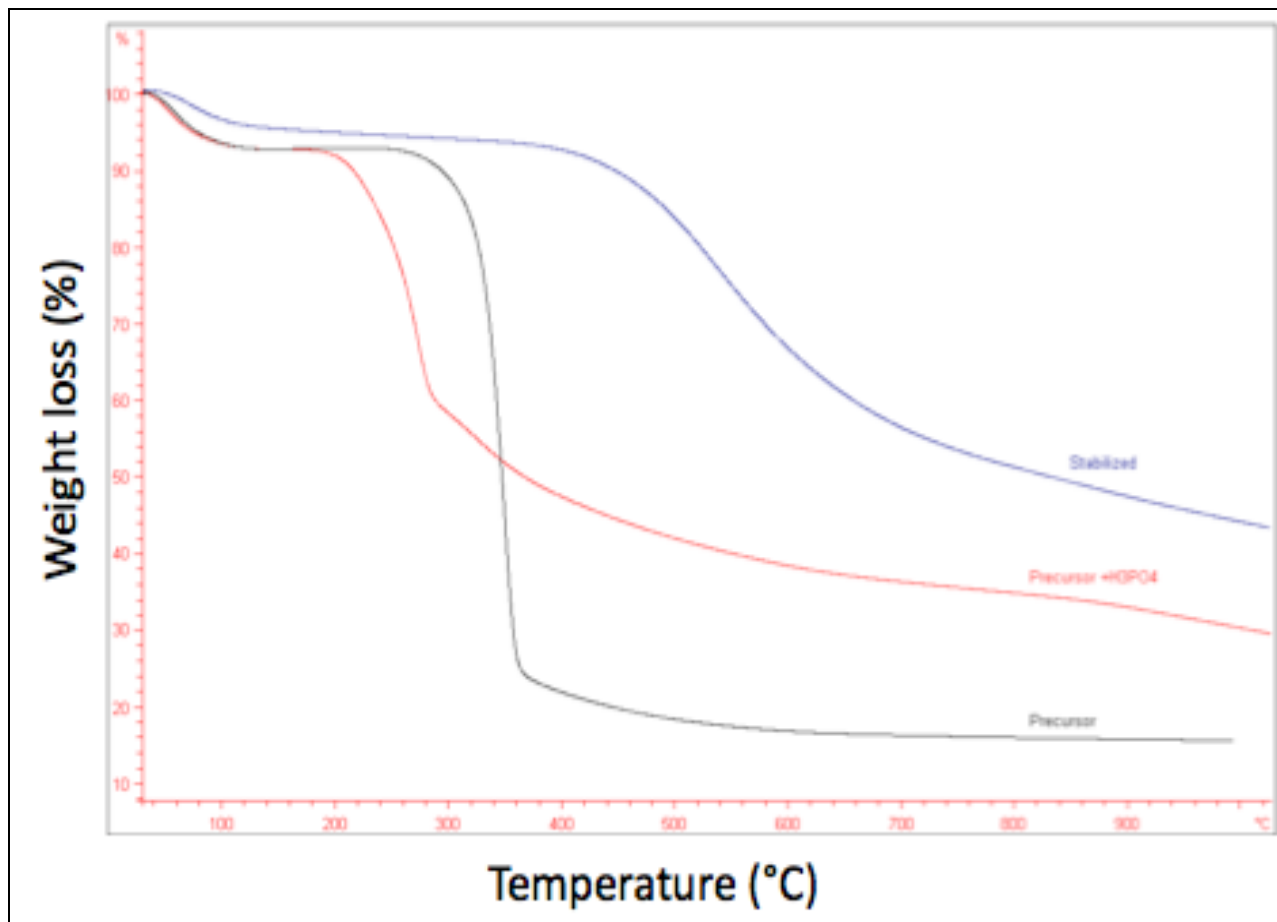


Figure 28 TGA curves of the precursor, the soaked precursor, and stabilized sample.

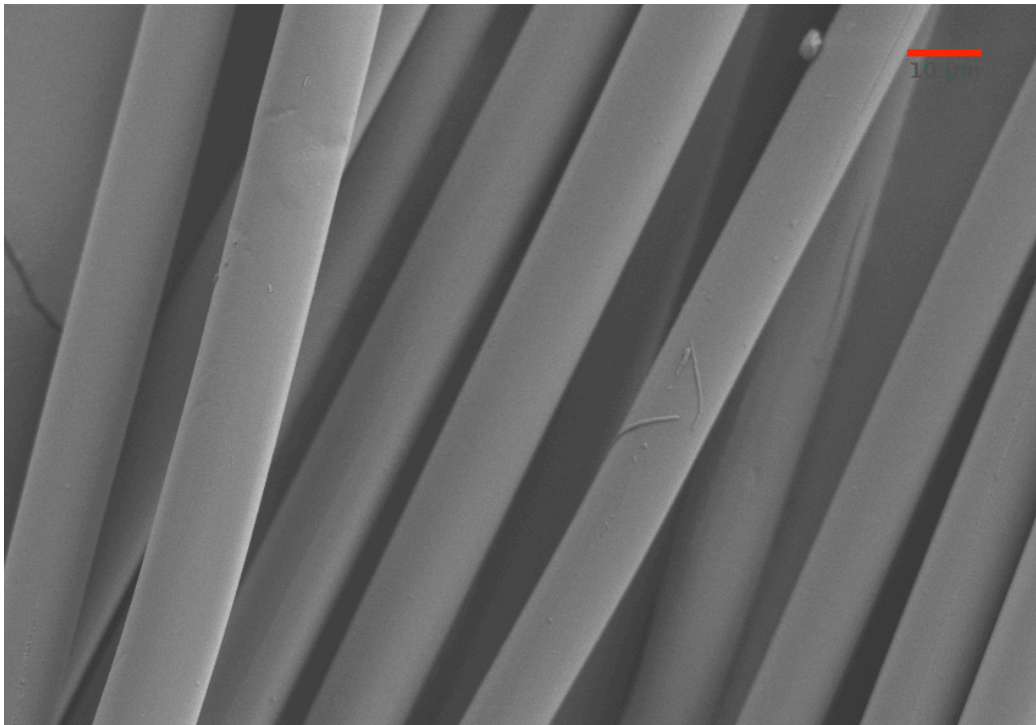
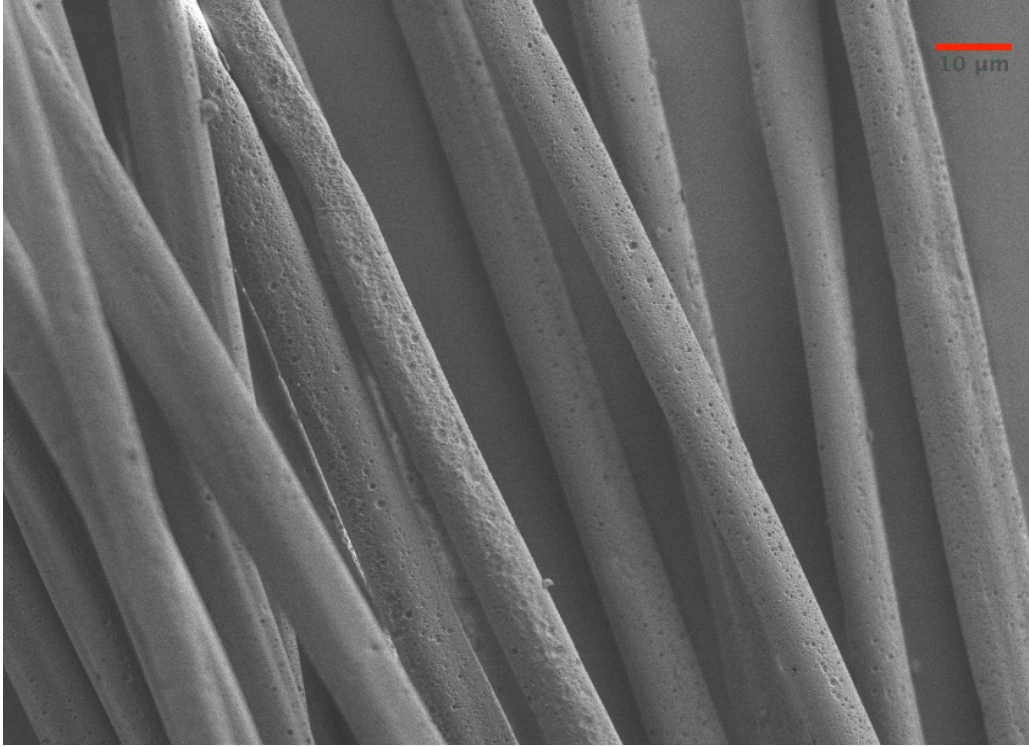


Figure 29 SEM micrographs of the untreated and treated rayon fibers after pyrolysis at 2KX.

At the end of the stabilization, the samples were thrust in a match flame. The results are recorded in Table 4. The samples that did not burn generally can be carbonized without burning at higher temperatures. It is noticeable that the treated samples did not burn, whereas the untreated samples after pyrolysis under similar conditions burned in the flame; though were self extinguishing in nature. The phosphoric acid helped produce a more thermally stable fiber at corresponding stabilization times and heat treatment temperatures.

Table 4 Burning test results of the untreated and soaked fibers after stabilization in air up to 380°C.

Sample ID	When in Flame	After Removal from Flame
5009	Burn	Self extinguish
5052P	Did not burn	
5011	Burn	Self extinguish
5050P	Did not burn	
5010	Burn	Self extinguish
5051P	Did not burn	

Note: Samples 5009, 5010, and 5011 were not treated with phosphoric acid. Samples 5051P, 5050P, and 5052P were treated with phosphoric acid.

4.2.1.2 Effect of temperature and residence time on stabilization

To investigate the effect of residence time and temperature on stabilization, fiber samples were heat treated for different time at different temperatures especially at 150°C and 200°C.

Table 5 Fiber diameters of stabilized samples.

Sample ID	5012	5053P	5009	5052P	5011	5050P	5010	5051P
Fiber diameter (micron)	6.51	8.91	6.48	8.89	6.10	8.72	5.94	8.27

From data in table 5; it is found that the fiber diameter decreases with increasing residence time. The observation is the same for the sample treated with phosphoric acid and the untreated samples. As the temperature rises and residence time increases, the samples start to dehydrate and shrink in both the longitudinal and cross-sectional direction. These reactions are part of the physico-chemical changes occurring during pyrolysis. The shrinkage is related to the breakage of hydrogen bond and also to the surface vulnerability to heat treatment. The fibers yielded from the untreated rayon had the smaller diameter than the fibers yielded from the soaked rayon fibers. The phosphoric acid plays the role of flame retardant and reduces the loss of volatiles and conserves most of the fiber morphology. Even though the untreated samples might have the smaller diameters, the lack of protection makes them vulnerable to heat with less char yield as observed by TGA.

Figure 30 shows the DSC curves of the precursor and selected stabilized samples. The curves show an endothermic reaction up to 160°C for some samples. As explained in earlier sections, the endothermic peak is related to the moisture and the adsorbed water removal. The endothermic peak at 341°C disappeared entirely after stabilization for all samples. Mild exotherms were discernible for sample 5009 at 270°C and 320°C. Sample 5050P also shows mild exotherms at 350°C and 400°C. The exotherms are so minimal and seem to be buried in the baseline.

A selection was made based on the two lowest residence times (180 min and 210 min) and DSC curves were obtained for comparison (figure 31). Both the untreated samples (5012 and 5013)

have small endothermic peaks at 130 and 140°C respectively. The peaks were absent on either treated samples. The difference is related to the effect of phosphoric acid. The phosphoric acid lowers the dehydration related reactions to occur at lower temperatures. It results in the merge of the small peak with the large endothermic peak. The curves are relatively similar.

The thermograms of the selected samples in nitrogen are shown in figure 32. There are four regions noticeable. A mass loss of 8% up to 110°C, followed by slight decrease up to 400°C, and sharp decrease in mass (34%) up to 760°C. The mass continues to decrease slowly up to 1000°C. It is noticeable that the products (amount of residue) did not change considerably. The difference in residue amount is less than 2%. Kilzer and Broido [63] studied the effect of time and temperature by holding cellulose samples at 250°C for 24 hours before heating it to 400°C, and also heating a sample directly to 400°C. The amount of char at 400 °C was three times higher for the sample held at 250°C than the sample heated directly. The long holding allows early char producing reaction to proceed to a greater extent. The sample directly heated to 400°C rushed through the char producing reaction and on into levoglucosan formation, some of which volatilizes before decomposition.

The char produced from the cellulose pyrolysis increases with longer preheating at low temperature. The heating rate is important during stabilization stage. Fast pyrolysis is non-beneficial to the formation of solid carbon fiber from rayon. The fast pyrolysis could accelerate side reactions to release volatile carbon containing substances that lead to low yields. Slow oxidation in air is more recommended. During pyrolysis, the physical interactions, such as coupling between thermal and mass diffusion can decelerate the local heating rate in the center of the fiber, hence controlled slow pyrolysis is suggested for the production of high quality carbon fibers from rayon precursors.

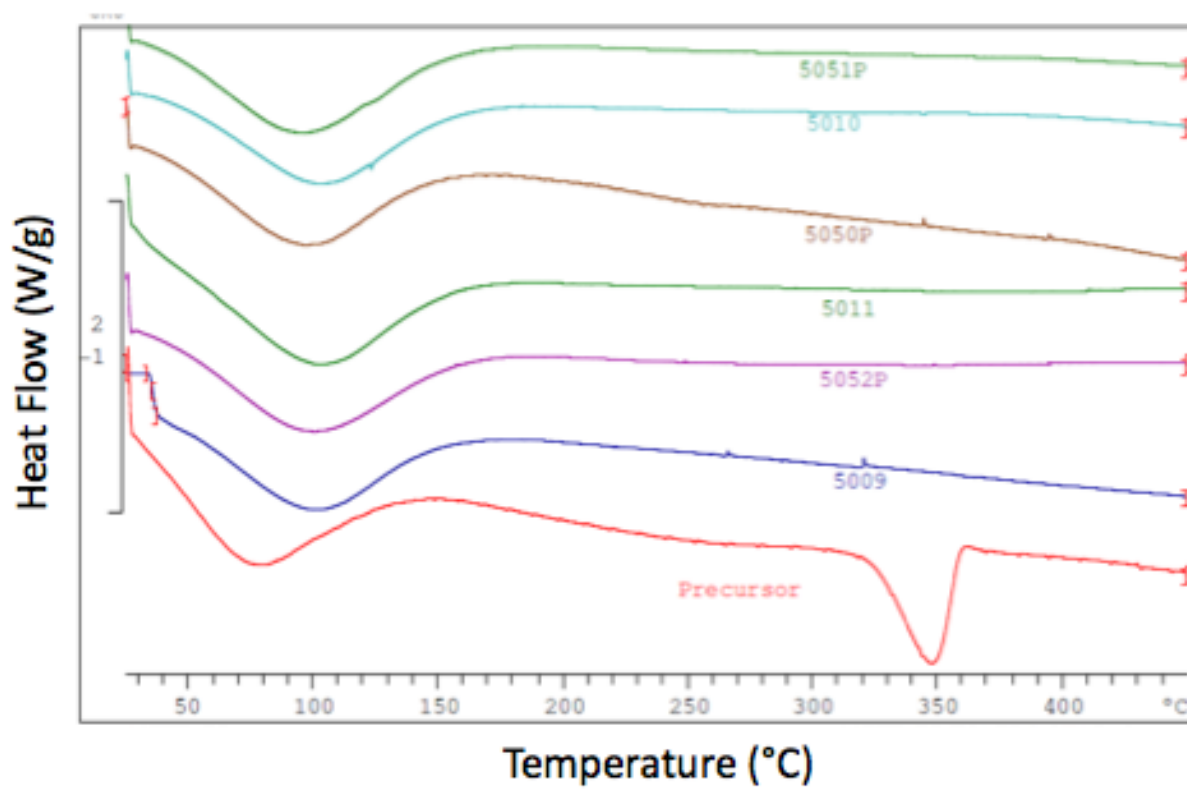


Figure 30 DSC curves of the samples after stabilization stage.

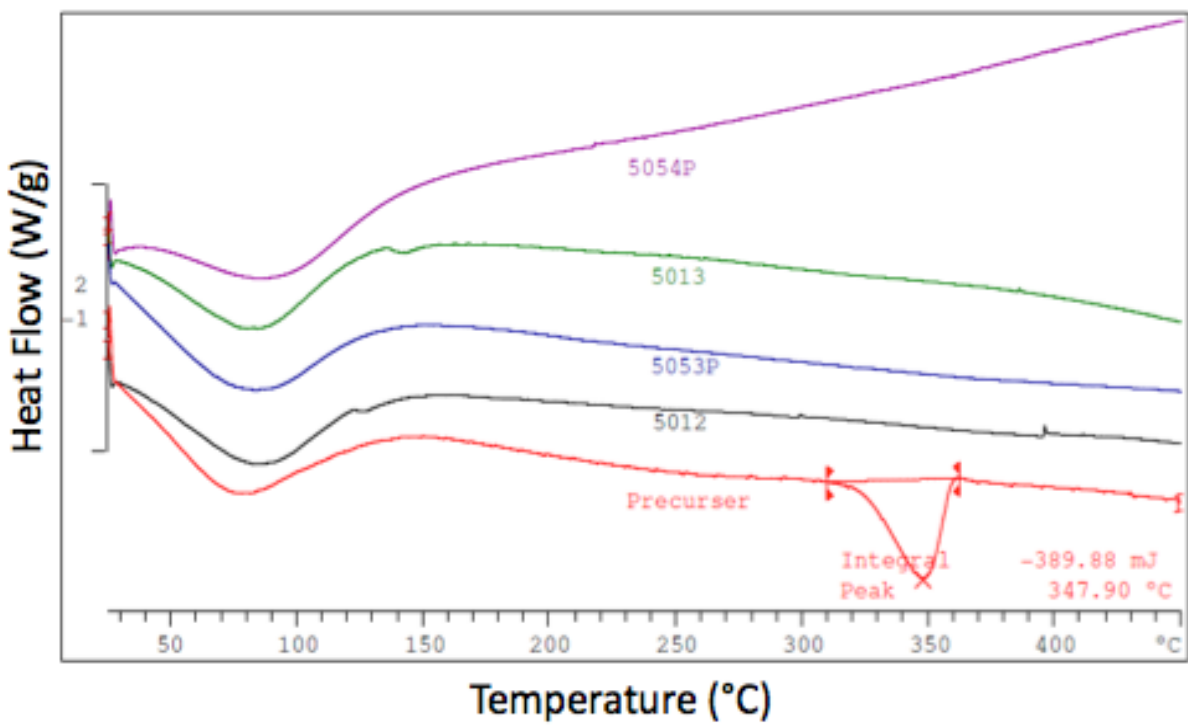


Figure 31 DSC curves of selected sample after stabilization in air up to 380°C.

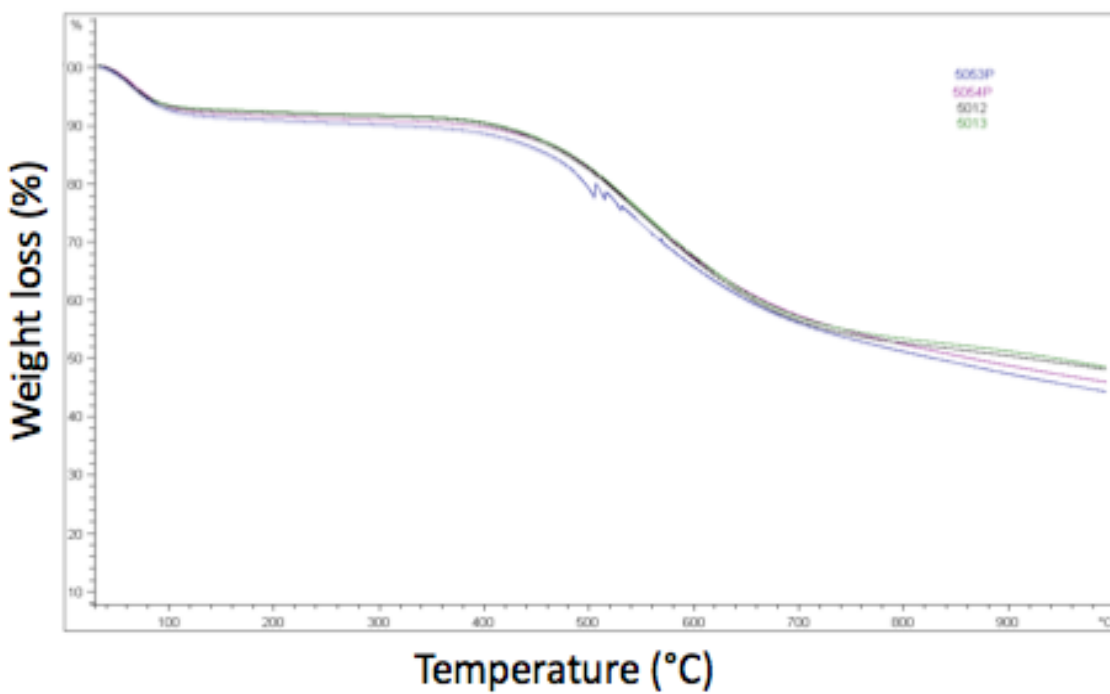


Figure 32 TGA curves of selected samples after stabilization from room temperature to 1000°C

4.2.1.3 Changes during stabilization

Table 6 and 7 have the temperature and residence time alongside the color change during low temperature pyrolysis. The color deepens as the temperature increases. The untreated samples and treated samples with phosphoric acid were profiled.

The DSC curves of the pure and treated rayon during heat treatment at different temperatures are shown in figures 33 and 34. There is an endothermic peak at the beginning of each curves associated with moisture removal. For the untreated samples, there is an endothermic peak at 341°C. The peak disappeared on the DSC curve of the soaked samples (figure 34). The endothermic peak was present for untreated samples A, B, and C. These samples were heated to 150°C, 200°C, and 250°C, respectively. The color changed from white to light yellow to light brown. The peak temperatures are relatively closed. At 300°C (sample D), the endothermic peak is replaced by exothermic peak at 325°C. The peak is evidence of decomposition activities. The color at this stage is dark brown. These reactions started around 280°C. The sample heated to 350°C (sample E) does not show either the endothermic peak or the exothermic peak. The thermal behavior is more stable after 350 °C. Both samples D and E are black that is evidence of higher extent of reactions indicating almost complete stabilization.

The treated samples DSC curves show the effect of phosphoric acid during decomposition. The precursor curve shows an exothermic peak at 260°C. The peak widened for sample Ap that was heated to 150°C for one half hour. As the temperature rises to 200°C (sample Bp), the exothermic peak disappeared with the appearance of a broad endothermic peak. The color is light brown but light yellow for the untreated sample. The color deepened to dark brown when heated to 250°C (sample Cp). This is evidence that phosphoric acid shifted the decomposition to lower temperature. In the untreated samples, changes were not noticed until 300°C. The DSC curves had the same profile for the precursor, samples A, B, and C but the soaked samples curves are different after each heat treatment for half an hour.

Table 6 Stabilization conditions of untreated samples with color change during heat treatment.

Sample ID	Treated with Phosphoric acid	Temperatures (°C) and Stabilization time (min)						Total Time (min)	Color change
		150°C	200°C	250°C	300°C	350°C	380°C		
5012 A	No	30						30	White
5012 B	No	30	30					60	Light yellow
5012 C	No	30	30	30				90	Light brown
5012 D	No	30	30	30	30			120	Dark brown
5012 E	No	30	30	30	30	30		180	Black
5012 F	No	30	30	30	30	30	30	240	Black

Table 7 Stabilization conditions of the treated samples with color change during heat treatment.

Sample ID	Treated with Phosphoric acid	Temperatures (°C) and Stabilization time (min)						Total Time (min)	Color change
		150°C	200°C	250°C	300°C	350°C	380°C		
5053PA	Yes	30						30	White
5053P B	Yes	30	30					60	Yellow
5053P C	Yes	30	30	30				90	Light brown
5053P D	Yes	30	30	30	30			120	Black
5053P E	Yes	30	30	30	30	30		180	Black
5053P F	Yes	30	30	30	30	30	30	240	Black

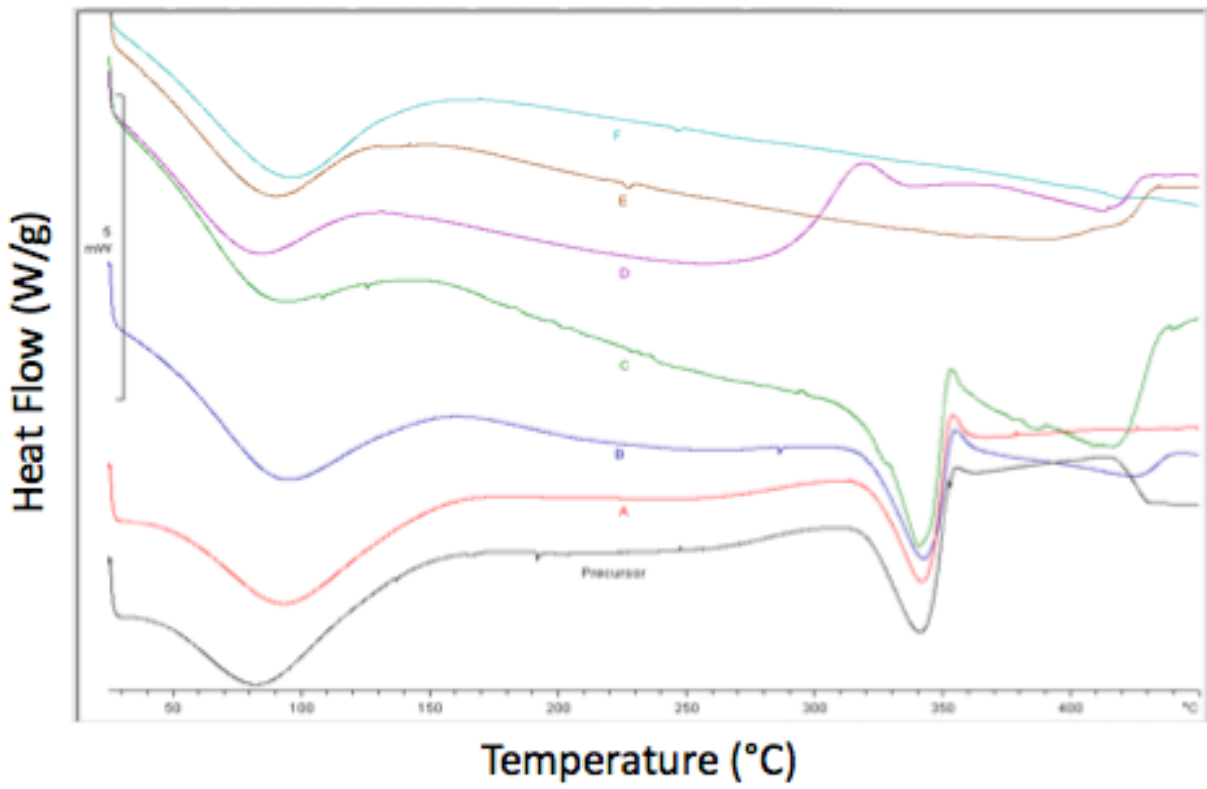


Figure 33 DSC curves of the untreated samples during heat treatment from 150°C to 380°C.

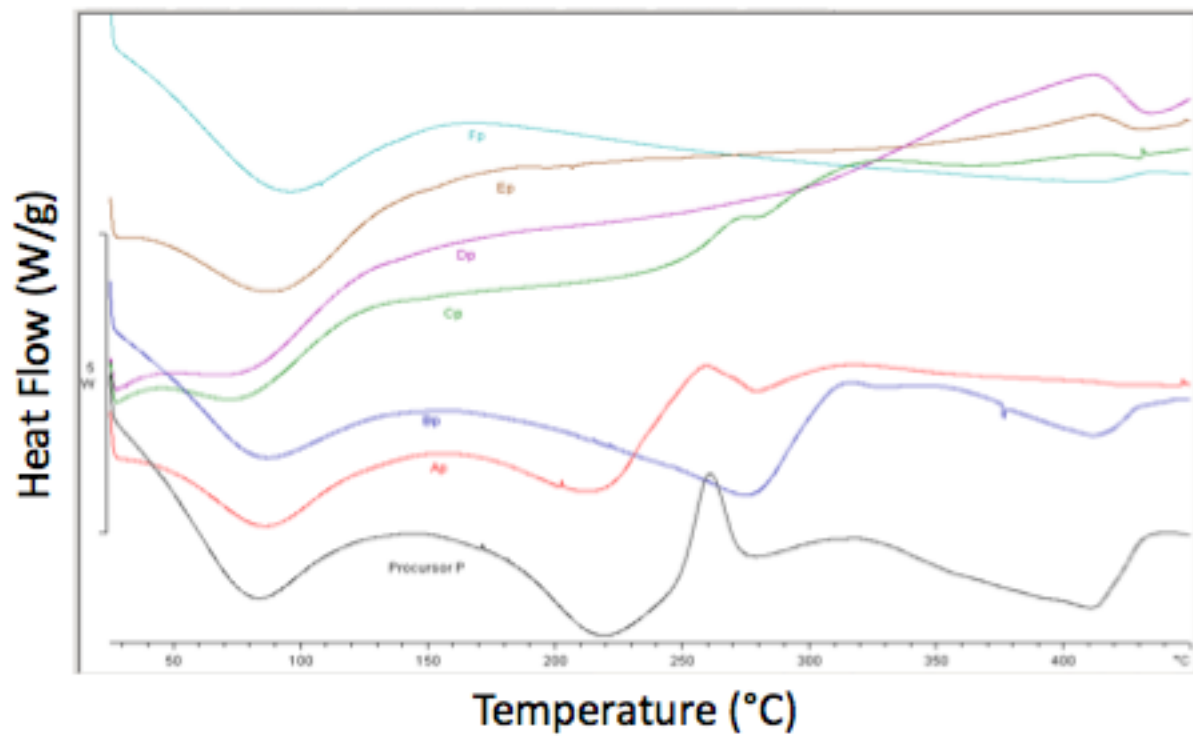


Figure 34 DSC curves of the soaked rayon with phosphoric acid during heat treatment from 150°C to 380°C.

There are chemical changes during pyrolysis associated with the physical changes. An example of physical change is the break down of crystallite structure and recrystallization later at high temperatures.

The WAXD patterns of the rayon pretreated with phosphoric acid during low temperature oxidation are shown in figure 35. The pure rayon has a small peak corresponding to $2\theta = 12^\circ$ and a very strong peak at $2\theta = 22^\circ$. These peaks correspond to the 101 and the 002 planes. There are two small double peaks at 38.5° and 42° . After heat treatment at 150°C for 0.5 hour, the double peak at 12° is changed slightly but the $2\theta = 38.5^\circ$ peak increases compared to the pure rayon precursor. Same behaviors are shown at 200°C . As the temperature rises to 250°C , the double peak at 12° starts to disappear and the double peak at 22° become broader. The crystal structure is partially damaged as the peaks became weak. After treatment at 300°C , the small peak at 12° diffused with the large peak at 22° . The results showed that the sample became amorphous with no crystalline order. The original crystal structures of rayon are entirely destroyed. At 350°C , the structure is confirmed to be completely amorphous as there is no a double peak present. At 380°C , a new small peak reappears at 10° with a broad peak starting to form around 25° .

The DSC and WAXD results were helpful to explain the chemical and physical changes occurring during low temperature heat treatment in air. During stabilization, little changes started to occur at 150°C . The untreated fiber (sample 5012A) DSC curve is similar to the precursor curve. The treated sample at the same temperature (sample Ap) curve is different from the treated precursor curve. There is similarity between the curves until the temperature reached 250°C for the untreated fibers. The treated samples curves show changes as the heating temperature increases up to 250°C . The effect of phosphoric acid is shown. The phosphoric acid lowers the degradation temperature. This explains the difference at early stages between the samples. The results are consistent with the color change. Dark colors are reached at much lower temperatures for the phosphoric acid treated fibers. The dark color formation is the result of dehydration. The H^+ in the acid promotes the dehydration and discoloration. The dehydration only changed the crystal structure partially. The WAXD results show very little changes in the

window of 150°C to 250°C. The basic chain, ring, and crystal structure of the cellulose are not damaged. It is important to mention the little change at 250°C marking the starting point of crystal damage. Most damages and changes occurred at 300°C (sample D and Dp). At this temperature, original chemical and crystal structures of rayon disappeared. Sample D showed an exothermic peak. Sample Dp showed the same peak but at a higher temperature. The cellulose break down based on the previous TGA and DSC studies, starts about 280°C. At this stage, the cleavage of bonds, profound degradation and formation of levoglucosan occur. The peaks on the WAXD curve are diffused as the fibers become amorphous at this point. The changes are marked by large rapid weight loss as observed by the TGA curve. The cellulose is transformed to a different material with different properties. The deeper dark color was a sign that hydroxyl, methyl, C-O and water were removed. Between 350°C and 380°C, the peaks disappeared totally on the DSC curves of both the treated and untreated fibers (sample D, F, Dp, and Fp). Only the low temperature endothermic related to moisture desorption is shown. In the 350°C to 380°C aromatization of carbon occurs with CO and CO₂ elimination. At 350°C, the WAXD peak still shows the amorphous character. The depolymerization reaction and later crosslinking don't change the crystallite structure. After 380°C, a new crystal structure started to develop. The appearance of new structure indicated the end of stabilization.

The SEM micrographs in figure 36 show the surface and cross-sections of the stabilized sample. The surface was smooth with high quality fibers. The fiber diameters are smaller after stabilization.

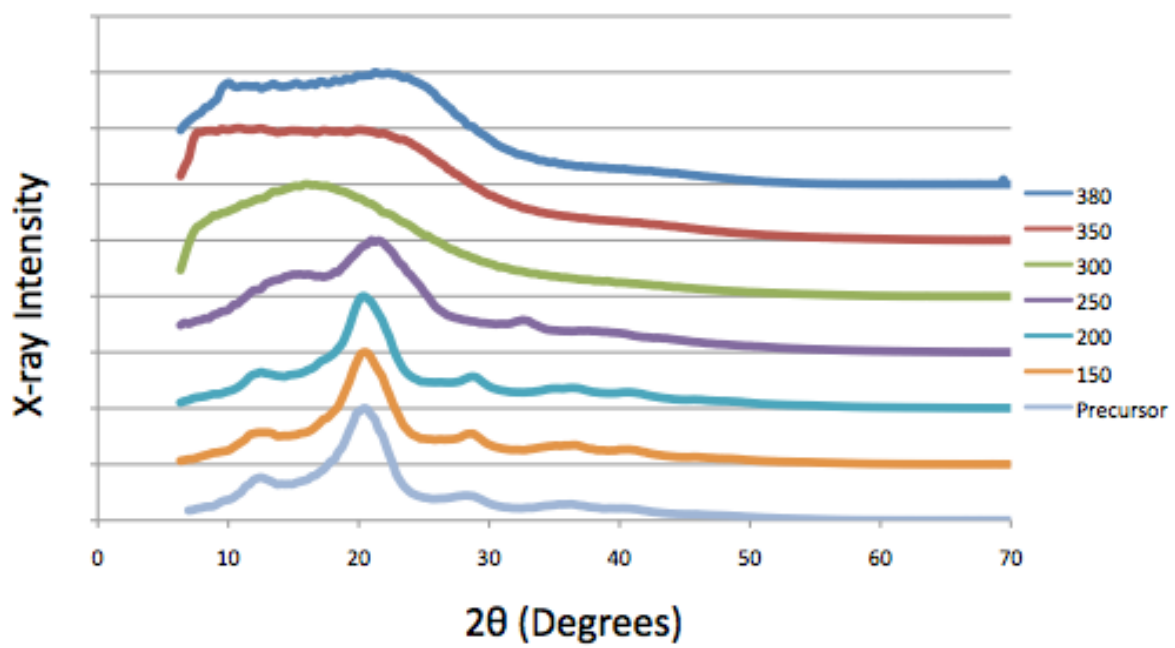


Figure 35 The WAXD of soaked rayon during heat treatment from 150°C to 380°C.

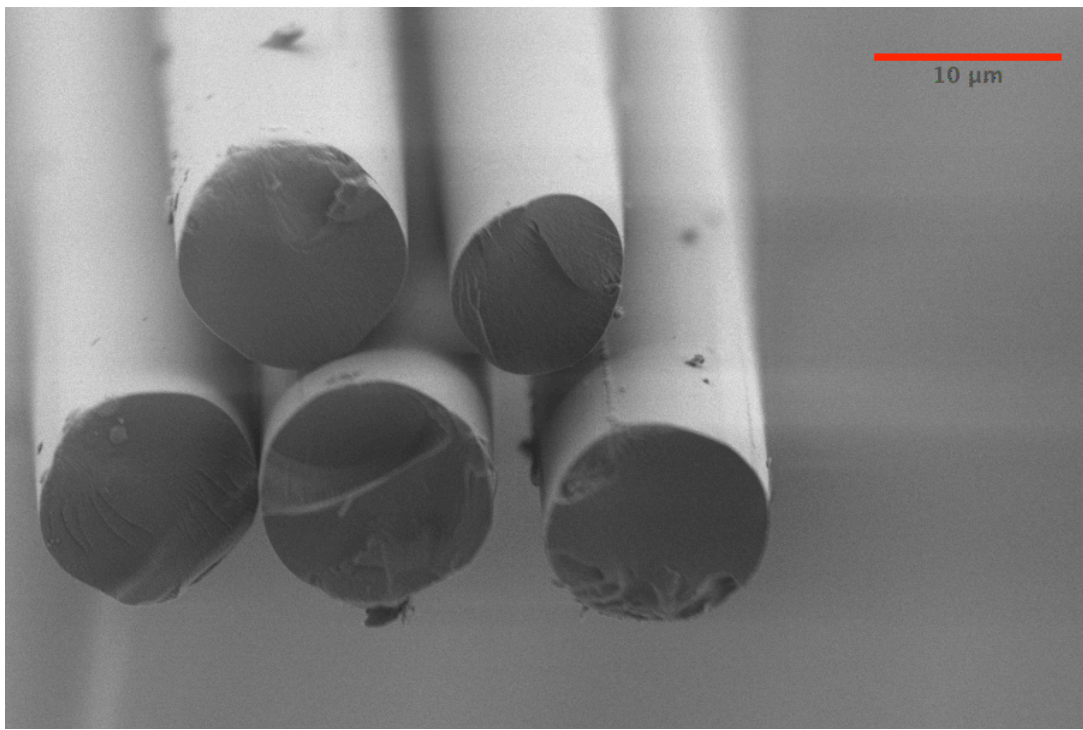
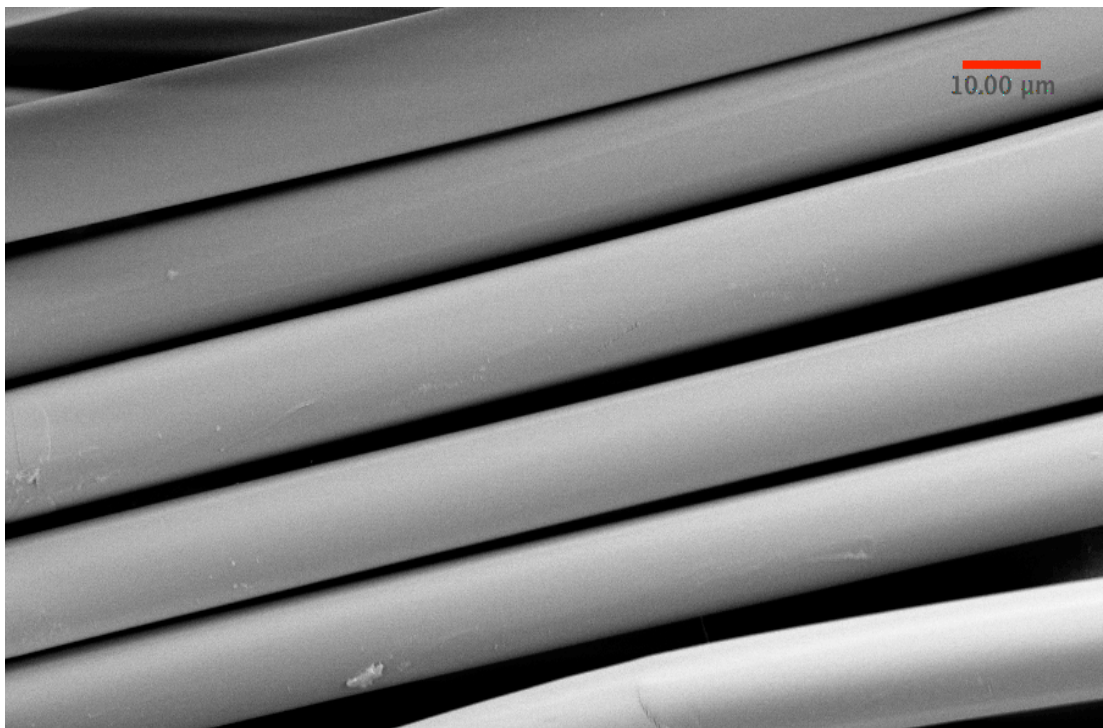


Figure 36 SEM micrographs of surface and cross-section of the treated commercial rayon at the end of stabilization.

4.2.2 High temperature heat treatments (Carbonization)

4.2.2.1 Effect of tension during carbonization

In order to understand the main effects of tension at high temperatures, the carbonization was completed under different loads. All samples were stabilized first from 110°C to 380°C in air for a total time of three hours. The samples were then carbonized from 400°C to 1200°C in nitrogen atmosphere. The loads used to apply tension during the heat treatment were 10g and 50g. The carbonization conditions are recorded in table 8. The commercial rayon was used for the present study.

Table 8 The carbonization conditions.

Carbonization Temp (°C)	400	500	600	800	900	1000	1100	1200
Residence Time (min)	30	30	30	20	10	5	5	5

Note: Applied load for sample 6003 is 10g and applied load for sample 6005 is 50g.

Figure 37 represents the WAXD curves. It was observed that for sample 6003, the major double peaks were at 23° and 44° and for the 6005; the 2θ peaks were at 24° and 44°. The peak at 24° is large and close to the carbon peak observed in the literature. It was suggested that the crystalline structure in the rayon is first damaged at low temperature and recrystallization occurred during high temperature treatment. When the 50g tension was applied, the peak intensity is higher and closer to carbon peak. The 10g sample showed the same peak but it was weaker. According to the literature, the first graphite peak appears at 26° so the carbonized samples are mostly carbon but not graphite.

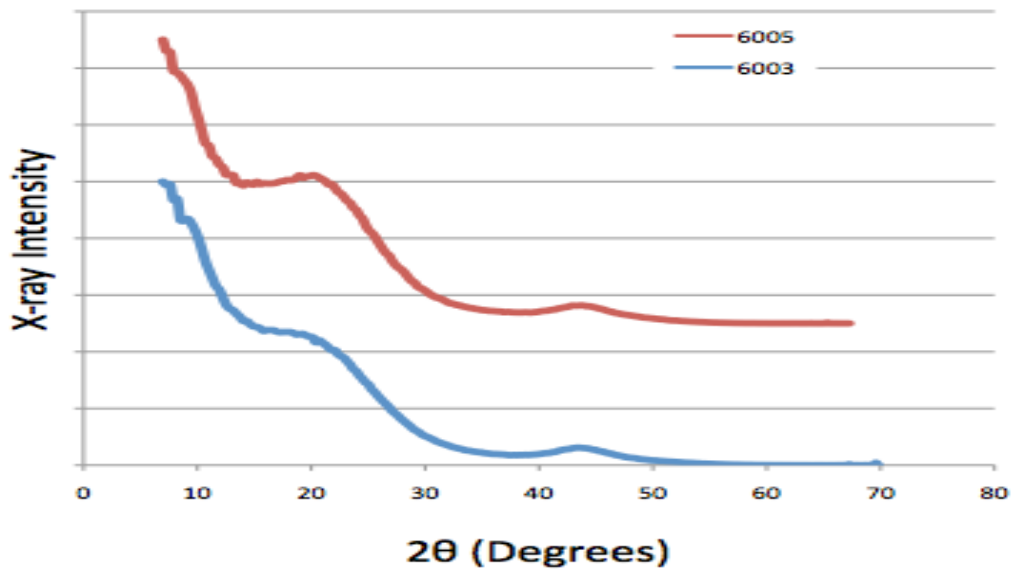


Figure 37 WAXD patterns of samples 6003 and 6005 with different applied tension (10g and 50g) during carbonization.

Table 9 shows the mechanical properties of the samples obtained from single fibers tensile test. The fiber diameter and the carbon content were also recorded.

Table 9 Mechanical properties, fiber diameter, and carbon content of sample 6003 and sample 6005

Sample ID	Tension (g)	Diameter (microns)	Tensile Strength (MPa)	Peak elongation (%)	Modulus (GPa)	Carbon Content (%)
6003	10	8.82	475.87	2.30	36.75	77.46
6005	50	6.72	579.61	0.80	58.83	80.91

It is observed that the fiber diameter decreased with increasing tension. The tensile strengths were 476 MPa and 580 MPa and the modulus were 37 GPa and 59 GPa respectively. The peak

elongations were less than 3%. The mechanical properties were better when the 50g tension was applied. The carbon content also increased slightly with the applied load. The properties are highly influenced by the tension applied during carbonization. The tension affects the orientation distribution of the carbon planes along the fiber axis. Bacon and Tang [112] suggested that repolymerization of the four carbon residue during carbonization involves the longitudinal and transversal polymerization. They reported that longitudinal polymerization results from the four carbon residue aligning with their “long dimension” parallel to the b-axis. Such alignment leads to formation of a chain polymer along the original cellulose chain direction. Application of tension favors the longitudinal repolymerization. The resulting structure is closely packed. This is an effective way to ensure high degree of orientation and thus high tensile strength.

4.2.2.2 Chemical transition and change in structure during carbonization

The stabilized samples were carbonized in nitrogen under different conditions, and the parameters are recorded in the table below. The difference between the samples carbonization conditions is that sample 6002 was held for 2 minutes at 1000°C, 1100°C, and 1200 °C and sample 6003 was held for 5 minutes at these temperatures (Table 10).

Table 10 Carbonization conditions (time and temperatures).

Sample ID	Temp (°C)	400	500	600	800	900	1000	1100	1200
6002	Time (min)	30	30	30	20	10	2	2	2
6003	Time (min)	30	30	30	20	10	5	5	5

The TGA curves in figure 38 showed the changes in thermal behavior from the pure precursor to the carbonized samples. The small weight loss in the 100°C is the removal of moisture. The larger weight loss started at 840°C and finished at 950°C. Sample 6003 had the highest carbon yield at 1000°C. The high carbon yield is due to longer carbonization time from 1000°C to 1200°C. During carbonization, the four carbons residue from stabilization is polymerized to give a new six carbons structure.

The FTIR results are shown in figure 39. The precursor spectra presented the same peaks as the cellulose. The pure rayon precursor spectrum has a large peak at 890 corresponding to the β -D-glucosyl. The intermediate peaks from 940 to 1200 are characteristics of the cellulose ring. The medium peaks at 1300 – 1420, represent the CH₂, OH and CH groups. The sharp peak at 1650 is due to the water molecules. The strong peak at 2900 represents the CH₂ and CH. The very strong broad peak at 3500 is due to the hydroxyl groups. The stabilized sample at 380°C shows the change that occurred after pyrolysis. This is the end of oxidative reactions. The β -D-glucosyl and methylene bands disappeared. The disappearance is the result of scissions of molecular chains and ring structure. The reactions are believed to start around 260°C. The TGA and DSC discussed in early sections support the FTIR findings. The band at 1650 is much bigger and broader. There is an overlap of new absorption of C=C and water peak. The hydroxyl peak at 3500 also disappeared because it was removed during dehydration. The oxidation led to the formation of double bond C=C and C=O. The stabilized sample results reveal the product of cellulose degradation at low temperature. The degradation is believed to occur through dehydration, formation of C=C and C=O groups. The spectrum of the carbonized sample showed a strong peak from 1000 to 1200. The main chemical reactions that are reported at this stage are: aromatization of carbon, polycondensation, and recombination of the four carbons residue to form six carbons ring. The peak at 1600 represents the water molecule. The presence of water can be related to the moisture absorbed by the sample. Most of the other bands disappeared confirming that the samples are mostly carbon.

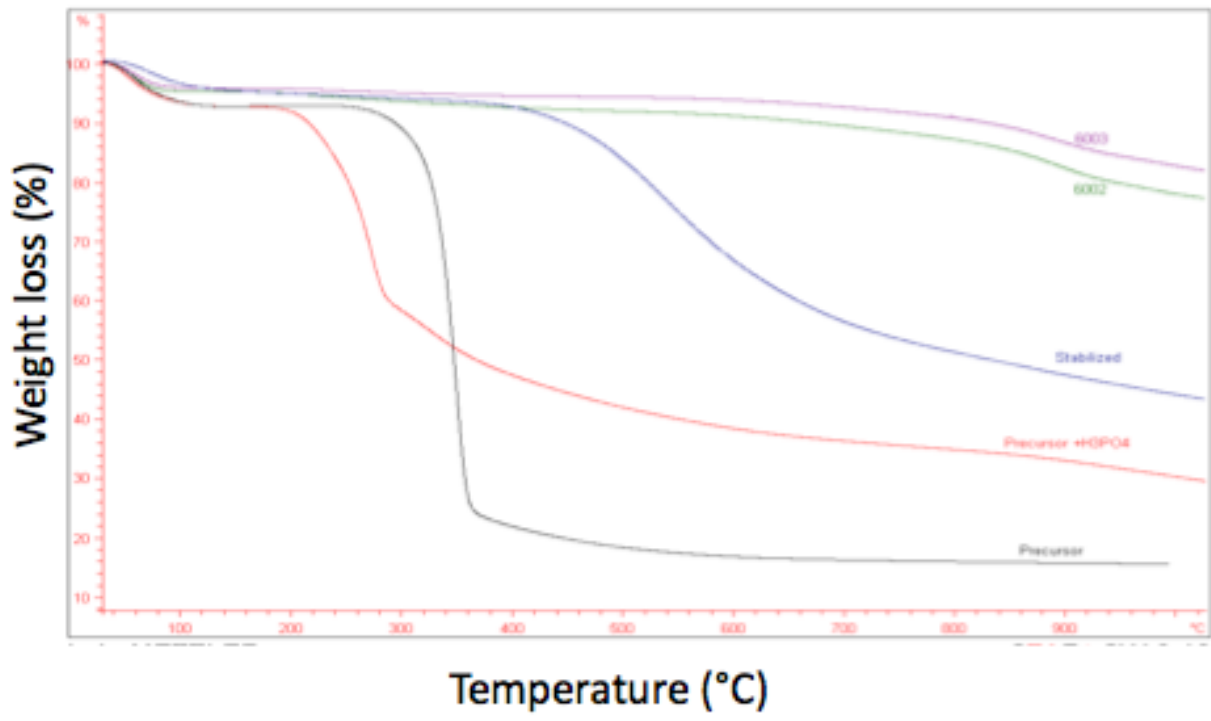


Figure 38 TGA curves of the precursor, the soaked precursor, the stabilized sample, sample 6002 and sample 6003.

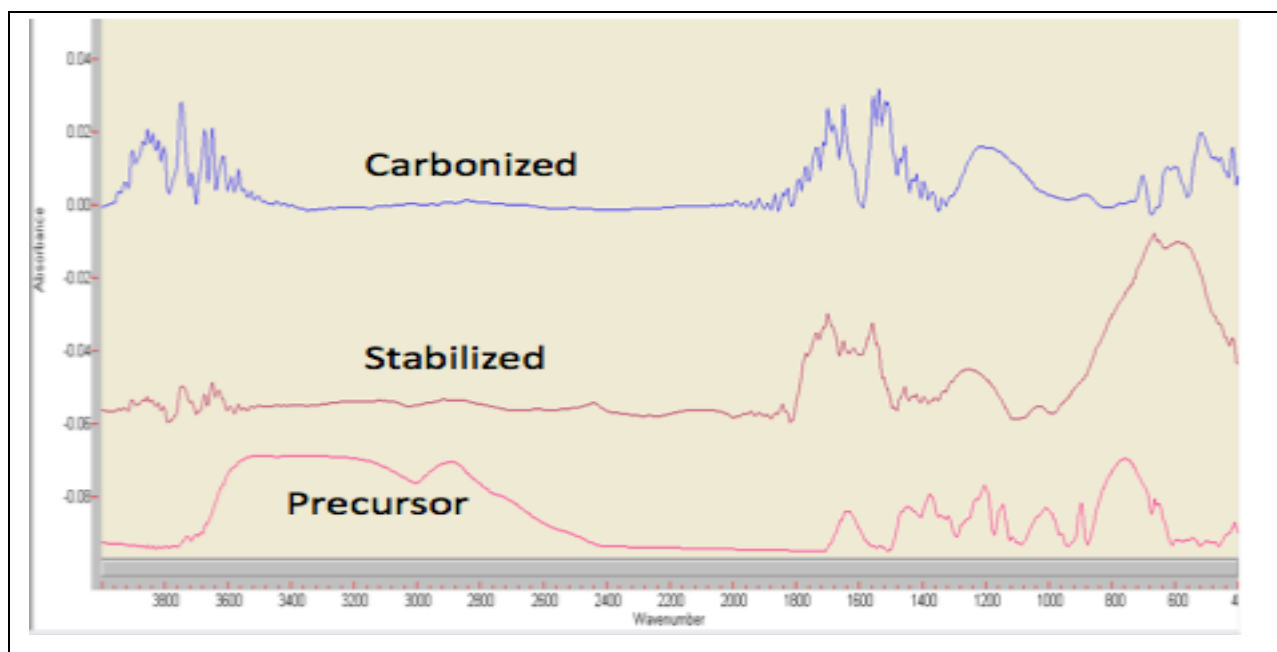


Figure 39 The FTIR spectra of precursor, stabilized and carbonized samples.

The WAXD results are shown in figure 40 at different temperature during carbonization. At 400°C, the sample is partially amorphous. Chain fragmentation during stabilization eliminates orientation and order present in the precursor. There is a double peak at 10° and another peak at 24°. At 500°C, the structure is the same as at 400°C. As the temperature reaches 600°C, both peaks lost intensity. The peaks reappeared at 800°C. A very tiny change occurred at this stage. Polycondensation and aromatization of carbon have been initiated and slowly ordered structure starts to develop. At 1000°C, the peak near 25° appears. This is a sign of crystallization but the crystal size is believed to be small. The crystalline order is still poor. The carbonization temperature is not high enough to enhance crystalline order. At 1200°C, the peak near 25° is broader and the peak at 45° is of low intensity. The sample has higher level of order and a relatively well-established crystal structure. Ruland explained that the original orientation texture of the fiber is almost completely lost during the carbonization process at 240°C, and remains low until 900°C and that rayon fiber with the highest initial orientation produced a carbon fiber with the lowest final orientation.

During the transition from rayon fiber to CF, the content of carbon increased with a simultaneous decrease in the hydrogen content (figure 41). The fibers were dried before the test. The carbon content increase is related to the oxidative reactions at low temperatures and removal of hydrogen atom when volatile gases are released. At 600°C, hydrogen is removed as water and partly in the form of hydrocarbon but above 600°C, it is removed as carbon containing compounds. Sample 6003 has higher carbon content. The TGA curves also showed a higher carbon yield at 1000°C. The longer residence time from 1000°C to 1200°C explains the difference in carbon yield between the 6002 and 6003 samples. The higher the treatment temperature, the higher the carbon content, and better carbon structures are formed.

The fiber diameter also changes with temperature. As seen in figure 42, the sample diameter decreases after carbonization at 1200°C. The SEM delineated a much smoother surface. The fibers appear to be of higher quality. It is mainly due to the usage of phosphoric acid. The EDAX results (figure 43) are consistent with the elemental analysis results. The results show how

oxygen decreases during transition of rayon fibers to CFs. The results also reveal the presence of phosphorus in all three samples (precursor, stabilized and carbonized fibers).

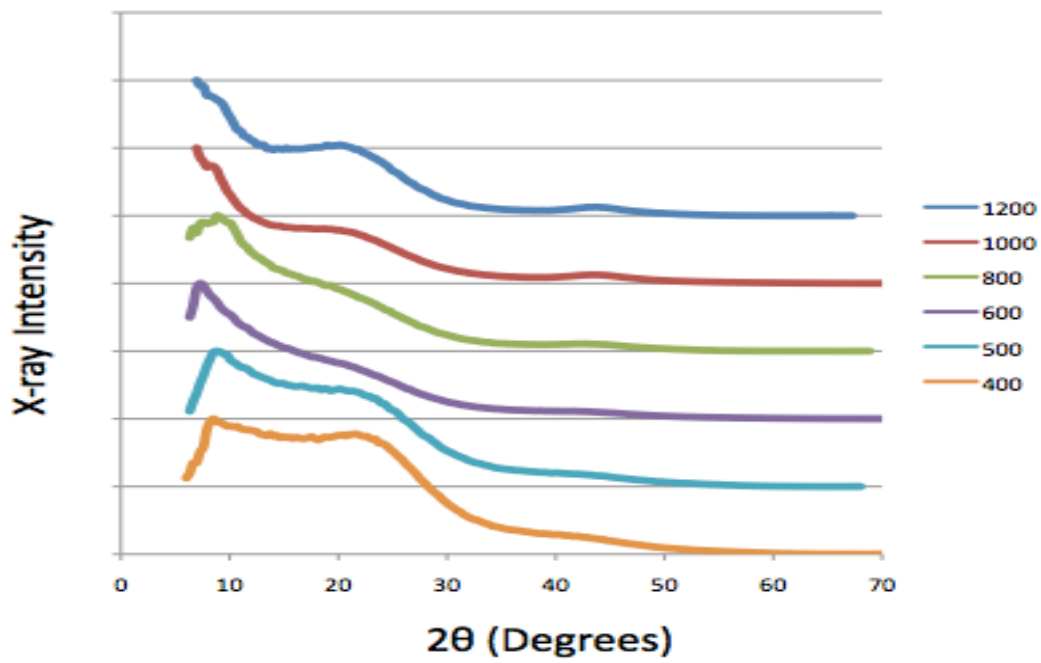


Figure 40 The WAXD of soaked sample during carbonization from 400C to 1200C in nitrogen.

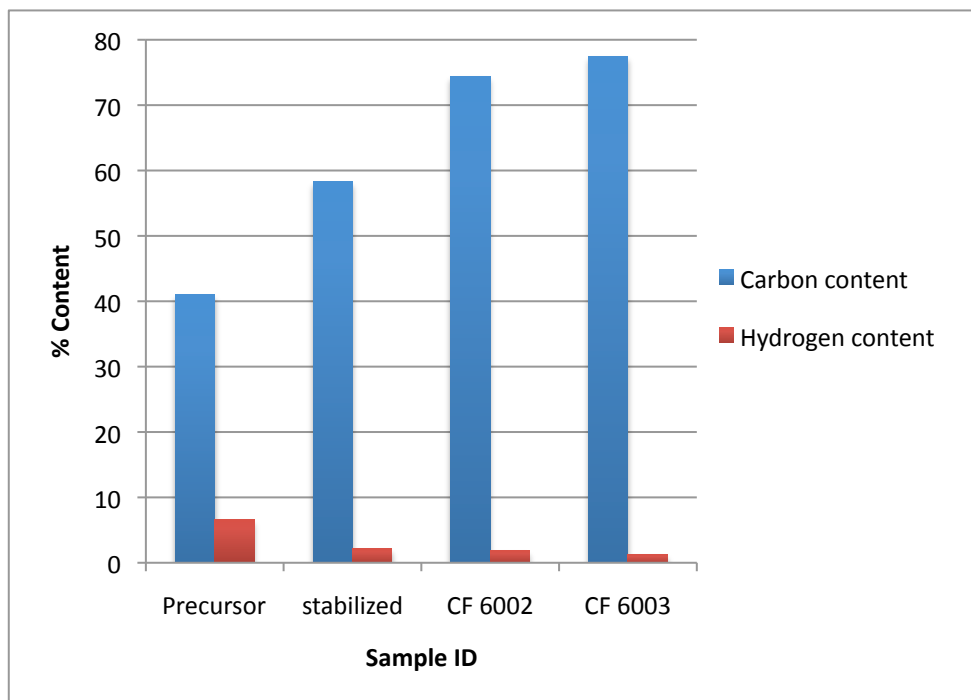


Figure 41 Elemental analysis results showing carbon and hydrogen content.

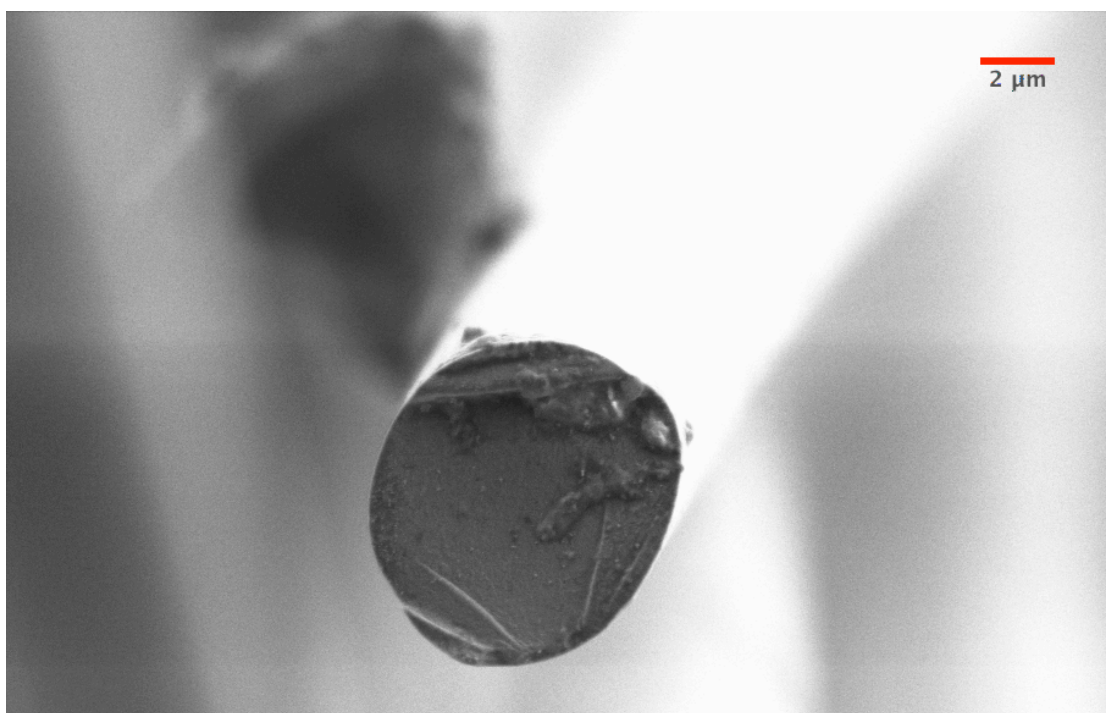
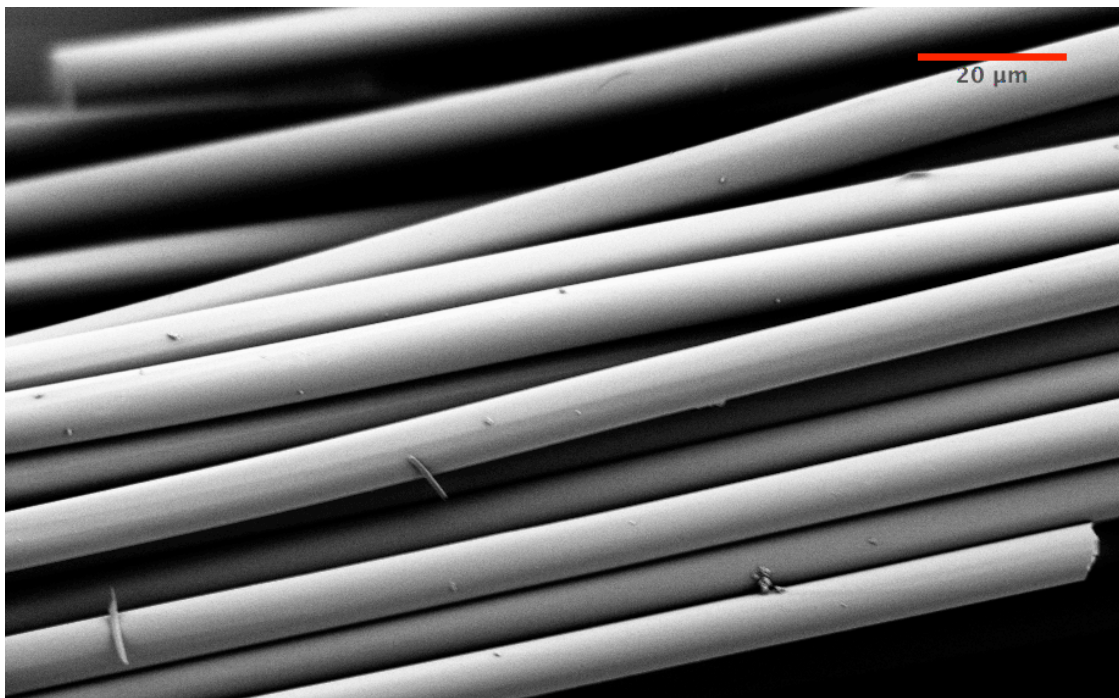


Figure 42 SEM micrographs of the surface and cross-section of the carbonized sample.

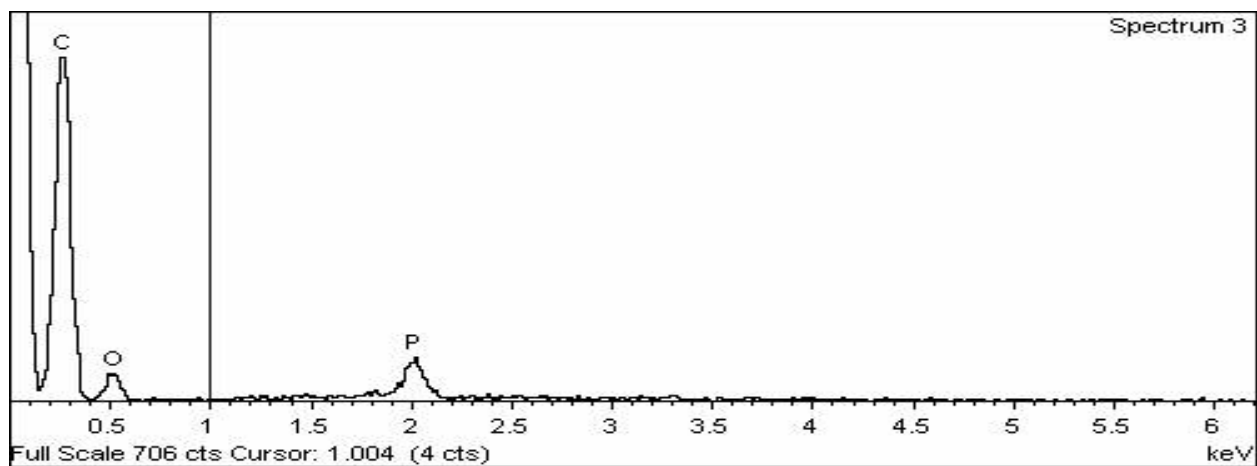
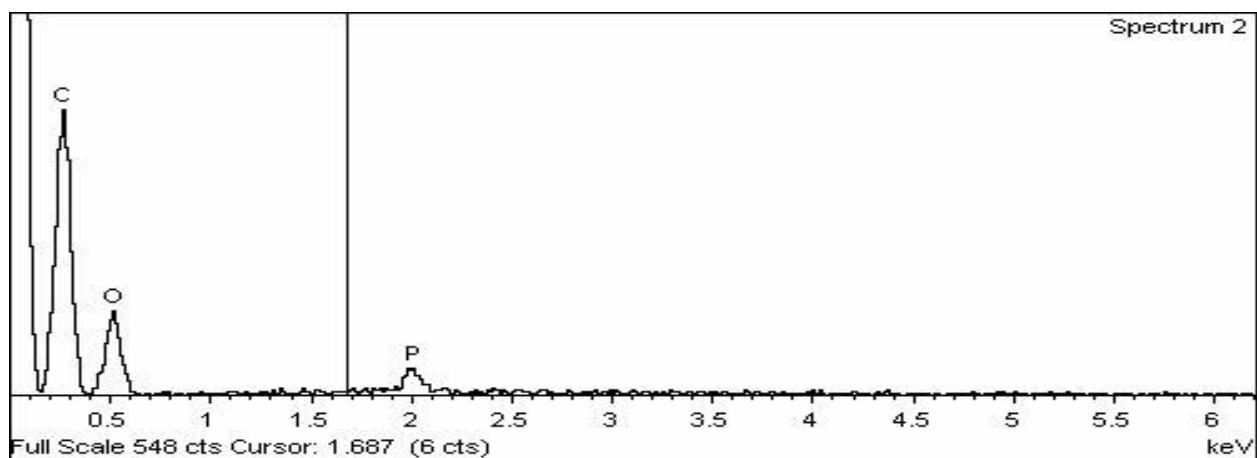
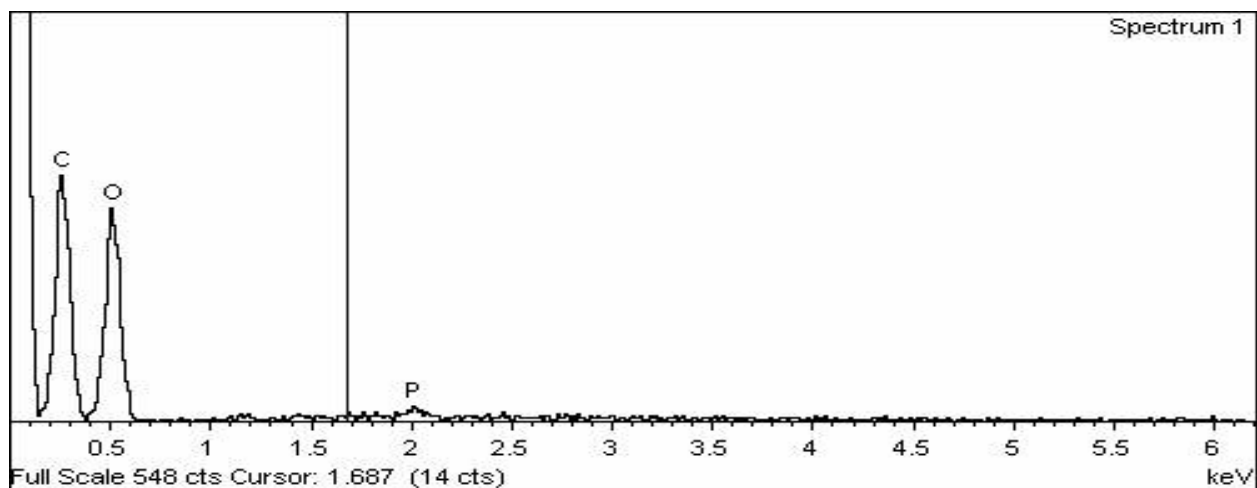


Figure 43 EDXA results of the commercial rayon precursor, the stabilized fibers to 380C and the carbonized fibers to 1200C respectively.

4.2.3 Mechanical properties

Table 11 Mechanical properties and fiber diameter of the precursor, the stabilized (6001) and carbonized samples (6002, 6003).

Sample ID	Diameter (microns)	Tensile Strength (MPa)	Peak elongation (%)	Modulus (GPa)
Precursor	14.98	275.57	8.20	32.35
6002	7.46	550.96	1.06	53.26
6003	6.72	579.61	0.80	58.83

The mechanical properties along the fiber diameter are recorded in table 11. The properties are compared with the precursor to show the change of mechanical properties at the end of carbonization at 1200°C. The mechanical properties are better based on time and temperature of treatment. Sample 6003 was treated for longer residence time and presents better mechanical properties. The tensile strength was 580 MPa and peak elongation less than 1%. It is well established that the temperature increase causes a modulus decrease and tensile strength increase to a maximum value. The average tensile strength for the precursor is 275 MPa. However, carbonization to 1200°C increased the tensile strength to as high as 580 MPa. This value is significantly lower than the tensile strength of commercially available carbon fibers, but such high values are obtained upon pyrolysis at much higher temperatures. As discussed previously, the four-carbon structure is an important piece in the process of producing rayon-based carbon fibers. Bacon and Tang explained that the four-carbon structure repolymerization and how it affects properties. The application of tension on fibers during carbonization is an effective way to ensure the repolymerization reactions in the longitudinal path. This results in higher degree of orientation and higher tensile strength. It is important to note that the 1200°C was not high enough for the formation of graphitic structure.

4.3 Precursor II: Experimental rayon fibers

Unlike with the commercial precursor, the studies were done with this precursor only with phosphoric acid pretreatment. The samples were kept in a normal solution of phosphoric acid for 5 hours and dried at room temperature for 2 hours.

4.3.1 Low temperature heat treatment

Recall that all samples were stabilized from 110°C to 380°C with a tension of 10g (Table 2). The data in table 12 show how the fiber diameter changes during stabilization. The diameter changes with temperature and time. The shrinkage percentage is in the range of 10 – 15%. The highest shrinkage is observed in sample 502. Sample 502 has the lowest heating rate. The considerable shrinkage is associated to loss of water molecules followed by cleavage of C-C and C-O linkages. All three samples were treated with phosphoric acid. The acid, as explained early plays a role of protecting agent and flame-retardant. The samples did not burn when thrust in flame after stabilization meaning the samples should withstand the high temperatures of carbonization.

Figure 44, shows the TGA curves of the precursor, soaked precursor and the stabilized samples. All samples have small weight loss in the 100°C region, which is related to moisture removal. The soaked precursor as expected shows a rapid weight loss starting at 180°C to 300°C, compared to the as- received precursor, for which the rapid weight loss did not start till 280°C. The results are consistent with the DSC curves in figure 45. There is an endothermic peak in the 100°C for both samples. The as received precursor has another endothermic peak at 340°C. The soaked precursor, shows the same peak but at lower temperatures (around 220°C). These results show the effect of phosphoric acid on stabilization. The phosphoric acid accelerated the pyrolysis reactions. It catalyzed the dehydration reaction. The fibers are protected and the pyrolysis reaction occurred from fiber surface to fiber core with tempered speed. The acid prevents the formation of skin-core structures at the surface. These results are consistent with what was observed for the commercial fiber.

The TGA scans of the stabilized samples show the rapid weight loss starting at 400°C. The low temperature stabilization changed the fiber structure. The stabilized samples had the smallest weight loss at 1000°C and high carbon yield because the acid suppressed the release of volatile organic substances and a great portion of the original fiber is conserved. All three stabilized samples TGA curves are similar. The SEM micrographs of the stabilized samples are shown in figure 46. The micrographs delineated smooth surfaces of the fibers. The cross section micrograph shows a hole in the center of the fibers. This is probably due to the rapid stabilization and larger diameter of the precursor fibers.

Table 12 Fiber diameter, shrinkage and burning test of the precursor and stabilized samples.

Sample ID	Fiber diameter (micron)	Shrinkage (%)	Burning test
Precursor	18.99	N/A	Burn
502	13.11	15	Did not burn
503	12.46	14	Did not burn
504	14.23	10	Did not burn

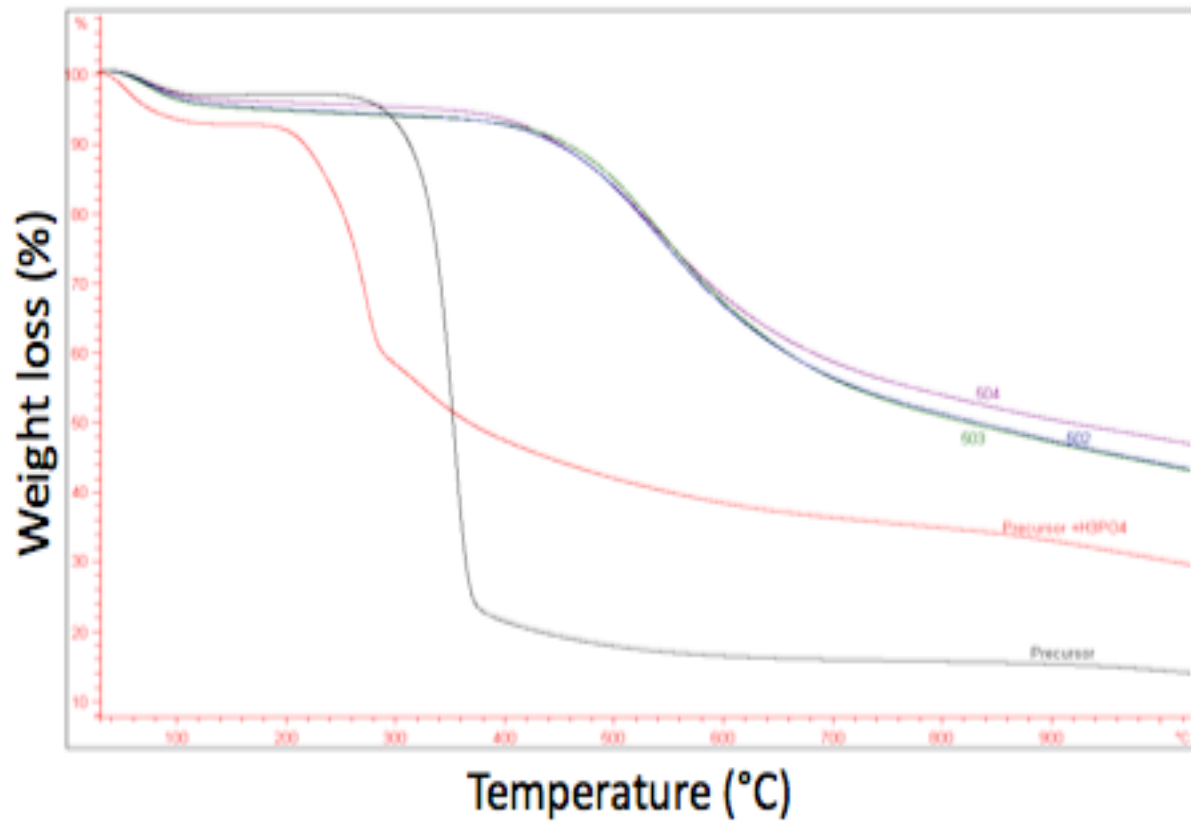


Figure 44 TGA curves of the precursor, the soaked precursor and the stabilized samples (502, 503 and 504) from room temperature to 1000°C in nitrogen.

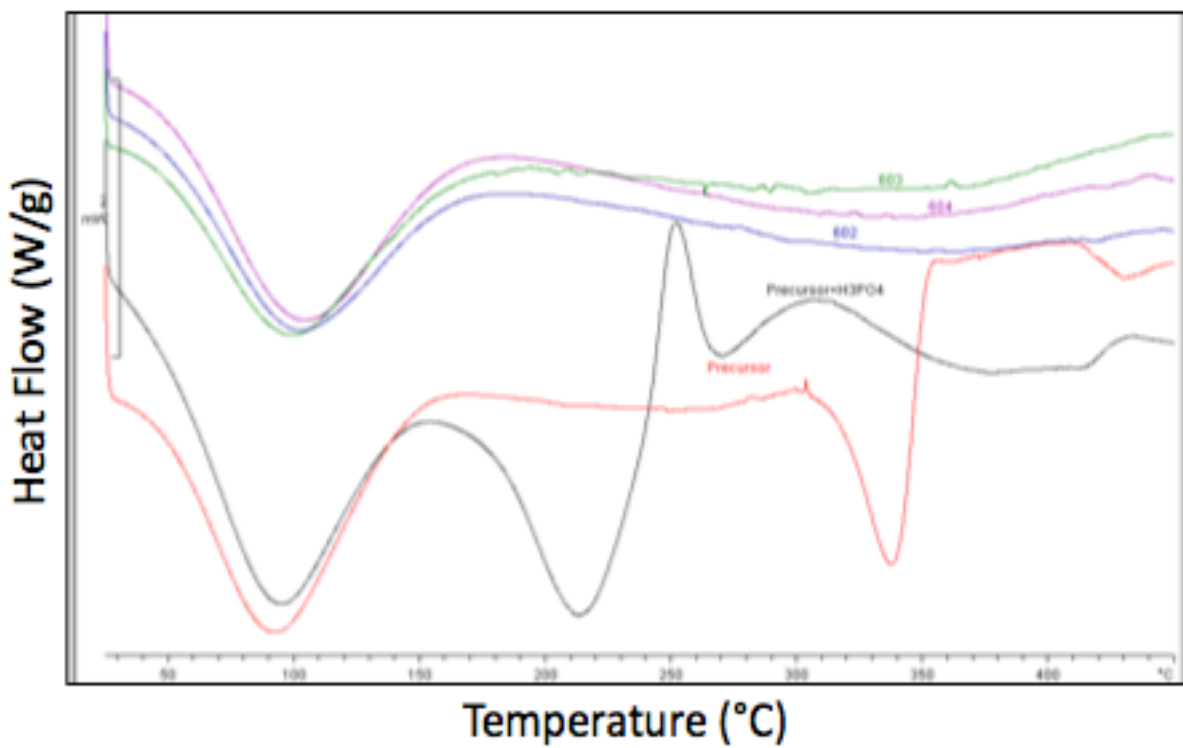


Figure 45 DSC curves of the precursor, soaked precursor, and the stabilized samples (502, 503, 504) from room temperature to 450°C in nitrogen.

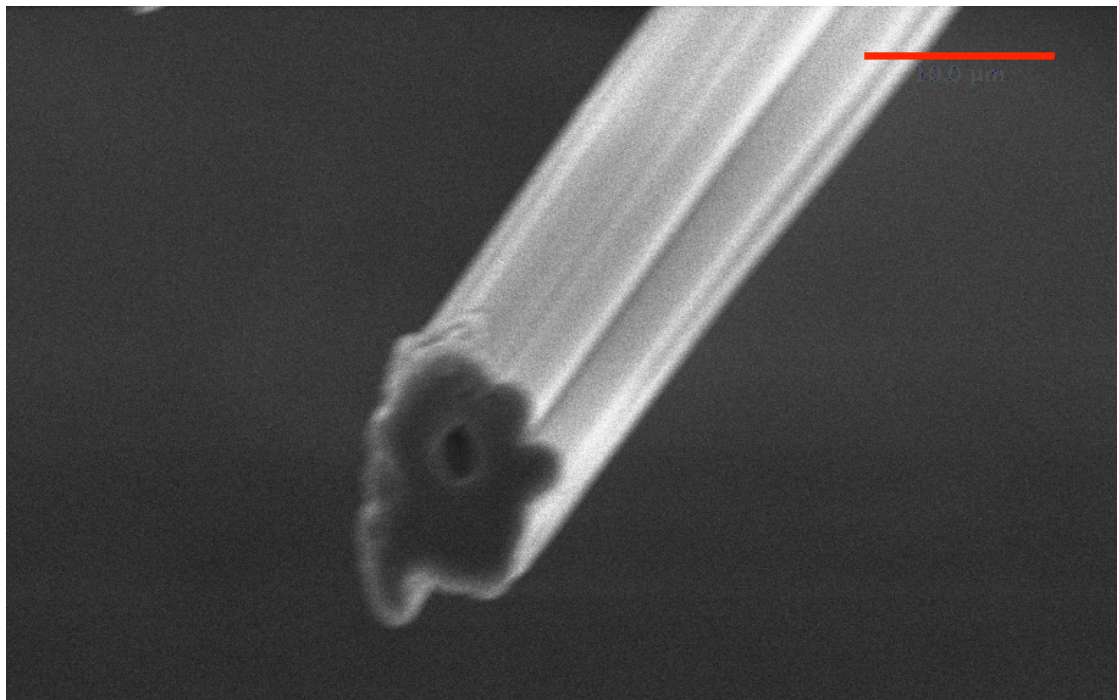
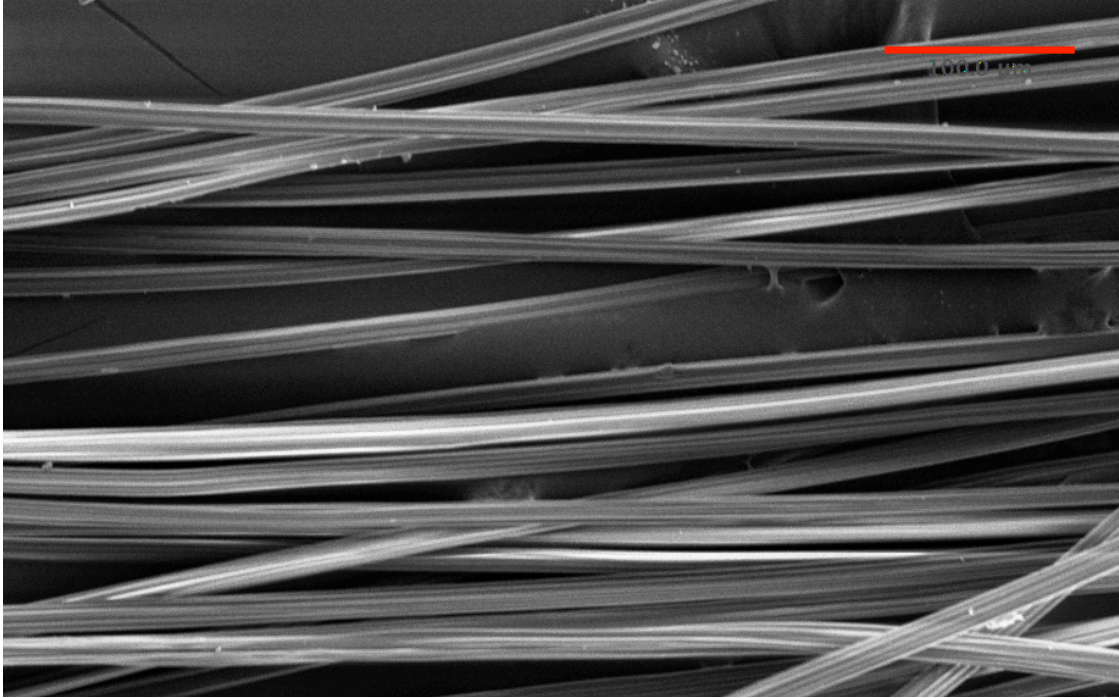


Figure 46 SEM micrographs of the surface and cross-section of the stabilized sample at 2KX.

4.3.2 High temperature heat treatment

After the stabilization, the fibers were carbonized under conditions shows in table 13.

Table 13 Carbonization conditions.

Carbonization Temp (°C)	400	500	600	800	900	1000	1100	1200
Residence Time (min)	30	30	30	20	10	5	5	5

Figure 47 shows the TGA curves of the transition of the precursor to the carbonized samples. As discussed before, the small rapid loss around 100°C is due to moisture removal. During the transition, the effect of phosphoric acid is noticeable. The carbonized sample (506) does not show any weight loss till after 900°C, the loss is minimal and less than 2%. Carbonization at much higher temperature is required to avoid this minimal weight loss. The carbonized sample had the highest carbon yield at 1000°C because the four- carbon residue from stabilization is polymerized during carbonization stage to give new six carbons structure.

FTIR was used to investigate changes during the transition to carbon fiber. The FTIR results are shown in figure 48. The very strong broad peak at 3500 is due to hydroxyl disappeared gradually from precursor to carbonized samples. Also the β -D-glucosyl and methylene bands disappeared at the end of stabilization due to scissions of molecular chains and ring structure. A new large peak appeared from 1000 to 1400. The peak is a result of numerous chemical reactions that occurred during carbonization. The main reactions are aromatization of carbon, polymerization, and recombination of the four carbons residue to form six carbon rings.

The XRD results in figure 49 shows the structure change during CF production. The pattern for precursor fiber shows 2θ peaks at 14°, a large peak at 23° followed by 3 small peaks at 30°, 35° and 42° indicating good amount of order. After stabilization at low temperatures in air, the crystalline order is completely damaged and the structure is amorphous. During stabilization,

chain fragmentation eliminates any order present in the precursor. Disorientation of cellulose started at 250°C and continued till about 350°C. As the treatment temperature increased to 1200°C, a large peak appeared at 25°. The peak is believed to be that of carbon. The temperature is not high enough to show complete graphite peak.

The elemental analysis in figure 50 shows an increase in carbon and decrease in hydrogen due to the reactions as expected. During low temperature stabilization, as discussed early, many reactions occurred. These results are consistent with the TGA results. Hydrogen is removed as water and partly in form of hydrocarbons at temperature higher than 600°C. It is found that high temperature treatment leads to high carbon content and more developed carbon structure. The cellulose polymer degrades at low temperatures through dehydration and cross-linking reactions leaving the sample with slight increase of carbon content. As the temperature rises, rearrangement of cellulose structure occurs and promotes the production of char residue rich in carbon. The EDAX results (figure 52) also show the change in oxygen content and the presence of phosphor. The oxygen content decreased during the transition to carbon fibers. The minimum oxygen present can be reduced further by carbonization at higher temperatures.

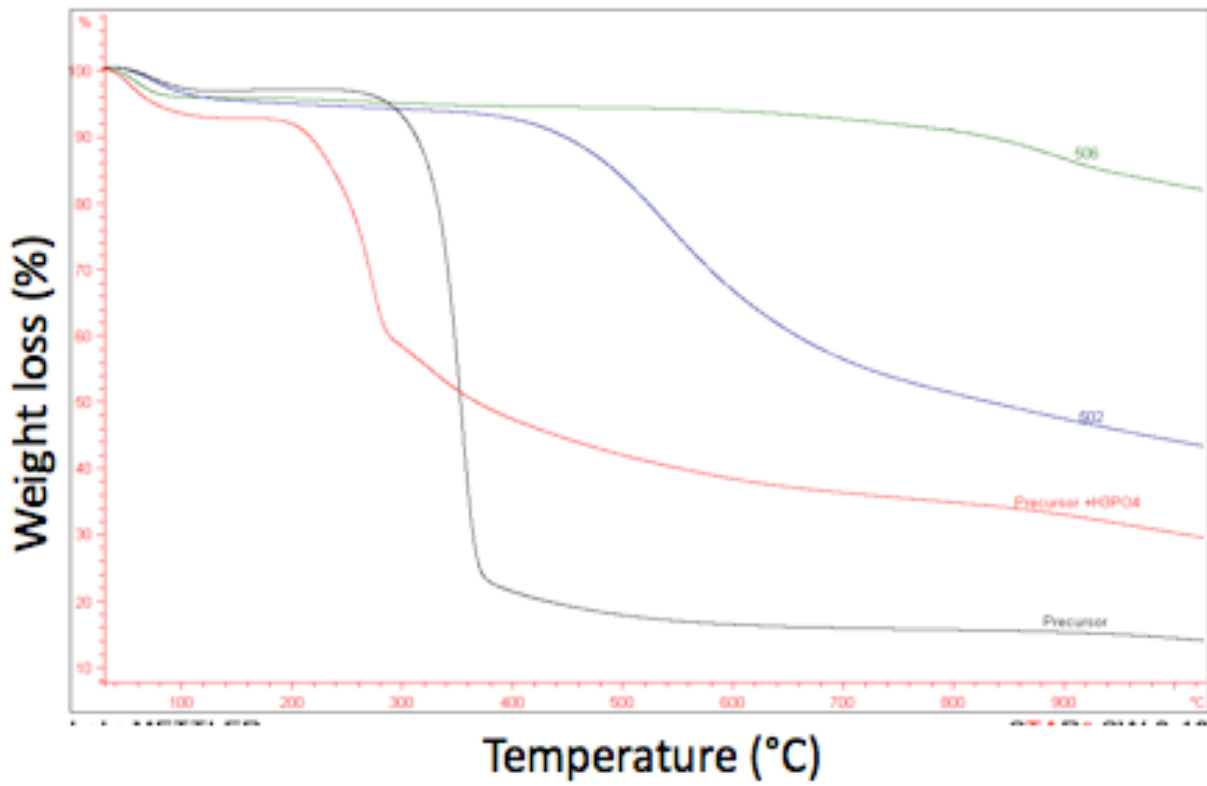


Figure 47 TGA curves of the precursor, soaked precursor, stabilized (502) and carbonized sample (506).

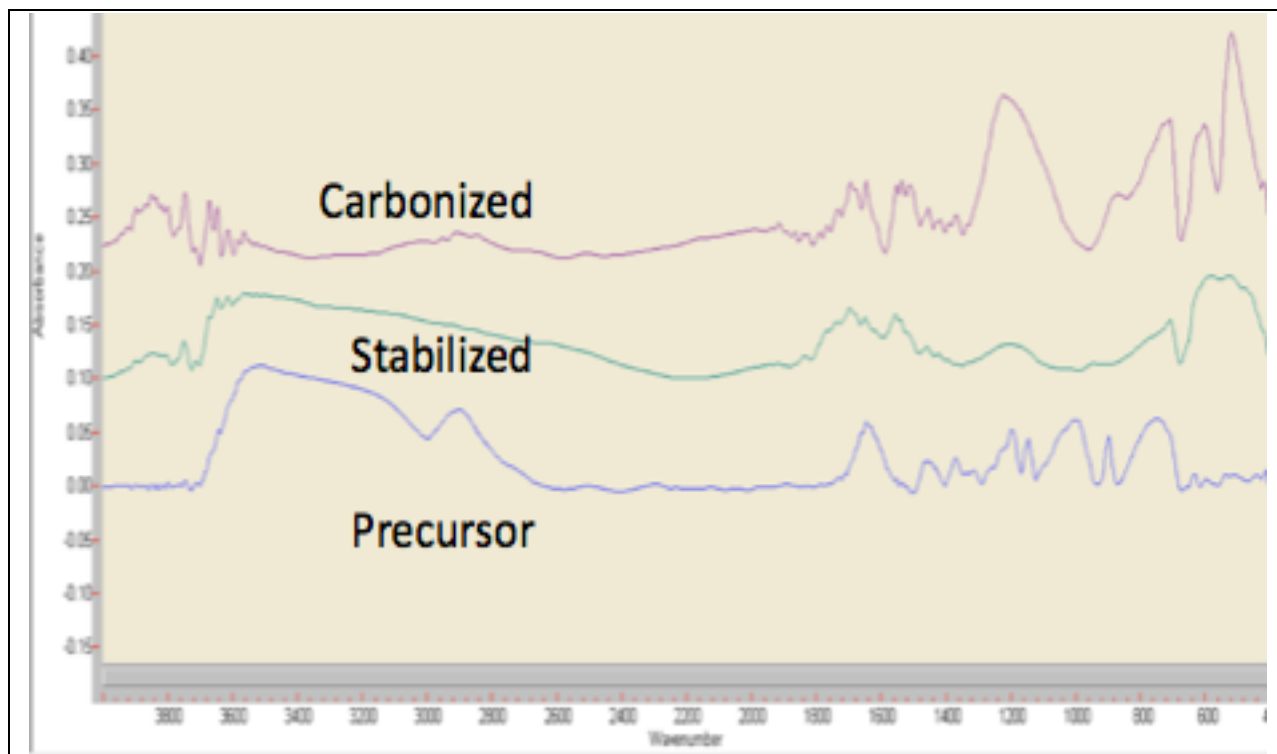


Figure 48 FTIR spectra of the experimental rayon (precursor, stabilized and carbonized samples).

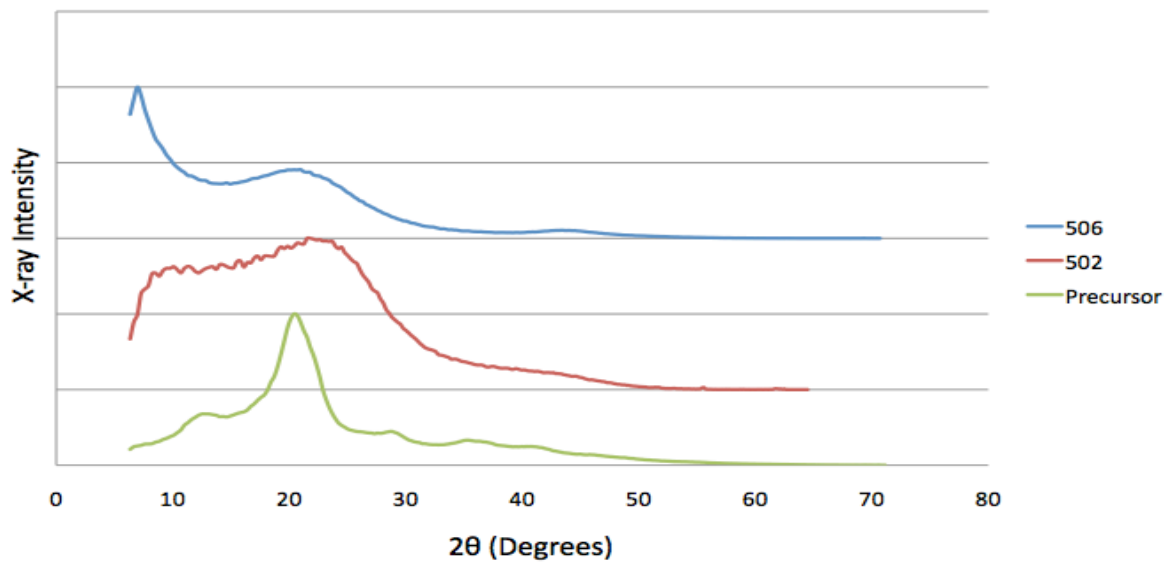


Figure 49 The WAXD patterns of the experimental rayon (precursor, stabilized and carbonized).

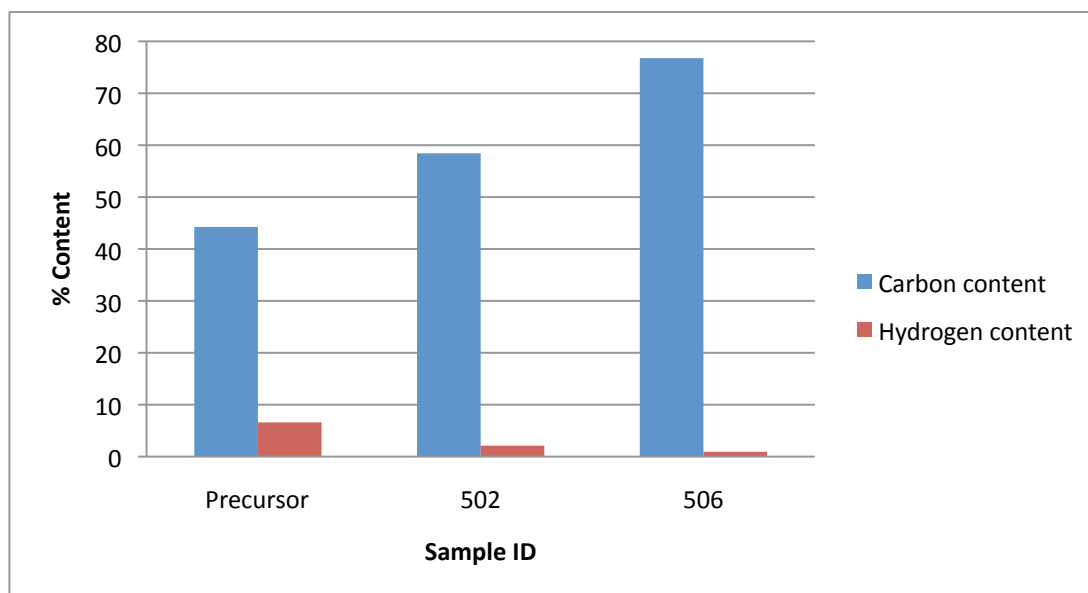


Figure 50 Elemental analysis results showing carbon and hydrogen content.

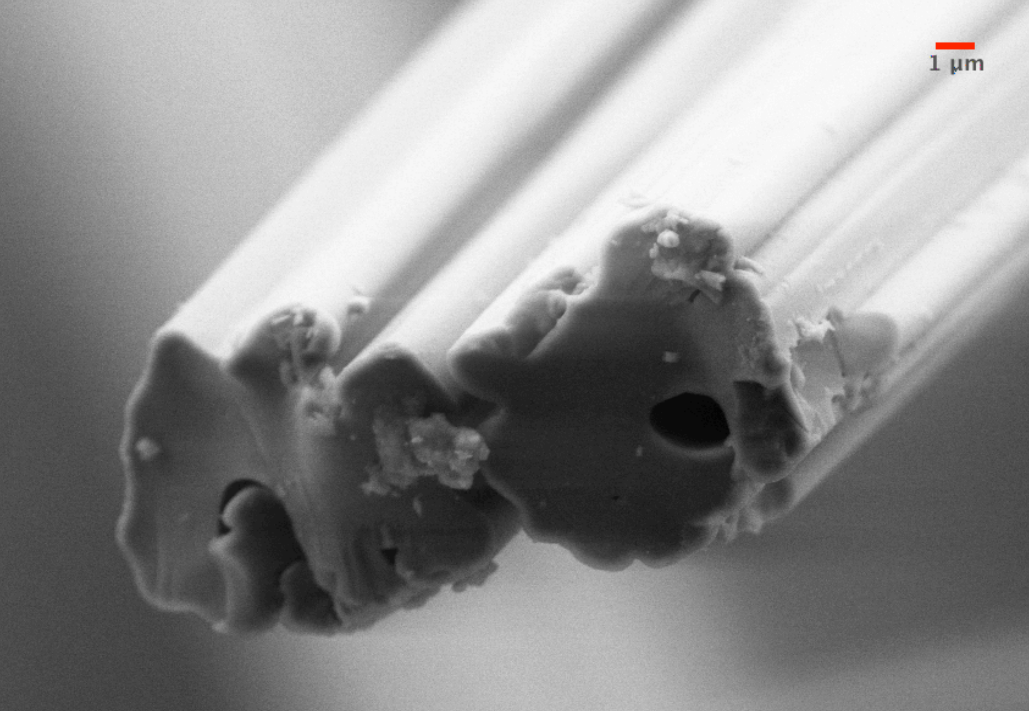
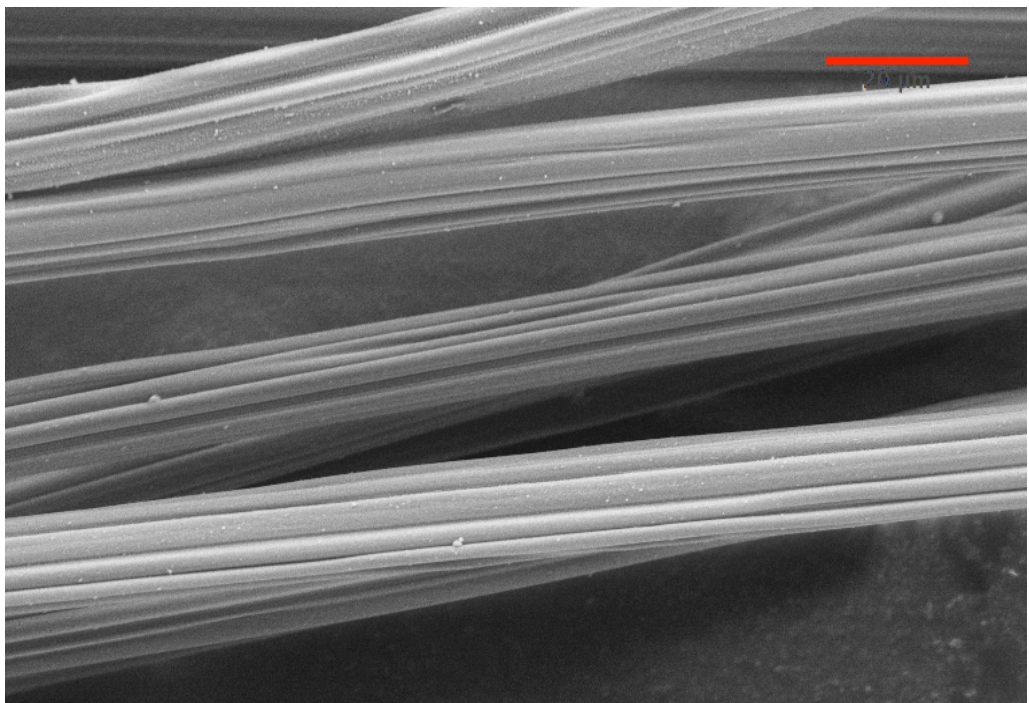


Figure 51 SEM micrographs of surface (5KX) and cross-section (10KX) of the experimental rayon fiber at the end of carbonization.

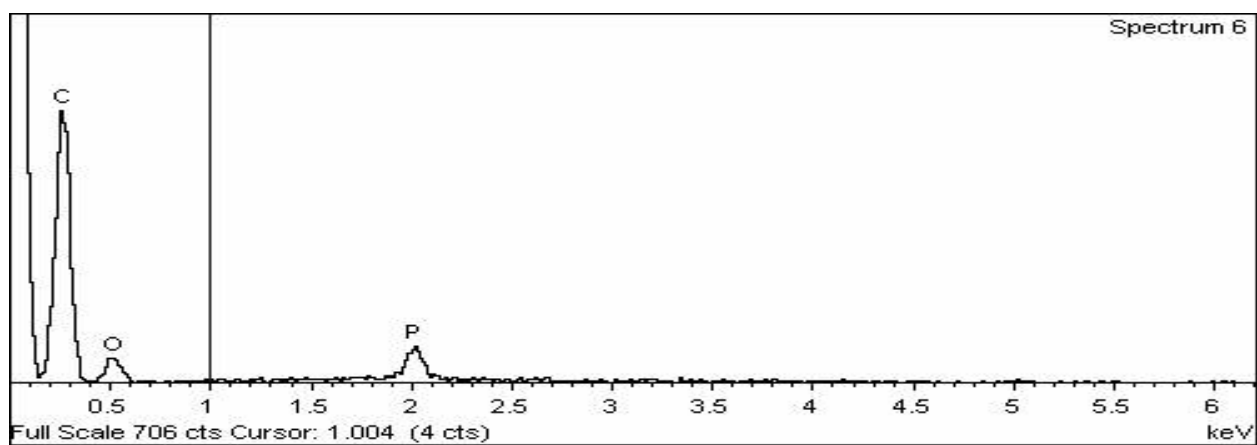
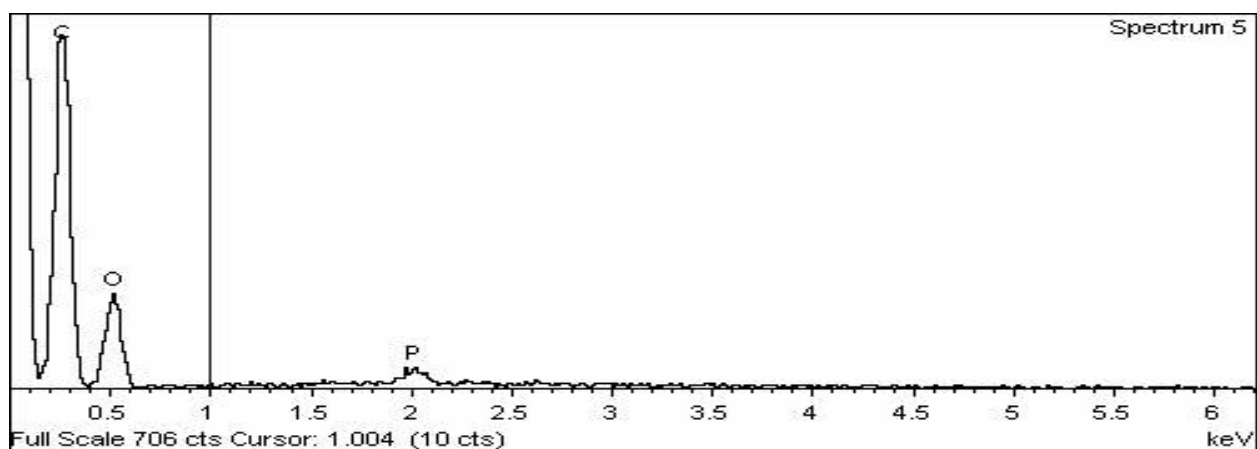
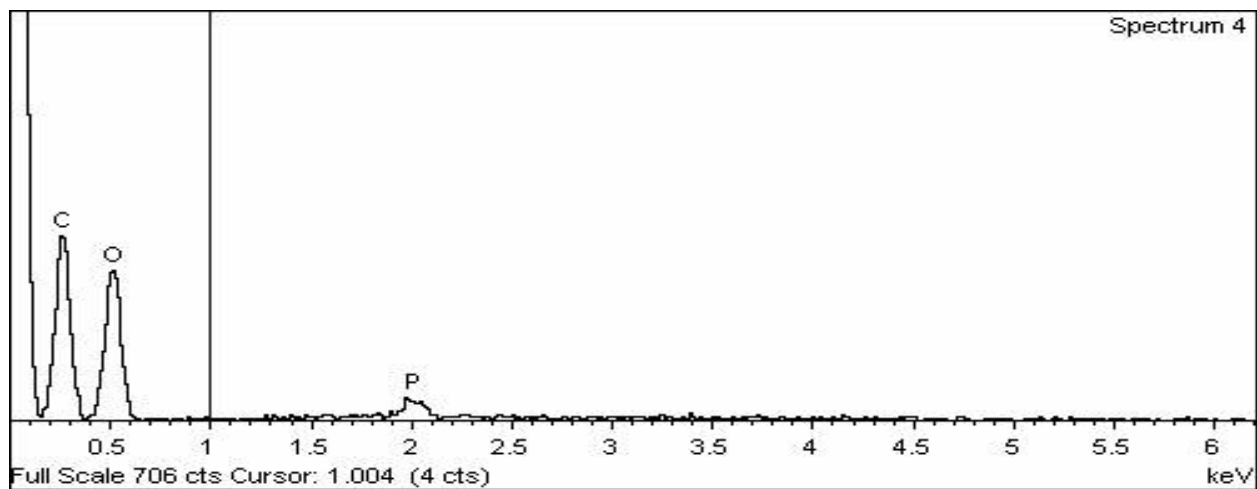


Figure 52 EDXA results of the precursor, stabilized and carbonized samples respectively.

4.3.3 Mechanical properties

Table 14 Mechanical properties and fiber diameter of precursor and carbonized sample

Sample Id	Fiber diameter (microns)	Tensile strength (MPa)	Peak elongation (%)	Modulus (GPa)
Precursor	18.99	174.69	5.21	26.71
506	10.52	349.43	0.68	46.57

The carbon fiber has a tensile strength of 349 MPa, the peak elongation of 0.67% and modulus of 47 GPa. The mechanical properties almost double in value as the fiber diameter decreases. Many parameters affect the improved mechanical properties. The temperature, treatment time, phosphoric acid as protective media, and tension applied all play an important role in the structure and texture of the produced fibers. The effects of each of these parameters were described in detail during the present study in previous sections. The overall mechanical properties could be improved by further treatment at higher temperature.

4.4 Comparison of commercial and experimental fibers

Two different rayon fibers used in the present investigation were a commercial grade rayon fiber and an experimental rayon fiber.

The experimental rayon fiber diameter was higher and tensile properties were poorer compared to the commercial fibers (Table 15). The reason is the difference in fiber structure

and texture. The experimental rayon has a fibrillar texture along its longitudinal direction. Both precursors were stabilized under similar conditions and the results were similar. The TGA curves in nitrogen show major degradation starting at 304°C for the experimental rayon and 317°C for the commercial rayon. The TGA in air curves also show the same pattern with degradation starting at 285°C and 305°C respectively. These degradation temperatures affect the stabilization time and temperature for each precursor. The phosphoric acid had the same effect on both the precursors and was found to be a useful catalyst for transition to carbon fiber.

The produced carbon fibers from both precursors mechanical properties are different (table 16). The commercial carbon fiber (6003) has a tensile strength of 580 MPa and the experimental CF (506) had 349 MPa. The moduli are found to be 59 GPa and 47 GPa and the peak elongations are 0.8 and 0.68% respectively. The differences are more related to the texture and structure of the precursor. A highly oriented rayon fiber produces highly oriented carbon fibers. The carbon layers are likely to be formed with orientation in the direction of the original cellulose chain. These aspects need to be explored further.

Also the degree of polymerization of the two precursors is not known (due to proprietary nature) and could have a role as well.

Table 15 Comparison of the commercial and experimental fibers as received precursor.

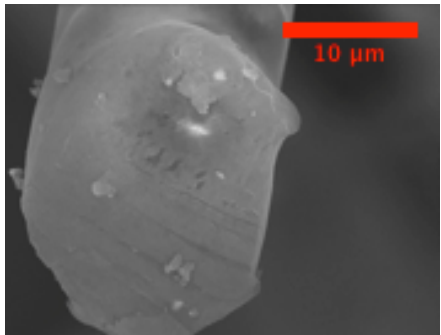
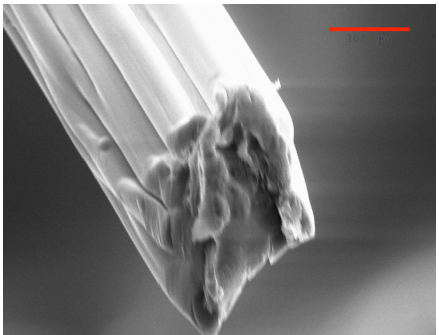
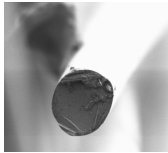
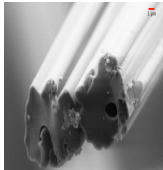
Properties	Commercial rayon fibers	Experimental rayon fibers
Fiber diameter (microns)	14.98	18.99
Tensile strength (MPa)	275.57	174.69
Peak elongation (%)	8.20	5.21
Modulus (GPa)	32.35	26.71
SEM micrographs of cross section		

Table 16 Comparison of the commercial and experimental fibers at the end of carbonization at 1200°C with commercial available carbon fibers.

Properties	Commercial rayon fibers	Experimental rayon fibers	Commercial available carbon fibers
Fiber diameter (microns)	6.72	10.52	4 to 8
Tensile strength (MPa)	579.61	349.43	4130 to 5650
Peak elongation (%)	0.80	0.68	< 0.70
Modulus (GPa)	58.83	46.57	Up to 530
SEM micrographs of cross section			

CHAPTER 5: CONCLUSIONS AND RECOMMENDATIONS FOR FUTURE WORK

5.1 Conclusions

In this work, two different rayon fibers were investigated as carbon fiber precursors. A detailed consideration was applied to the cellulose fiber to carbon fiber transition. After initial studies with a commercially available rayon fiber, an experimental rayon fiber produced in the US was investigated for its potential as a precursor to produce carbon fibers with good mechanical properties. The effect of pretreatment with phosphoric acid, time, temperature and tension during stabilization was analysed. It was concluded that the structural effects are sensitive to the conditions of stabilization (temperature, applied tension, medium). The structural changes were described using results from X-ray diffraction, FTIR and other tests.

The thermal behaviors of the precursor are important during the production of carbon fibers. DSC and TGA analyzed the behaviors in air and nitrogen environment. The two precursors showed a small difference in thermal response as far as the reaction kinetics and the weight loss are concerned. It was observed that during the oxidative decomposition of cellulose at low temperature, dehydration is followed by crosslinking reactions. Concurrently there is rearrangement of the cellulose structures. Two competitive pathways are believed to occur during the pyrolysis stage. Thermal analyses helped in monitoring the progress in stabilization. In addition to observed changes in thermal analyses, color change and burning test help determine the suitability of the stabilized fiber for carbonization. Although DSC scans show the disappearance of the reaction peaks first, color change to black, and passing-burning test take additional stabilization time. Passing of the burning test may be critical to indicate that the fiber is stabilized and can withstand higher temperatures of carbonization. All the samples that pass burning test are black in color, which is another indication of completion of most of the stabilization reactions.

The use of phosphoric acid shifts the pyrolysis reactions to lower temperatures over a wider range. The acid also catalyzes the dehydration reactions and serves as a protectant of the fiber surface so the pyrolysis reaction can happen from fiber surface to fiber core with a tempered speed. The surface protection by phosphoric acid will likely reduce the weight loss and leads to higher yield of carbon fibers. The presence of phosphoric moieties within the fiber probably helps stabilization reactions to progress faster within the interior of the fiber as well at a lower temperature. Carrying out the reactions at lower temperatures can help in maintaining the aromatic structure within the fiber during the conversion reactions leading to lower amount of loss of material due to breakdown of the structure and volatile release. Although these reactions have not been investigated here, it is possible to draw these conclusions based on earlier studies.

The heating rate is important during the stabilization stage. Fast pyrolysis is non-beneficial to the formation of solid carbon fiber from rayon. Slower oxidation in air is highly recommended. As the temperature rises and the residence time increases, the samples start to dehydrate and shrink in both the longitudinal and cross-sectional direction.

As the pyrolysis progresses, the crystalline structure becomes amorphous. The orders in the rayon fiber disappear during pyrolysis as those regions participate in the reactions. During carbonization, as the temperature increases, the basal planes expand and recrystallization occurs. That is when the structure of carbon starts to form. The FTIR results confirm the formation of double bond carbon and the carbon content increases.

Being chemically similar, both precursors showed a comparable response, but the domestic rayon was more susceptible to initiation of reactions. However due to larger diameter, the total time for the reaction to complete was higher. Even during carbonization, the effect of difference in fiber diameter shows up as the larger diameter domestic rayon fiber, which ended up with a small hole in the center of the fiber. The formation of the hole is due to the incomplete stabilization of the fiber in the center, which leads to burning off during carbonization. Also, due to the diffusion kinetics, as the stabilization or carbonization proceeds, the formation of denser sheath further reduces the rate of diffusion leading to additional

slowing down of reactions in the center of the fiber. All these contribute to the formation of hole in the fiber, and further slowing down the heat treatment rates and starting with lower temperatures of treatment may help prevent this.

5.2 Recommendations for future work

To improve the mechanical properties of the obtained fibers, the carbonization temperature can be elevated to 1500°C. Also, stabilization and carbonization at much slower rates may have to be tried. Different impregnants need be evaluated as well. By carefully investigating their effects, the best impregnants can be selected for the production of carbon fiber from rayon. Another improvement to be considered in future research is the impregnants concentration. One can choose to vary the concentration and investigate the influence on pyrolysis.

The diameter of the domestic rayon fiber was almost twice that of many commercial carbon fiber precursors. As the reactions during stabilization and carbonization involve diffusion of gases into and out of the fiber, the reaction kinetics are affected by the fiber diameter. It is recommended that rayon fibers with fiber diameters in the range of 10 microns be produced and then investigated. Also, if possible, the catalysts or flame-retardants could be added during the fiber production process. That will avoid the special impregnation or pretreatment step, and better dispersion of the additives can be achieved.

REFERENCES

1. Kauffman, G.B., *Rayon: first semi-synthetic fiber product*. Journal of chemical education 1993. 70(11): p. 887-893.
2. Shunjin Peng, H.S., *Lyocell Fibers as the Precursor of Carbon Fibers*, 2003, State Key Laboratory of Chemical Fiber & Polymer Material Modification: Shanghai.
3. DONNET, J., *CARBON FIBERS*, ed. second 1990, New York and Basel: MARCEL DEKKER.
4. Konkin, A.A., *Production of Cellulose Based Carbon Fibrous Materials*, in *Handbook of Composites*, W. Watt, Editor 1985, Elsevier Science: Moscou. p. 275.
5. Ruland, W., Journal of Applied Physics, 1967. 38: p. 35-85.
6. Zeng, F.L., D. Pan, and N. Pan, *Choosing the impregnants by thermogravimetric analysis for preparing rayon-based carbon fibers*. Journal of Inorganic and Organometallic Polymers and Materials, 2005. 15(2): p. 261-267.
7. Reinoso, F.R., *Carbon* 38: p. 379.
8. Lewin, M., *Chemical Processing of Fiber and Fabrics, Functional Finishes: Part B*, in *Handbook of Fiber Science and Technology*, S.B. Sello, Editor 1983, Marcel Dekker, Inc.: New York. p. 2-93.
9. Ehrburger, P., *Carbon and graphite fibers*. 1981: p. 169-219.
10. Diefendorf, R.J., *High Performance Carbon Fibers*. Polymer Engineering and Sciences, 1975. 63(3): p. 64-68.
11. Hatta, H., *Strengths of C/C Composites under Tensile, Shear, and Compressive Loading: Role of Interfacial Shear Strength*. Composites Science and Technology 2005. 65: p. 2550-2562
12. Edison, T., 1880: U.S. Patent. p. 223-898.
13. Bacon, R., *Carbon Fibers from Rayon Precursor*. Chemistry and Physics of Carbon, 1973. 9: p. 2.
14. Cranch, G.E., *Unique Properties of flexible Carbon Fibers*. Proceedings of 5th Conference on Carbon, 1962. 11: p. 589.
15. Ford, C.E., 1963: U.S. Patent. p. 107,152.
16. Shindo, A., Journal of Ceramic Assoc. Japan, 1961. 69: p. 195.
17. Watt, W., *New Materials Make Their Mark*. Nature, 1968. 220: p. 835.
18. Clark, A.J. and B. J.E., *Carbon 72 Preprints*. 1972: p. 299.
19. Johnston, J.W., 1968: French Patent. p. 511.
20. Johnston, W., 1969: British Patent. p. 874.
21. Stangedege, A. and R. Prescott, 1966: Belgian Patent. p. 072.
22. Otani, S., *On the Raw Materials of MP Carbon Fiber*. Carbon, 1966. 4: p. 425.
23. Morita, K., H. Miyachiand, and T. Hiramatsu, Carbon, 1981. 19: p. 1-18.
24. Hawthorne, H.M., *High Strength, High Modulus Graphite Fibers from Pitch*. Nature, 1970. 227: p. 946.
25. Hawthorne, H.M. *Carbon Fibers: Their Composites and Applications*. in *The first International Conference on Carbon Fibers*. 1971. London.
26. Brooks, J.D., *The Formation of Grapitizing Carbons from the liquid Phase*. Carbon, 1965. 3: p. 185.
27. Otani, S., *Effects of Heat Treatment under Stress on MP Carbon Fiber*. Appl. Polym. Symp, 1969. 9: p. 325.
28. Boucher, E.A., *Preparation and Structure of Saran-Carbon Fibers*. carbon, 1970. 8: p. 597.
29. Weedon, G.C., *New PE Fibers for High-end Composites*. Modern Plastics, 1986.
30. Hughes, J.D., *The evaluation of Current Carbon Fibers*. J. Phys and Apply. Phys, 1987. 20: p. 1987.
31. Bhat, G.S., *Stabilization of PAN-based precursors for Carbon fibers*, in *Georgia Tech 1990*, Georgia Tech. Inst.: atlanta.
32. Riggs, J.P., *Carbon Fibers*. Enciclopedia of Polym. Sci. & Tech 1985.

33. Morgan, P., *Carbon fibers and their Composites*, 2005. p. 121.
34. Cook, J.G., *Man-Made Fibers*. 15 ed. In *The New Enciclopedia Britannica*. Vol. 7. 1979, Chicago: Enciclopedia Britannica.
35. Stepanik, T.M.E., D.; Whitehouse, R. *Electron processing technology: a promising application for the viscose industry*. in *10th International meeting on Radiation Processing 2000*.
36. Summerlin, L.R., ; Ealy, J. I. Jr, *Chemical Demonstrations: A Sourcebook for Teachers*, ed. A.C. Society. Vol. 1. 1985, Washington, DC.
37. Schuntzenberger, P., *Ann. Chim*, 1870. 21: p. 235.
38. Bunsell, A.R., *Fibre Reinforcements for Composite Materials*, 1988, The Netherlands: Elsevier Science Publishers B.V.: Amsterdam. p. 90.
39. Grassie, N. and R. McGuchan, *Eur. Polym. Jour.*, 1970. 6: p. 1277.
40. Fitzer, E. and D. Muller, *Carbon*, 1975. 13: p. 63.
41. Turner, W., *appl. Polym. Sci.*, 1968. 39: p. 1245.
42. Endrey, A., *J. Polym. Sci. Polym. Chem*, 1982. 20: p. 2105.
43. DiEdwardo, 1974, 3: U.S. Patent.
44. Sato, H., 1975, 3: U.S. Patent.
45. Kalnin, I., 1982, 4: U.S. Patent.
46. DiEdwardo, A. *Organic Chemistry and Plastic Chemistry*. in *175th American Chemical Society Meeting*. Anaheim, Calif.: ACS, Washington, DC.
47. Bacon, R. and M. Tang, *Carbon*, 1964. 2: p. 221.
48. Singer, L.S. and S. Mitchell, *Diffusion of Oxygen into Pitch. Carbon. Carbon*, 1997. 35(5): p. 599-604.
49. Vakili, A., *Low Cost Mesophase Pitch-based Carbon Fiber*, in *TANCON2006*: Knoxville, TN.
50. Shindo, A., Y. Nakanishi, and I. Sema, *Appl. Polym. Symp.*, 1969. 9: p. 271.
51. Bacon, R., A. Pallozzi, and S. Slosarik. in *the 21st Annual Reinforced Plastics Conference*. 1966. New York.
52. Edison, T., 1880: U.S. Patent.
53. DONNET, J. and R.C. Bansal, *Carbon Fibers*, Dekker, Editor 1990: New York. p. 51.
54. shafizadeh, F. and G.W. Bradbury, *Thermal Degradation of Cellulose in air and Nitrogen at low temperature*. *Journal of Applied Polymer Science*, 1979. 23: p. 1431-1442.
55. Qingfeng, L.c., Lv.; Yonggang, Y.; lichen, I., *Investigation on the effects of fire retardants on the thermal decomposition of wood derived rayon fiber in an inert atmosphere by thermogravimetry-mass spectrometry*. *Thermochimica Acta*, 2004(419): p. 205-209.
56. Pappa, A.M., K.; Tzamtzis, N.; Statheropoulos, M., *Chemometric methods for studing the effetc of chemicals on cellulose pyrolysis by thermogravimetry-mass spectrometry*. *Journal of Analytical and Applied Pyrolysis*, 2002. 67: p. 221-235.
57. Statheropoulos, M.K., S.A., *Quantitative thermogravimetric-mass spectrometric analysis for monitoring the effects of fire retardants on cellulose pyrolysis*. *Analytica Chimica Acta*, 2000. 409: p. 203-214.
58. Kim, D.Y.N., Y.; Wada, M.; Kuga, S., *High-yield carbonization of cellulose by sulfuric impregnation*. *Cellulose*, 2001. 8: p. 29-33.
59. Baker, R.R., *Thermal decomposition of cellulose*. *Journal of Thermal Analysis*, 1974. 8: p. 163-173.
60. Ball, R., A.C. McIntosh, and J. Brindley, *The role of char-forming processes in thermal decomposition of cellulose*. *Phys. Chem. Chem. Phys*, 1999. 1: p. 5035-5043.
61. Arseneau, D.F., *Competitive reactions in thermal decomposition of cellulose*. *Canadian Journal of chemistry*, 1970. 49: p. 632.

62. Broido, A. and M. Weinstein, *kinetics of solid-phase cellulose pyrolysis*, in *3rd International Conference of thermal Analysis*, B. Verlag, Editor 1971: Bassel. p. 285.
63. Kilzer, F.J. and A. Broido, *Pyrodynamics*. 1965. 2: p. 151.
64. Mamleev, V. and S. Bourbigot, *J. Anal. Appl. Pyrolysis*, 2007. 80: p. 151.
65. Shafizadeh, F. and G.W. Bradbury, *J. Appl. Polym. Sci.*, 1979. 23: p. 1431.
66. Piskorz, J. and G.V. Peacocke, *Pyrolysis fundamentals Review*, in *Fast pyrolysis of Biomass: A handbook*, Radlein, Editor 2002, Bridgewater, A.V.: Newbury. p. 14.
67. Banyasz, J.L. and S. Li, *J. Anal. Appl. Pyrolysis*, 2001. 57: p. 223.
68. Conesa, J.A., et al., *Analysis of Different Kinetic-Models in the Dynamic Pyrolysis of Cellulose*. *Thermochimica Acta*, 1995. 254: p. 175-192.
69. Agrawal, R.K., *Kinetics of reactions involved in pyrolysis of cellulose I. The three-reaction model*. *Canadian Journal of chemistry*, 1988. 66: p. 403-412.
70. Alves, S.S. and J.L. Figueiredo, *Pyrolysis kinetics of lignocellulosic materials by multi-stage isothermal thermogravimetry*. *J. Anal. Appl. Pyrolysis*, 1988. 17: p. 37.
71. Zhsbankov, R.G., A.A. Konkin, and G.S. Bychkova, ed. *K. volokna*. Vol. 4. 1976.
72. Phillip, B., *Pure Appl. Chem.*, 1984. 56: p. 391.
73. Suuberg, E.M., E.M. Milosavljevic, and V. Oja. in *26th symposium (International) on combustion* 1996. Pittsburgh.
74. Diebold, J.P., *Biomass bioenergy*, 1994. 7: p. 75.
75. Antal, M.J., *Cellulose Pyrolysis Kinetics: The Current State of knowledge*. *Industrial & Engineering Chemistry Research*, 1995. 34: p. 703-717.
76. Valenzuela-Calahorra, C., V. Gomez-Serrano, and M.J. Bernalte-Garcia, *Influence of particle size and pyrolysis conditions on yield, density and some textural paramaters of chars prepared from Holm-oak wood*. *J. Anal. Appl. Pyrolysis*, 1987. 12: p. 61-70.
77. Simmons, G.M. and M. Gentry, *Size limitations due to heat transfer in determining pyrolysis kinetics of biomass*. *J. Anal. Appl. Pyrolysis*, 1986. 10: p. 117-127.
78. Szekely, T., G. Varhegyi, and O. Faix, *Effects of heat and mass transport on the results of thermal decomposition studies*. *J. Anal. Appl. Pyrolysis*, 1987. 11: p. 83-92.
79. Bradbury, G.W., Y. Sakai, and F. Shafizadeh, *J. Appl. Polym. Sci.*, 1979. 23: p. 3271.
80. Lin, Y.C., et al., *Kinetics and mechanism of cellulose pyrolysis*. *J. Phys. Chem.*, 2009. 113: p. 20097-20107.
81. Dillon, A.C., et al., *Nature*, 1997(386): p. 377-379.
82. Li, Y. and R.T. Yang, *J. Am. Chem.Soc.*, 2006(128): p. 8136-8137.
83. Suzuki, M., *Carbon*, 1994. 32: p. 577.
84. Johnson, D.J., *In Chemistry and Physics of Carbon*, ed. P.A. Thrower. Vol. 20. 1987, New York: Marcel Dekker.
85. Wu, Q.L., et al., *SEM/STM studies on the surface structure of a novel carbon fiber from lyocell*. *Syntetic Metals*, 2005(156): p. 792-795.
86. Wu, Q.L. and D. Pan, *Scanning Tunnel Microscopy Study of rayon-Based Carbon fiber Surfaces*, 2002: Shangai, China.
87. Bennett, S.C. and D.J. Johnson, *Carbon*, 1979. 17: p. 145-152.
88. Johnson, D.J., *J. Phys and Apply. Phys*, 1987. 20: p. 286-291.
89. Fourdeaux, A., A. Perret, and W. Ruland. in *First International conference on Carbon Fibers* 1971. London.
90. Johnson, D.J., *Carbon Fibers*, in *Structure Formation in Polymeric Fibers*, D.R. salem, Editor 2001, Hanser Gardner Plublication: Cincinnati. p. 329-358.
91. Singer, L.S., *Carbon*, 1978. 16: p. 409-415.

92. Wu, Q.L. and D. Pan, *A new cellulose based carbon fiber from a lyocell precursor*. Textile Research Journal, 2002. 72(5): p. 405-410.
93. Watt, W. and W. Johnson. in *The Third London International Carbon and Graphite conference*. 1970. london.
94. McClintock, F.A. and A.S. Argon, *Mechanical behavior of materials*1996, Reading,MA: Addison-Wesley.
95. Bacon, R. and W.H. Smith. *Carbon Graphite*. in *2nd Conf. Ind.* . 1965. London.
96. Prandy, J.M. and H.T. Hahn. *Challenge next Decade*. in *International SAMPE Symp. and Exhib.* 1990.
97. Mostovoi, G.E., et al., 1977. 4(626): p. 30 (translated).
98. Tanable, Y., et al., J. Material Sci., 1991. 26(1601): p. 4.
99. Sauder, C., J. Lamon, and R. Pailler, *The Tensile behavior of carbon fiber at high temperatures up to 2400C*. Carbon, 2003. 42: p. 715-725.
100. Ridge, O., Workshop, and Results, *Low cost carbon fiber composites for energy applications*, 2009: Oak Ridge, TN.
101. Rogers, K., G. Sidney, and D. Kingston-Lee, *Royal Aircraft Establishment technical Report*, 1970: UK.
102. in *Polymer News*1982. p. 278.
103. *Market Research Report: Strategic Business Expansion of Carbon Fiber, 2007*, Toray Industries press release. .
104. Bruderick, M., D. Douglas, and S. Michael, *CARBON FIBER COMPOSITE BODY STRUCTURES FOR THE 2003 DODGE VIPER*, 2003, DaimlerChrysler Corporation and Michael Kiesel.
105. Dry, A., *The Development of the Carbon Fiber Industry*, in *42nd International SAMPE Symposium & Exhibition*1997.
106. Yuanwen, W.D., D., *Kinetic studies of thermal degradation of natural cellulosic materials*. Thermochemica Acta, 1998. 324: p. 49-57.
107. Baker, R.R., *Thermal-Decomposition of Cellulose*. Journal of Thermal Analysis, 1975. 8(1): p. 163-173.
108. Tang, M.B., R., *Carbonization of cellulose fibers I low temperature pyrolysis*. Carbon, 1964. 2: p. 211-220.
109. Sekiguchi, Y.S., F., *The effect of inorganic additives on the formation, composition, and combustion of cellulose char*. J. Appl. Polym. Sci., 1984(29): p. 1267-1286.
110. Wodley, F., *Pyrolysis products of untreated and flame retardant treated cellulose and levoglucosan*. J. Appl. Polym. Sci., 1971(15): p. 835-851.
111. Zeng, F.P., D., *Choosing the impregnants for rayon based activated carbon fiber by thermogravimetric analysis*. J. Inorg and Organomet Polym and Mat, 2005. 15(2): p. 261-267.
112. Bacon, R.T., M., *Carbonization of cellulose fibers- II physical property study*. carbon, 1964. 2: p. 221-225.

APPENDICES

VITA

Kokouvi Akato was born in Lome, Togo to Mr. and Mrs. Kokou Akato. He received a Bachelor's degree in Material Science and Engineering from the University of Tennessee, Knoxville in 2010. He then enrolled in the Polymer Engineering Masters program at the same institution in January 2011 and received the graduate research assistantship. After the completion of his Masters, Kokouvi plans on continuing at the University of Tennessee, Knoxville to attain his doctorate degree.